

Hexagonal Grid Approximation of the Solution of Two Dimensional Heat Equation

Nouman Arshad

Submitted to the
Institute of Graduate Studies and Research
in partial fulfillment of the requirements for the degree of

Doctor of Philosophy
in
Mathematics

Eastern Mediterranean University
August 2020
Gazimağusa, North Cyprus

Approval of the Institute of Graduate Studies and Research

Prof. Dr. Ali Hakan Ulusoy
Director

I certify that this thesis satisfies all the requirements as a thesis for the degree of Doctor of Philosophy in Mathematics.

Prof. Dr. Nazım Mahmudov
Chair, Department of Mathematics

We certify that we have read this thesis and that in our opinion it is fully adequate in scope and quality as a thesis for the degree of Doctor of Philosophy in Mathematics.

Assoc. Prof. Dr. Suzan Cival Buranay
Supervisor

Examining Committee

1. Prof. Dr. Hüseyin Aktuğlu _____
2. Prof. Dr. Elimhan Mahmudov _____
3. Prof. Dr. Nazım Mahmudov _____
4. Prof. Dr. Emine Mısırlı _____
5. Assoc. Prof. Dr. Suzan Cival Buranay _____

ABSTRACT

We consider the first type boundary value problem of heat equation $\frac{\partial u}{\partial t} = \omega \left(\frac{\partial^2 u}{\partial x_1^2} + \frac{\partial^2 u}{\partial x_2^2} \right) + f(x_1, x_2, t)$ in two space dimensions on special polygons with interior angles $\alpha_j \pi$, $j = 1, 2, \dots, M$, where $\alpha_j \in \left\{ \frac{1}{2}, \frac{1}{3}, \frac{2}{3} \right\}$, ω is positive constant and f is the heat source. To approximate the solution we develop two difference problems on hexagonal grids using two layers with 14 points. It is proved that the given implicit schemes in Difference Problem 1 and Difference Problem 2 are unconditionally stable. We also show that the convergence of the given difference problems to the exact solution are the order of $O(h^2 + \tau^2)$ and $O(h^4 + \tau)$ respectively on the grids, where h and $\frac{\sqrt{3}}{2}h$ are the step sizes in space variables x_1 and x_2 respectively and τ is the step size in time. The theoretical results are justified by numerical examples on rectangle, trapezoid and parallelogram.

Furthermore, a two layer implicit method on hexagonal grids is also proposed for approximating the solution to first type boundary value problem of the heat equation $\frac{\partial u}{\partial t} = \omega \left(\frac{\partial^2 u}{\partial x_1^2} + \frac{\partial^2 u}{\partial x_2^2} \right) - bu + f(x_1, x_2, t)$ on rectangle where $\omega > 0$, $b \geq 0$ are constants and f is the heat source. For the hexagonal grids that have centers $\frac{h}{2}$ units away from the sides of the rectangle at time moment t with one of the neighboring point in the pattern emerging through the sides a special scheme is given. The unconditional stability of the implicit scheme and the convergence of the approximate solution having order $O(h^4 + \tau^2)$ where h and $\frac{\sqrt{3}}{2}h$ are the step sizes in space variables x_1 and x_2 respectively and τ being the step size in time, are proved. The method is applied on test problems and the obtained numerical results justify the given theoretical results.

Keywords: Finite difference method, Hexagonal grid, Stability analysis, Error bounds,

Two dimensional heat equation.

ÖZ

İç açılı $\alpha_j\pi$, $j = 1, 2, \dots, M$, $\alpha_j \in \{\frac{1}{2}, \frac{1}{3}, \frac{2}{3}\}$ olan özel çokgenler üzerinde, iki boyutlu ısı denkleminin $\frac{\partial u}{\partial t} = \omega(\frac{\partial^2 u}{\partial x_1^2} + \frac{\partial^2 u}{\partial x_2^2}) + f(x_1, x_2, t)$, $\omega > 0$ sabit, f ise ısı kaynağı olmak üzere birinci tip sınır değer problemi ele alınır. Çözümün yaklaşık hesaplanması için, altıgen ızgara düğümler üzerinde 14 nokta kullanarak iki adet farklar problemleri geliştirilir. Farklar Problemi 1 ve Farklar Problemi 2’de verilen örtük şemaların koşulsuz kararlı olduğu kanıtlanmıştır. Ayrıca, verilen farklar problemlerinin çözümlerinin, sırası ile $O(h^2 + \tau^2)$ ve $O(h^4 + \tau)$ mertebelerinden ızgaralar üzerindeki kesin çözüme yaklaştığı gösterilmiştir ki sırası ile h ve $\frac{\sqrt{3}}{2}h$, x_1 ve x_2 uzay değişkenlerine ait adım uzunlukları, τ ise zaman değişkenine ait adım uzunluğudur. Teorik sonuçlar dikdörtgen, yamuk ve paralelkenar üzerindeki sayısal örneklerle doğrulanmaktadır.

Ayrıca, dikdörtgen üzerinde ısı denkleminin $\frac{\partial u}{\partial t} = \omega(\frac{\partial^2 u}{\partial x_1^2} + \frac{\partial^2 u}{\partial x_2^2}) - bu + f(x_1, x_2, t)$, $\omega > 0, b \geq 0$ sabitler, f ise ısı kaynağı olmak üzere birinci tip sınır değer probleminin yaklaşık çözümü için altıgen ızgaralar üzerinde iki katmanlı örtük yöntem de önerilmektedir. Her t zaman anında dikdörtgenin kenarlarından merkezi $h/2$ birim uzaklıkta olan altıgen ızgaralar için ki model içinde bir komşuluğu dikdörtgenin kenarından dışarı çıkar, özel bir şema verilmiştir. Verilen örtük şemanın koşulsuz kararlılığı ve yaklaşık çözümün düğümler üzerinde $O(h^4 + \tau^2)$ mertebeden u kesin çözümüne yakınsadığı ispatlanmıştır ki sırası ile h ve $\frac{\sqrt{3}}{2}h$, x_1 ve x_2 uzay değişkenlerine ait adım uzunlukları, τ ise zaman değişkenine ait adım uzunluğudur. Daha sonra, yöntem test problemlerine uygulamış ve elde edilen sayısal sonuçların verilen teorik sonuçları doğruladığı görülmüştür.

Anahtar Kelimeler: Sonlu farklar yöntemi, Altıgen ızgara, Kararlılık analizi, Hata sınırları, İki boyutlu ısı denklemi.

To the Little Angel who Always Brings Smile to my Face

ACKNOWLEDGMENTS

At first and foremost, thanks to Almighty Allah, for His assistance in my success reaching such a sophisticated level of education, through my journey at EMU. I wish to express my sincere appreciation to my supervisor, Assoc. Professor Dr. Suzan Cival Buranay, who has the substance of a genius: she convincingly guided and encouraged me to be professional and do the right thing even when the road got tough. Without her persistent help, patience, motivation and the immense knowledge she has, the goal of this project would not have been realized. I could not have imagined having a better supervisor for my PhD study. Besides my supervisor, I would like to thank the rest of my thesis committee members, for their insightful comments and encouragement, but also for the hard questions which incited me to widen my research from various perspectives.

Not neglecting the vital role of my parents, brother, sister, and other family members for helping me survive all the stress throughout my journey to this prestigious qualification and not letting me give up, and for supporting me both on and off the water. I exceptionally want to thank all academic and non-academic staff in the Mathematics department for their kindness, support, and confidence throughout my departmental research and teaching duties.

Most of all, i am fully indebted to all those who refused to help me, so i did it myself.

TABLE OF CONTENTS

ABSTRACT	iii
ÖZ.....	v
DEDICATION	vii
ACKNOWLEDGMENTS	viii
LIST OF TABLES.....	xi
LIST OF FIGURES	xiii
1 INTRODUCTION	1
2 Hexagonal Grid Approximation of the Solution to Heat Equation on Special Polygons	6
2.1 Introduction	6
2.2 First Type Boundary Value Problem of Heat Equation on Special Polygons .	7
2.3 Second Order Accurate Difference Problem	9
2.3.1 The Stability and Convergence Analysis for Difference Problem 1....	15
2.4 Fourth Order Accurate Implicit Difference Problem.....	22
2.4.1 The Stability and Convergence Analysis of Difference Problem 2.....	23
3 Implicit Method of High Accuracy on Hexagonal Grids for Approximating the Solution to Heat Equation on Rectangle	30
3.1 Introduction	30
3.2 First Type Problem on Rectangle and Basic Notations	31
3.3 Implicit Method of High Accuracy for the Solution of Problem (3.2)-(3.4) ..	33
3.3.1 The Stability and Convergence Analysis for HADP (3.8)-(3.11)	35
4 Numerical Results	44
4.1 Introduction	44
4.2 Numerical Results for the Problem (2.9) - (2.11)	44

4.3 Numerical Results for the Problem (3.2) - (3.4)	52
5 Conclusion and Further Research	67
REFERENCES	68

LIST OF TABLES

Table 4.1: Computational time, maximum norm of the errors and the order of convergence by using Difference Problem 1 for the Example 4.1 and Example 4.2 on rectangle.....	48
Table 4.2: Computational time, maximum norm of the errors and the order of convergence by using Difference Problem 1 for the Example 4.1 and Example 4.2 on trapezoid.....	48
Table 4.3: Computational time, maximum norm of the errors and the order of convergence by using Difference Problem 1 for the Example 4.1 and Example 4.2 on parallelogram.	49
Table 4.4: Computational time, maximum norm of the errors and the order of convergence by using Difference Problem 2 for the Example 4.1 and Example 4.2 on rectangle.....	49
Table 4.5: Computational time, maximum norm of the errors and the order of convergence by using Difference Problem 2 for the Example 4.1 and Example 4.2 on trapezoid.....	49
Table 4.6: Computational time, maximum norm of the errors and the order of convergence by using Difference Problem 2 for the Example 4.1 and Example 4.2 on parallelogram.	49
Table 4.7: Solution at some points on $t = 1$, and the order of convergence by using Difference Problem 1 for the Example 4.3.	52
Table 4.8: Solution at some points on $t = 1$, and the order of convergence by using Difference Problem 2 for the Example 4.3.	53

Table 4.9: Computational time, maximum norm of the errors and the order of convergence obtained by using the proposed method M_{14P}^H and the method M_{14P}^R for the Example 4.4 when $\alpha = 0.8$	58
Table 4.10: Computational time, maximum norm of the errors and the order of convergence obtained by using the proposed method M_{14P}^H and the method M_{14P}^R for the Example 4.4 when $\alpha = 0.01$	59
Table 4.11: sizes of the stiffness matrices, preconditioning times and the condition numbers of the preconditioned stiffness matrices and the total computational time required by the methods M_{14P}^H and M_{14P}^R for the Example 4.4 when $\alpha = 0.8$	59
Table 4.12: Solution at some points on $t = 1$, and the order of convergence obtained by M_{14P}^H for the Example 4.5.	62
Table 4.13: Solution at some points on $t = 1$, and the order of convergence obtained by M_{14P}^R for the Example 4.5.	63
Table 4.14: Computational efficiency comparison of the methods M_{14P}^H , M_{14P}^R , and $M_{An(200)}$ for the solution at $t = 1$ for the Example 4.5.	63
Table 4.15: Computational times, maximum norm of the errors and the order of convergence obtained by using the proposed method M_{14P}^H for the Example 4.6. ..	65

LIST OF FIGURES

Figure 2.1: Hexagonal grid on rectangle.....	10
Figure 2.2: Hexagonal grid on parallelogram.	10
Figure 2.3: Hexagonal grid on trapezoid.....	11
Figure 2.4: The illustration of the solution $u_{P_2}^{k+1}$ and $u_{P_2}^k$ on the left ghost points..	13
Figure 2.5: The illustration of the solution $u_{P_5}^{k+1}$ and $u_{P_5}^k$ on the right ghost points.	13
Figure 3.1: Hexagonal grid structure and ghost points on rectangle	32
Figure 4.1: Absolute error function $\left \epsilon_{Rec}^{Ex2(2^{-6}, 2^{-14})} \right $ at $t = 0.25$ and $t = 0.75$ obtained by using Difference Problem 2 for the Example 4.2.	50
Figure 4.2: Absolute error function $\left \epsilon_{Par}^{Ex2(2^{-6}, 2^{-14})} \right $ at $t = 0.25$ and $t = 0.75$ obtained by using Difference Problem 2 for the Example 4.2.	50
Figure 4.3: Absolute error function $\left \epsilon_{Tra}^{Ex2(2^{-6}, 2^{-14})} \right $ at $t = 0.25$ and $t = 0.75$ obtained by using Difference Problem 2 for the Example 4.2.	51
Figure 4.4: The approximate solution $u_{2^{-6}, 2^{-14}}(x_1, x_2, t)$ at time moments $t = 0.25$ and $t = 1$ for the Example 4.3 obtained by using Difference Problem 2.	53
Figure 4.5: The absolute error function $\left \epsilon_{M_{14P}^H(2^{-6}, 2^{-10})} \right $, at time moments $t = 0.25, 0.5, 0.75, 1$ obtained by using the proposed method M_{14P}^H for the Example 4.4.	59
Figure 4.6: The absolute error function $\left \epsilon_{M_{14P}^R(2^{-6}, 2^{-10})} \right $, at time moments $t = 0.25, 0.5, 0.75, 1$ obtained by using the proposed method M_{14P}^R for the Example 4.4.	60
Figure 4.7: The approximate solution $u_{2^{-6}, 2^{-10}}^H(x_1, x_2, t)$ for the Example 4.5 obtained by using the given method M_{14P}^H at time moments $t = 0.25, 0.5, 0.75, 1$	64
Figure 4.8: The approximate solution $u_{2^{-6}, 2^{-10}}^R(x_1, x_2, t)$ for the Example 4.5 obtained by using the given method M_{14P}^R at time moments $t = 0.25, 0.5, 0.75, 1$	64

Figure 4.9: The absolute error function $\left| \mathcal{E}^{M_{14P}^H(2^{-6}, 2^{-10})} \right|$, at time moments $t = 0.25, 0.5, 0.75, 1$ obtained by using the proposed method M_{14P}^H for the Example 4.6. 66

Chapter 1

INTRODUCTION

There are many real world applications, particularly partial differential equations for which the solution cannot be calculated using standard analytical methods. Therefore, the numerical methods to approximate the solution of such problems have gained much importance in recent years. For example the dynamical problem of thermodiffusion in an elastic solid given in Dryja [1] where, finite difference and finite element methods were used to approximate the solution. It is also well known that by finite difference method for the approximation of the partial differential equation, the construction of economical schemes is of great importance because one of the most important issues in numerical methods for the solution of dynamical problems is the well-founded choice of stable and economical computational algorithms. By an economical scheme we mean a scheme which is unconditionally stable and total number of arithmetic operations needed to solve this difference scheme is proportional to the number of the grid points.

In numerical calculations of nuclear reactors it has been found worthwhile to use the implicit schemes for the solution of two dimensional age-diffusion equation by Ehrlich and Hurwitz [2]. Most recently, in Ahmed et al. [3] a novel and time efficient positivity preserving numerical scheme to find the solution of epidemic model involving reaction-diffusion system in three dimension has been designed. In Iqbal et al. [4] an unconditionally stable and structure preserving computational technique for fractional order Schnakenberg model has been given.

Icosahedral-hexagonal grids were investigated more than half century ago for their suitability to meteorological application. Sadourny et al. [5], and Williamson [6] solved the nondivergent barotropic vorticity equation with finite difference methods on such grids. Their results were more favorable than those of the more usual spherical grids. Since then the hexagonal grid was extended to the integration of the primitive equations of fluid dynamics by Sadourny [7], Sadourny and Morel [8] and Masuda [9]. They tried to apply the governing equations of momentum form to the hexagonal grid directly and develop a conservative finite difference scheme. Masuda and Ohnishi [10] reinvestigated the integration scheme of the primitive equation model with icosahedral-hexagonal grid system and its application to the shallow water equation. The authors used the stream function and velocity potential as the dependent variables of the primitive equations instead of the velocity components and obtained satisfactory approximation to the integration of the shallow water equation. Also, Sadourny [7], Thacker [11], Thacker [12], Salmon and Talley [13], Ničkovič [14], considered various aspects of the finite differencing on hexagonal grids. Later, Ničkovič et al. [15] showed that hexagonal lattices have some advantages over commonly used square grids. As the authors in Ničkovič et al. [15] state “having better isotropy, they provide more accurate dispersion of gravity waves than square grids do and therefore they can be more appropriate for simulation of smaller-scale divergent processes”.

Hexagonal grid approach was also studied in reservoir simulation and simulation of electrical wave phenomena. Pruess and Bodvarsson [16] used seven-point finite difference method for improved grid orientation performance in pattern steam floods of heavy oil reservoirs. It was shown that for seven-point floods, hexagonal grid method provides good numerical accuracy at substantially less computational work

than rectangular grid method (five or nine point methods).

Taking into consideration that the hexagonal grid is a more natural choice to emulate the isotropy of the Laplacian operator, the approximation of the solution of the Dirichlet type boundary value problems for the two dimensional Laplace equation and heat equations were of interest. Such as high accuracy implicit schemes on triangular nets whose meshes are equilateral triangles for the two dimensional homogeneous diffusion equation were studied by Richtmyer and Morton [17]. Therein, the analogue of $O(h^2 + \tau^2)$ accurate, unconditionally stable three layer scheme with 9-point on hexagonal grids and a three layer scheme with 21-point, a two layer scheme with 14-point both converging with order $O(h^4 + \tau^2)$ to the exact solution on hexagonal grids were given. However, the diffusion problem with heat source on hexagonal grids that have centers $\frac{h}{2}$ units away from the sides of the rectangle at any time moment t with neighboring points emerging through these sides were not considered. Kara [18] gave the compact scheme of 4th order using hexagonal grid for convection diffusion equation to approximate its solution. Numerical results were given on parallelogram showing more accurate results with less computational time than the standard central difference scheme. In the article of Lee et al. [19] hexagonal grid finite difference methods were derived in finite volume approach involving standard Laplacian. The obtained schemes were used in the simulation of electrical wave phenomena propagated in two dimensional reserved-C type cardiac tissue, exhibiting both linear and spiral waves more efficiently than similar computation carried on rectangular finite volume schemes. Most recently, Dosiyeu and Celiker [20] gave the approximation on the hexagonal grid of the Dirichlet problem for Laplace's equation. The fourth order matching operator on the hexagonal grid was constructed and applied to justify a hexagonal version of the combined Block-Grid method for the

Dirichlet problem with corner singularity. Thus, they obtained $O(h^4)$ order of accuracy where, h is the step size when using the 7-point scheme on the hexagonal grid instead of using 9-point scheme on the rectangular grid giving the computational advantages such as memory space and computational cost. Further, Dosiyeve and Celiker [21] investigated a fourth order block-hexagonal grid approximation for the solution of Laplace's equation on special polygons with singularities. It has been justified that in these polygons if the boundary functions away from the singular corners are from the Hölder classes $C^{4,\lambda}, 0 < \lambda < 1$, the uniform error is of order $O(h^4)$ when the hexagon grid is applied in the "nonsingular" part of the domain.

The solution to first type boundary value problem of heat equation,

$$\frac{\partial u}{\partial t} = \omega \left(\frac{\partial^2 u}{\partial x_1^2} + \frac{\partial^2 u}{\partial x_2^2} \right) + f(x_1, x_2, t) \quad (1.1)$$

on special polygons with interior angles $\alpha_j\pi, j = 1, 2, \dots, M$, for $\alpha_j \in \{\frac{1}{2}, \frac{1}{3}, \frac{2}{3}\}$ where, $\omega > 0$ and f is the heat source by using hexagonal grids, two implicit methods on two layers with 14-point has been given in Buranay and Nouman [22]. Under the assumption that the heat source and the initial and boundary functions are given such that the exact solution belongs to the Hölder space $C_{x,t}^{6+\alpha, 3+\frac{\alpha}{2}}, 0 < \alpha < 1$, it is proved that the given Difference Problem 1 and Difference Problem 2 converge to the exact solution with $O(h^2 + \tau^2)$ and $O(h^4 + \tau)$ order of accuracy on the grids respectively.

In this study we give the findings of Buranay and Nouman [22], that the theoretical results are given in Chapter 2 and numerical results are given in Chapter 4. Furthermore, we also propose a highly accurate two layer implicit scheme on hexagonal grids to approximate the solution of the first type boundary value problem

of heat equation

$$\frac{\partial u}{\partial t} = \omega \left(\frac{\partial^2 u}{\partial x_1^2} + \frac{\partial^2 u}{\partial x_2^2} \right) - bu + f(x_1, x_2, t) \quad (1.2)$$

on rectangle where, $\omega > 0$, $b \geq 0$ are constants, A special scheme is given for the grid points having the ghost points in the pattern with centers $\frac{h}{2}$ units away. We prove that the given scheme is unconditionally stable and the constructed difference problem converge to exact solution on the grids with order of accuracy of $O(h^4 + \tau^2)$. Then we consider several test problems in Chapter 5, to justify the theoretical results obtained in Chapter 2 and Chapter 3. Numerical results are accompanied by the tables and figures. We also pre announce the various research areas where the methodology given in this thesis may be extended.

Chapter 2

HEXAGONAL GRID APPROXIMATION OF THE SOLUTION TO HEAT EQUATION ON SPECIAL POLYGONS

2.1 Introduction

In this chapter, we give two layer implicit schemes with 14-point by using the hexagonal grids for approximating the solution of first type boundary value problem of heat equation in two space dimensions on special polygons Ω with interior angles $\alpha_j\pi$, $j = 1, 2, \dots, M$, where $\alpha_j \in \{\frac{1}{2}, \frac{1}{3}, \frac{2}{3}\}$. The heat source, initial and boundary functions are given such that on $\overline{Q}_T = \overline{\Omega} \times [0, T]$, where $x = (x_1, x_2) \in \overline{\Omega}$ and $t \in [0, T]$ the solution belongs to the Hölder space $C_{x,t}^{6+\alpha, 3+\frac{\alpha}{2}}(\overline{Q}_T)$, $0 < \alpha < 1$. Special difference schemes are proposed for the hexagonal grids that have centers $\frac{h}{2}$ units away from the sides of these polygons at time moment t , which have a neighboring point in the pattern emerging through these sides. In Section 2.2, we give the boundary value problem of first type for two dimensional heat equation on special polygons. In Section 2.3, a two layer implicit difference scheme with 14-point on hexagonal grids called Difference Problem 1 is proposed and it is proved that this scheme is unconditionally stable. The solution of the constructed Difference Problem 1 converges to the exact solution on the grids with $O(h^2 + \tau^2)$ order of accuracy. In Section 2.4, we give a two layer implicit unconditionally stable scheme with 14-point on hexagonal grids called Difference Problem 2. We showed that the solution of the constructed Difference Problem 2 converges to the exact solution on the grids with

$O(h^4 + \tau)$ order of accuracy. Here, h and $\frac{\sqrt{3}}{2}h$ are the step sizes in space variables x_1 and x_2 respectively, and τ being the time step size. Numerical results are given in Chapter 4 to justify the theoretical results. Three test problems are constructed of which for the Example 4.1 and Example 4.2 the exact solution is known but for Example 4.3, the exact solution is not given.

We remark that the theoretical results given in this chapter are published in [22].

2.2 First Type Boundary Value Problem of Heat Equation on Special Polygons

Let $x = (x_1, x_2)$, and Ω be an open simply connected polygon and ν_j , $j = 1, 2, \dots, M$, be its sides, including the ends, enumerated counterclockwise ($\nu_0 \equiv \nu_M$, $\nu_1 \equiv \nu_{M+1}$), and also let $\alpha_j\pi$, $j = 1, 2, \dots, M$, where $\alpha_j \in \{\frac{1}{2}, \frac{1}{3}, \frac{2}{3}\}$ be the interior angles formed by the sides ν_{j-1} and ν_j . Furthermore, let $S = \bigcup_{j=1}^M \nu_j$ be the boundary for Ω and denote by $\bar{\Omega} = \Omega \cup S$ the closure of Ω . Let $Q_T = \Omega \times (0, T)$, with lateral surface S_T more accurately the set of points (x, t) , $x \in S$ and $t \in [0, T]$ also \bar{Q}_T shows the closure of Q_T . Let l be a noninteger positive number, $C_{x,t}^{l, \frac{l}{2}}(\bar{Q}_T)$ be the Banach space of functions $u(x, t)$ that are continuous in \bar{Q}_T together with all derivatives of the form

$$\frac{\partial^{r+s_1+s_2} u}{\partial t^r \partial x_1^{s_1} \partial x_2^{s_2}} \text{ for } 2r + s_1 + s_2 < l \quad (2.1)$$

with bounded norm

$$\|u\|_{C_{x,t}^{l, \frac{l}{2}}(\bar{Q}_T)} = \langle u \rangle_{Q_T}^{(l)} + \sum_{j=0}^{[l]} \langle u \rangle_{Q_T}^{(j)}, \quad (2.2)$$

where,

$$\langle u \rangle_{Q_T}^{(j)} = \sum_{2r+s_1+s_2=j} \max_{\bar{Q}_T} \left| \frac{\partial^{r+s_1+s_2} u}{\partial t^r \partial x_1^{s_1} \partial x_2^{s_2}} \right|, j = 0, 1, 2, \dots, [l] \quad (2.3)$$

$$\langle u \rangle_{Q_T}^{(l)} = \langle u \rangle_x^{(l)} + \langle u \rangle_t^{(\frac{l}{2})} \quad (2.4)$$

$$\langle u \rangle_x^{(l)} = \sum_{2r+s_1+s_2=[l]} \left\langle \frac{\partial^{r+s_1+s_2} u}{\partial t^r \partial x_1^{s_1} \partial x_2^{s_2}} \right\rangle_x^{l-[l]} \quad (2.5)$$

$$\langle u \rangle_t^{(\frac{l}{2})} = \sum_{0 < l-2r-s_1-s_2 < 2} \left\langle \frac{\partial^{r+s_1+s_2} u}{\partial t^r \partial x_1^{s_1} \partial x_2^{s_2}} \right\rangle_t^{\frac{l-2r-s_1-s_2}{2}} \quad (2.6)$$

and the quantities $\langle u \rangle_x^\alpha, \langle u \rangle_t^\beta$ for $\alpha, \beta \in (0, 1)$ are defined as

$$\langle u \rangle_x^\alpha = \sup_{(x,t), (x',t) \in \bar{Q}_T} \frac{|u(x,t) - u(x',t)|}{|x - x'|^\alpha} \quad (2.7)$$

$$\langle u \rangle_t^\beta = \sup_{(x,t), (x,t') \in \bar{Q}_T} \frac{|u(x,t) - u(x,t')|}{|t - t'|^\beta} \quad (2.8)$$

We consider the first type boundary value problem for two space dimensional heat equation BVP1:

$$Lu = f(x, t) \text{ on } Q_T, \quad (2.9)$$

$$u(x, 0) = \varphi(x) \text{ on } \bar{\Omega}, \quad (2.10)$$

$$u(x, t) = \phi(x, t) \text{ on } S_T, \quad (2.11)$$

where, $x = (x_1, x_2)$ and $L \equiv \frac{\partial}{\partial t} - \omega \left(\frac{\partial^2}{\partial x_1^2} + \frac{\partial^2}{\partial x_2^2} \right)$ and $\omega > 0$ is a constant.

The differentiability properties of solutions of boundary value problems for the Laplace's equation on polygons were given by Volkov [23]. For elliptic equations, the behaviour of solutions near singularities of the boundary of the domain had been treated by Kondrat'ev [24]. For the differentiability properties of solutions of the parabolic equations on cylindrical domains with smooth boundary, see Ladyženskaja

et al. [25], and Friedman [26]. The smoothness of solutions of parabolic equations in regions with edges was studied by Azzam and Kreyszig in [27] for the Dirichlet and for the mixed boundary value problems in [28]. Hence, in this paper the obtained subsequent theoretical and numerical results are given under the assumption that the heat source function $f(x,t)$ and the initial and boundary functions $\varphi(x)$ and $\phi(x,t)$ are given such that the BVP1 (2.9) - (2.11) has unique solution u belonging to the class $C_{x,t}^{6+\alpha,3+\frac{\alpha}{2}}(\overline{Q_T})$.

Remark 2.1: It is known that the use of classical finite difference method to solve the boundary value problems with singularities is ineffective. Therefore, a special construction is usually needed for the numerical scheme near the singularities in such a way that the order of convergence is the same as in the case of a smooth solution (see Dosiyeu and Celiker [20], Dosiyeu [29] and Dosiyeu et al. [30]).

2.3 Second Order Accurate Difference Problem

Let $h > 0$, we assign Ω^h a hexagonal grid on Ω , with step size h , defined as the set of nodes

$$\Omega^h = \left\{ x = (x_1, x_2) \in \Omega : x_1 = \frac{i' - j'}{2}h, x_2 = \frac{\sqrt{3}(i' + j')}{2}h, \right. \\ \left. i' = 1, 2, \dots; j' = 0 \pm 1 \pm 2, \dots \right\} \quad (2.12)$$

as shown in Figure 2.1, Figure 2.2 and Figure 2.3 when Ω is a rectangle, parallelogram and trapezoid respectively.

Let $v_j^h, j = 1, 2, \dots, M$ be the set of nodes on the interior of v_j and let $\widehat{v}_j^h = v_{j-1} \cap v_j$ be the j -th vertex of Ω , $S^h = \bigcup_{j=1}^M (v_j^h \cup \widehat{v}_j^h)$, $\overline{\Omega}^h = \Omega^h \cup S^h$. We assume that the lengths of the sides of the polygon are given such that irregular hexagonal grids only have a right neighboring point or a left neighboring point emerging through the side of Ω when the

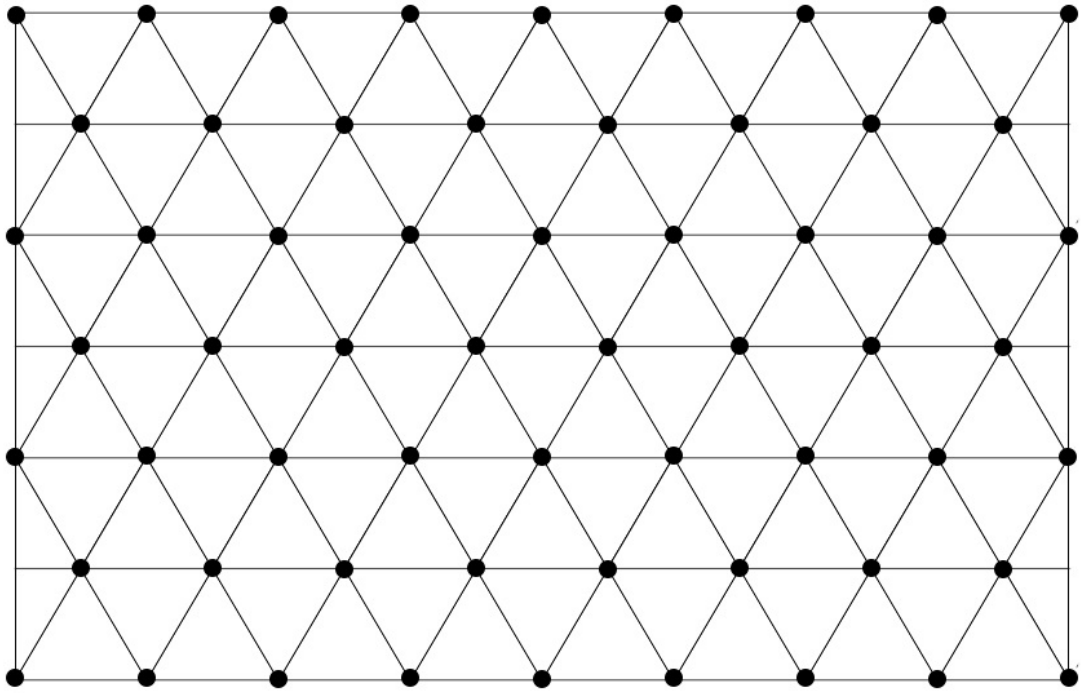


Figure 2.1: Hexagonal grid on rectangle.

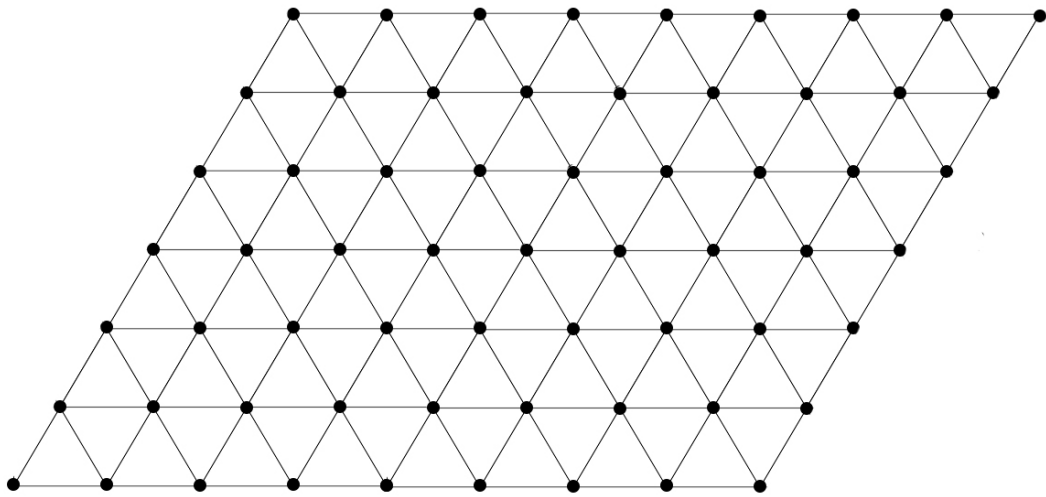


Figure 2.2: Hexagonal grid on parallelogram.

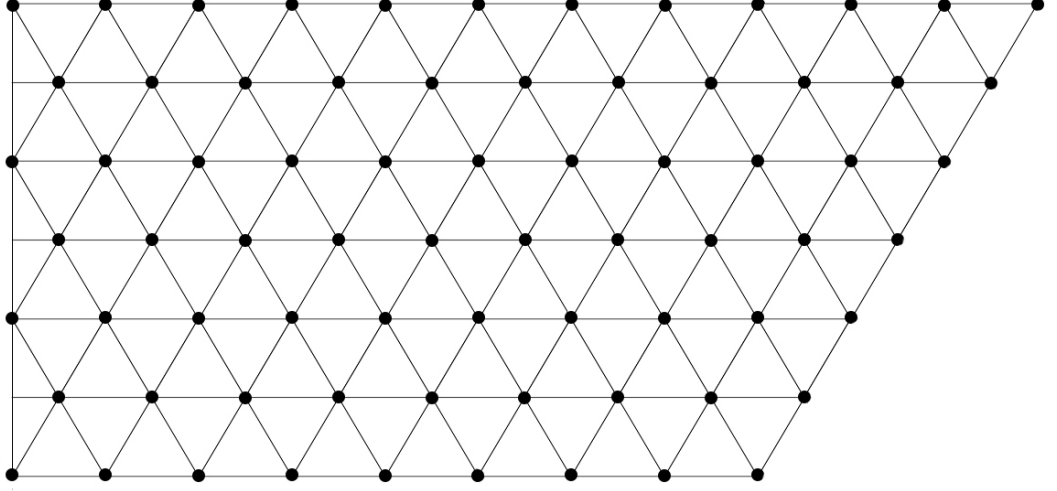


Figure 2.3: Hexagonal grid on trapezoid.

center of the hexagon is $\frac{h}{2}$ units away from this side. Accordingly, we shall call these points right ghost points and left ghost points. Further, let Ω^{*lh} , Ω^{*rh} denote the set of interior nodes whose distance from the boundary is $\frac{h}{2}$ and the hexagon has a left ghost point as shown in Figure 2.4 or a right ghost point given in Figure 2.5 respectively. We also denote by $\Omega^{*h} = \Omega^{*lh} \cup \Omega^{*rh}$ and $\Omega^{0h} = \Omega^h \setminus \Omega^{*h}$. Next, let

$$\gamma_\tau = \left\{ t_k = k\tau, \tau = \frac{T}{M'}, k = 1, \dots, M' \right\} \quad (2.13)$$

$$\bar{\gamma}_\tau = \left\{ t_k = k\tau, \tau = \frac{T}{M'}, k = 0, \dots, M' \right\}, \quad (2.14)$$

and the set of internal nodes and lateral surface nodes be defined by

$$\Omega^h \gamma_\tau = \Omega^h \times \gamma_\tau = \left\{ (x, t) : x \in \Omega^h, t \in \gamma_\tau \right\} \quad (2.15)$$

$$S_T^h = S^h \times \bar{\gamma}_\tau = \left\{ (x, t) : x \in S^h, t \in \bar{\gamma}_\tau \right\}. \quad (2.16)$$

Let $\Omega^{*lh} \gamma_\tau = \Omega^{*lh} \times \gamma_\tau \subset \Omega^h \gamma_\tau$ and $\Omega^{*rh} \gamma_\tau = \Omega^{*rh} \times \gamma_\tau \subset \Omega^h \gamma_\tau$ and $\Omega^{*h} \gamma_\tau = \Omega^{*lh} \gamma_\tau \cup$

$\Omega^{*rh}\gamma_\tau$, also $\Omega^{0h}\gamma_\tau = \Omega^h\gamma_\tau \setminus \Omega^{*h}\gamma_\tau$. We use the following notations:

P_0 denotes the center of the hexagon.

$Patt(P_0)$ is the pattern of the hexagon consisting the neighboring points $P_i, i = 1, \dots, 6$.

Inc denotes the incidence matrix related to the neighborhood topology of all the hexagon centers.

$\lambda_s(K)$ present the eigenvalues $\lambda_s, s = 1, 2, \dots, N$ of real matrix $K \in R^{N \times N}$.

Also

$$\begin{aligned}
u_{P_1}^{k+1} &= u(x_1 - \frac{h}{2}, x_2 + \frac{\sqrt{3}}{2}h, t + \tau), \quad u_{P_3}^{k+1} = u(x_1 - \frac{h}{2}, x_2 - \frac{\sqrt{3}}{2}h, t + \tau) \\
u_{P_2}^{k+1} &= u(x_1 - h, x_2, t + \tau), \quad u_{P_5}^{k+1} = u(x_1 + h, x_2, t + \tau) \\
u_{P_4}^{k+1} &= u(x_1 + \frac{h}{2}, x_2 - \frac{\sqrt{3}}{2}h, t + \tau), \quad u_{P_6}^{k+1} = u(x_1 + \frac{h}{2}, x_2 + \frac{\sqrt{3}}{2}h, t + \tau) \\
u_{P_0}^{k+1} &= u(x_1, x_2, t + \tau), \quad u_{P_A}^{k+1} = u(\hat{p}, x_2, t + \tau), \quad (\hat{p}, x_2, t + \tau) \in S_T^h. \quad (2.17)
\end{aligned}$$

where, the value of $\hat{p} = x_1 - \frac{h}{2}$ if $P_0 \in \Omega^{*lh}\gamma_\tau$ and $\hat{p} = x_1 + \frac{h}{2}$ if $P_0 \in \Omega^{*rh}\gamma_\tau$ as also given in (2.29). Analogously, the values $u_{P_i}^k, i = 0, \dots, 6$ and $u_{P_A}^k$ present the exact solution at the same space coordinates of $P_i, i = 0, \dots, 6$ and P_A respectively, but at time level t . Also we use the notations $u_{h,\tau,P_i}^{k+1}, i = 0, \dots, 6, u_{h,\tau,P_A}^{k+1}$, and $u_{h,\tau,P_i}^k, i = 0, \dots, 6, u_{h,\tau,P_A}^k$ to present the numerical solution at the same space coordinates of $P_i, i = 0, \dots, 6$ and P_A for time moments $t + \tau$ and $t = k\tau$, respectively. Further, $f_{P_0}^{k+\frac{1}{2}} = f(x_1, x_2, t + \frac{\tau}{2})$ and $f_{P_A}^{k+\frac{1}{2}} = f(\hat{p}, x_2, t + \frac{\tau}{2})$ where \hat{p} is as defined in (2.29).

For the numerical solution of the BVP we propose the following difference problem

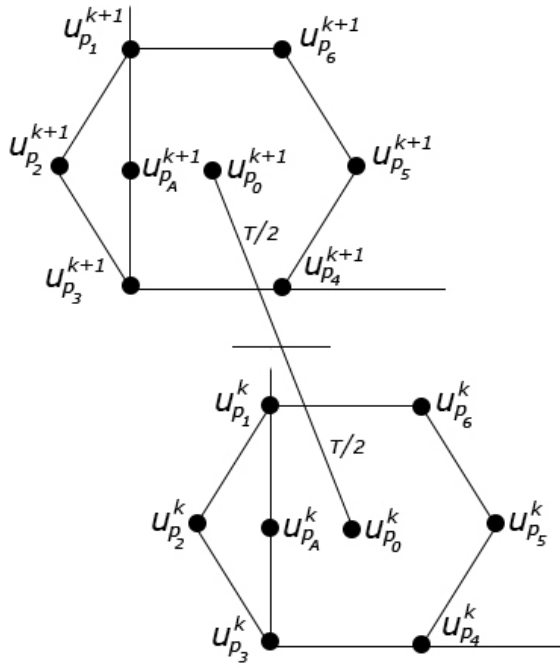


Figure 2.4: The illustration of the solution $u_{p_2}^{k+1}$ and $u_{p_2}^k$ on the left ghost points.

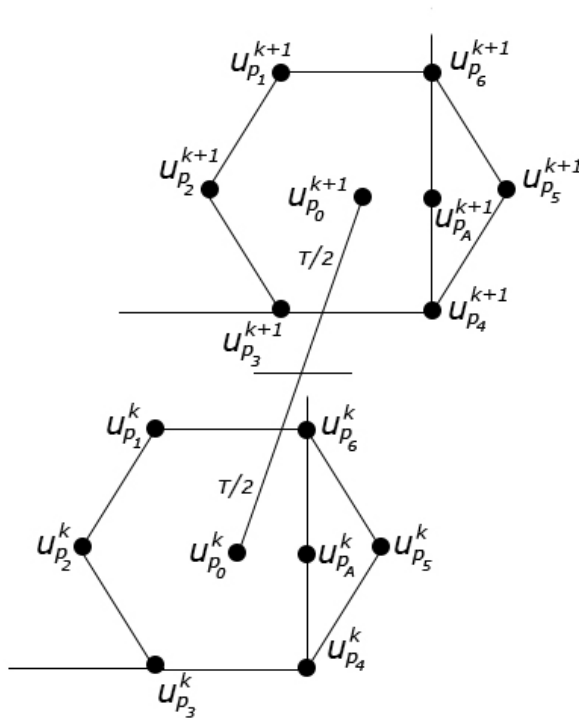


Figure 2.5: The illustration of the solution $u_{p_5}^{k+1}$ and $u_{p_5}^k$ on the right ghost points.

Difference Problem 1

$$\Theta_{h,\tau} u_{h,\tau}^{k+1} = \Lambda_{h,\tau} u_{h,\tau}^k + \Psi \text{ on } \Omega^{0h} \gamma_\tau \quad (2.18)$$

$$\Theta_{h,\tau}^* u_{h,\tau}^{k+1} = \Lambda_{h,\tau}^* u_{h,\tau}^k + E_{h,\tau}^* \phi + \Psi^* \text{ on } \Omega^{*h} \gamma_\tau \quad (2.19)$$

$$u_{h,\tau} = \varphi(x), \quad t = 0 \text{ on } \bar{\Omega}^h \quad (2.20)$$

$$u_{h,\tau} = \phi(x, t) \text{ on } S_T^h \quad (2.21)$$

for $k = 0, \dots, M' - 1$, where

$$\Psi = f_{P_0}^{k+\frac{1}{2}}, \quad (2.22)$$

$$\Psi^* = f_{P_0}^{k+\frac{1}{2}} - \frac{1}{6} f_{P_A}^{k+\frac{1}{2}}, \quad (2.23)$$

$$\Theta_{h,\tau} u^{k+1} = \left(\frac{1}{\tau} + \frac{2\omega}{h^2} \right) u_{P_0}^{k+1} - \frac{\omega}{3h^2} \sum_{i=1}^6 u_{P_i}^{k+1}, \quad (2.24)$$

$$\Lambda_{h,\tau} u^k = \left(\frac{1}{\tau} - \frac{2\omega}{h^2} \right) u_{P_0}^k + \frac{\omega}{3h^2} \sum_{i=1}^6 u_{P_i}^k, \quad (2.25)$$

$$\begin{aligned} \Theta_{h,\tau}^* u^{k+1} = & \left(\frac{1}{\tau} + \frac{7\omega}{3h^2} \right) u_{P_0}^{k+1} - \frac{\omega}{3h^2} \left(u(p + \eta, x_2, t + \tau) \right. \\ & \left. + u(p, x_2 + \frac{\sqrt{3}}{2}h, t + \tau) + u(p, x_2 - \frac{\sqrt{3}}{2}h, t + \tau) \right), \end{aligned} \quad (2.26)$$

$$\begin{aligned} E_{h,\tau}^* \phi = & \frac{2\omega}{9h^2} \left(\phi(\hat{p}, x_2 + \frac{\sqrt{3}}{2}h, t + \tau) + \phi(\hat{p}, x_2 - \frac{\sqrt{3}}{2}h, t + \tau) \right. \\ & \left. + \phi(\hat{p}, x_2 + \frac{\sqrt{3}}{2}h, t) + \phi(\hat{p}, x_2 - \frac{\sqrt{3}}{2}h, t) \right) \\ & + \left(\frac{1}{6\tau} + \frac{8\omega}{9h^2} \right) \phi(\hat{p}, x_2, t + \tau) + \left(-\frac{1}{6\tau} + \frac{8\omega}{9h^2} \right) \phi(\hat{p}, x_2, t), \end{aligned} \quad (2.27)$$

$$\begin{aligned} \Lambda_{h,\tau}^* u^k = & \left(\frac{1}{\tau} - \frac{7\omega}{3h^2} \right) u_{P_0}^k + \frac{\omega}{3h^2} \left(u(p, x_2 + \frac{\sqrt{3}}{2}h, t) \right. \\ & \left. + u(p, x_2 - \frac{\sqrt{3}}{2}h, t) + u(p + \eta, x_2, t) \right), \end{aligned} \quad (2.28)$$

and,

$$\begin{cases} p = x_1 + \frac{h}{2}, \hat{p} = x_1 - \frac{h}{2}, \eta = \frac{h}{2} \text{ if } P_0 \in \Omega^{*lh}\gamma_\tau, \\ p = x_1 - \frac{h}{2}, \hat{p} = x_1 + \frac{h}{2}, \eta = -\frac{h}{2} \text{ if } P_0 \in \Omega^{*rh}\gamma_\tau. \end{cases} \quad (2.29)$$

2.3.1 The Stability and Convergence Analysis for Difference Problem 1

Theorem 2.1 (Theorem 2 of Buranay and Nouman [22]): The order of approximation of the implicit scheme in Difference Problem 1 is $O(h^2 + \tau^2)$.

Proof. (Proof of Theorem 2 of Buranay and Nouman [22]) Let $(x_1, x_2, t + \tau) \in \Omega^*\gamma_\tau$ be the center of the hexagon (P_0) at time moment $t + \tau$. By the continuity of the solution u , the heat equation (2.9) is also satisfied at the boundary points $(\hat{p}, x_2, t + \frac{\tau}{2})$ denoted by P_A . Therefore, we give $O(h^2 + \tau^2)$ difference approximation of the heat equation (2.9) at $(\hat{p}, x_2, t + \frac{\tau}{2})$ when $\hat{p} = x_1 - \frac{h}{2}$ as

$$\begin{aligned} \frac{u_{h,\tau,P_A}^{k+1} - u_{h,\tau,P_A}^k}{\tau} &= \omega \left(\frac{2}{h^2} \left(u_{h,\tau,P_0}^{k+1} - 2u_{h,\tau,P_A}^{k+1} + u_{h,\tau,P_2}^{k+1} \right) \right. \\ &\quad + \frac{2}{3h^2} \left(u_{h,\tau,P_1}^{k+1} - 2u_{h,\tau,P_A}^{k+1} + u_{h,\tau,P_3}^{k+1} \right) + \frac{2}{h^2} \left(u_{h,\tau,P_0}^k - 2u_{h,\tau,P_A}^k + u_{h,\tau,P_2}^k \right) \\ &\quad \left. + \frac{2}{3h^2} \left(u_{h,\tau,P_1}^k - 2u_{h,\tau,P_A}^k + u_{h,\tau,P_3}^k \right) \right) + f_{P_A}^{k+\frac{1}{2}}. \end{aligned} \quad (2.30)$$

Using the equation (2.30) the following equation can be derived for the sum of the approximate solution at left ghost points P_2 at time moments $t + \tau$, and $t = k\tau$

$$\begin{aligned} u_{h,\tau,P_2}^{k+1} + u_{h,\tau,P_2}^k &= \frac{h^2}{2\tau\omega} u_{h,\tau,P_A}^{k+1} + \frac{8}{3} u_{h,\tau,P_A}^{k+1} - u_{h,\tau,P_0}^{k+1} - \frac{1}{3} u_{h,\tau,P_1}^{k+1} - \frac{1}{3} u_{h,\tau,P_3}^{k+1} - \frac{h^2}{2\tau\omega} u_{h,\tau,P_A}^k \\ &\quad + \frac{8}{3} u_{h,\tau,P_A}^k - u_{h,\tau,P_0}^k - \frac{1}{3} u_{h,\tau,P_1}^k - \frac{1}{3} u_{h,\tau,P_3}^k - \frac{h^2}{2\omega} f_{P_A}^{k+\frac{1}{2}}. \end{aligned} \quad (2.31)$$

Analogously, we use the following difference approximation of the heat equation (2.9)

at the boundary points $(\hat{p}, x_2, t + \frac{\tau}{2})$ when $\hat{p} = x_1 + \frac{h}{2}$

$$\begin{aligned}
\frac{u_{h,\tau,P_A}^{k+1} - u_{h,\tau,P_A}^k}{\tau} &= \omega \left(\frac{2}{h^2} \left(u_{h,\tau,P_0}^{k+1} - 2u_{h,\tau,P_A}^{k+1} + u_{h,\tau,P_5}^{k+1} \right) \right. \\
&+ \frac{2}{3h^2} \left(u_{h,\tau,P_4}^{k+1} - 2u_{h,\tau,P_A}^{k+1} + u_{h,\tau,P_6}^{k+1} \right) + \frac{2}{h^2} \left(u_{h,\tau,P_0}^k - 2u_{h,\tau,P_A}^k + u_{h,\tau,P_5}^k \right) \\
&\left. + \frac{2}{3h^2} \left(u_{h,\tau,P_4}^k - 2u_{h,\tau,P_A}^k + u_{h,\tau,P_6}^k \right) \right) + f_{P_A}^{k+\frac{1}{2}}. \tag{2.32}
\end{aligned}$$

with order of approximation $O(h^2 + \tau^2)$. The sum of the approximate solution at right ghost points P_5 at time moments $t + \tau$, and $t = k\tau$ is obtained from (2.32)

$$\begin{aligned}
u_{h,\tau,P_5}^{k+1} + u_{h,\tau,P_5}^k &= \frac{h^2}{2\tau\omega} u_{h,\tau,P_A}^{k+1} + \frac{8}{3} u_{h,\tau,P_A}^{k+1} - u_{h,\tau,P_0}^{k+1} - \frac{1}{3} u_{h,\tau,P_4}^{k+1} - \frac{1}{3} u_{h,\tau,P_6}^{k+1} - \frac{h^2}{2\tau\omega} u_{h,\tau,P_A}^k \\
&+ \frac{8}{3} u_{h,\tau,P_A}^k - u_{h,\tau,P_0}^k - \frac{1}{3} u_{h,\tau,P_4}^k - \frac{1}{3} u_{h,\tau,P_6}^k - \frac{h^2}{2\omega} f_{P_A}^{k+\frac{1}{2}}. \tag{2.33}
\end{aligned}$$

Using (2.31), (2.33) and (2.18) we obtain the scheme (2.19). Let the error function be $\varepsilon_{h,\tau} = u_{h,\tau} - u$. Then $\varepsilon_{h,\tau}$ satisfies the following difference problem

$$\Theta_{h,\tau} \varepsilon_{h,\tau}^{k+1} = \Lambda_{h,\tau} \varepsilon_{h,\tau}^k + \Psi_1^k \text{ on } \Omega^{0h}\gamma_\tau, \tag{2.34}$$

$$\Theta_{h,\tau}^* \varepsilon_{h,\tau}^{k+1} = \Lambda_{h,\tau}^* \varepsilon_{h,\tau}^k + \Psi_2^k \text{ on } \Omega^{*h}\gamma_\tau, \tag{2.35}$$

$$\varepsilon_{h,\tau} = 0, \quad t = 0 \text{ on } \overline{\Omega}^h, \tag{2.36}$$

$$\varepsilon_{h,\tau} = 0 \text{ on } S_T^h. \tag{2.37}$$

where,

$$\Psi_1^k = \Lambda_{h,\tau} u^k - \Theta_{h,\tau} u^{k+1} + \psi, \tag{2.38}$$

$$\Psi_2^k = \Lambda_{h,\tau}^* u^k - \Theta_{h,\tau}^* u^{k+1} + \psi^*. \tag{2.39}$$

Let $\widehat{\Theta}_{h,\tau}$ be the operator that coincides with $\Theta_{h,\tau}$ for the points in $\Omega^{0h}\gamma_\tau$, and coincides with $\Theta_{h,\tau}^*$ for the points in $\Omega^{*h}\gamma_\tau$. Analogously, let $\widehat{\Lambda}_{h,\tau}$ be the operator that coincides with $\Lambda_{h,\tau}$ for the points in $\Omega^{0h}\gamma_\tau$ and coincides with $\Lambda_{h,\tau}^*$ for the points in $\Omega^{*h}\gamma_\tau$. Further $\widehat{\Psi}^k$ denotes the truncation error Ψ_1^k and Ψ_2^k for the points belonging to $\Omega^{0h}\gamma_\tau$ and $\Omega^{*h}\gamma_\tau$ respectively. Then the system (2.34)-(2.37) can be given as

$$\widehat{\Theta}_{h,\tau}\boldsymbol{\varepsilon}_{h,\tau}^{k+1} = \widehat{\Lambda}_{h,\tau}\boldsymbol{\varepsilon}_{h,\tau}^k + \widehat{\Psi}^k \text{ on } \Omega^h\gamma_\tau, \quad (2.40)$$

$$\boldsymbol{\varepsilon}_{h,\tau} = 0, t = 0 \text{ on } \overline{\Omega}^h, \quad (2.41)$$

$$\boldsymbol{\varepsilon}_{h,\tau} = 0 \text{ on } S_T^h. \quad (2.42)$$

Using Taylor's expansion around the point $(x_1, x_2, t + \frac{\tau}{2})$ and from the assumption that $u \in C_{x,t}^{6+\alpha, 3+\frac{\alpha}{2}}(\overline{Q}_T)$, we obtain the approximation order to be $\widehat{\Psi}^k = O(h^2 + \tau^2)$. Thus, the approximation order for the implicit scheme in Difference Problem 1 is $O(h^2 + \tau^2)$. \square

Next we analyze the stability for the Difference Problem 1 by using spectral method. Let us label the interior grid points in $\Omega^h\gamma_\tau$ by Q_j , $j = 1, 2, \dots, N$ at every time level along spatial variable x_1 (lexicographical ordering). The neighbouring topology of all hexagon centers can be given by the set

$$T = \{(i, j) : \text{if the grid } Q_i \in \text{Patt}(Q_j), i \neq j, 1 \leq i, j \leq N\}, \quad (2.43)$$

and shows the sparsity pattern of the incidence matrix Inc . Thus, the entries of the matrix $Inc \in \mathbb{R}^{N \times N}$ are

$$Inc_{ij} = \begin{cases} 0 & \text{if } (i, j) \notin T, \\ 1 & \text{if } (i, j) \in T. \end{cases} \quad (2.44)$$

The algebraic linear system of equations obtained by the Difference Problem 1 can be given in matrix form:

$$KU^{k+1} = SU^k + \tau \left(F^{k+\frac{1}{2}} + G^{k*} \right), \quad (2.45)$$

where, $K, S \in R^{N \times N}$ are given as

$$K = \left(I + \frac{\omega\tau}{h^2} B \right), \quad S = \left(I - \frac{\omega\tau}{h^2} B \right), \quad (2.46)$$

and

$$B = D_1 - \frac{1}{3} Inc \in R^{N \times N}. \quad (2.47)$$

Here $U^{k+1}, U^k, F^{k+\frac{1}{2}}$ and G^{k*} are vectors of order N and $F^{k+\frac{1}{2}}$ and G^{k*} are obtained by evaluating the heat source function in (2.22), (2.23) at time level $(k + \frac{1}{2})\tau$ and the boundary and initial functions in Difference Problem 1 (2.18)-(2.21) respectively. Also k^* denotes that values at time moments $t + \tau$, and $t = k\tau$ are used and I is the identity matrix, D_1 is a diagonal matrix with entries

$$d_{1,jj} = \begin{cases} 2 & \text{if } Q_j \in \Omega^{0h}\gamma\tau \\ \frac{7}{3} & \text{if } Q_j \in \Omega^{*h}\gamma\tau \end{cases}, \quad j = 1, 2, \dots, N. \quad (2.48)$$

Lemma 2.1 (Lemma 6.2 of Axelsson [31]): Let $K = [k_{ij}]$ be $N \times N$ matrix with $k_{ij} \leq 0$ for all $i \neq j$ and $k_{ii} > 0$. If K is strictly diagonally dominant then K is an M -matrix.

Theorem 2.2 (Theorem 4.9 of Axelsson [31]): If $K = [k_{ij}]$ is strictly diagonally dominant or irreducibly diagonally dominant then K is nonsingular. If in addition its diagonal entries are positive i.e. $k_{ii} > 0$ then $Re(\lambda_s(K)) > 0$ for all eigenvalues λ_s of K .

Lemma 2.2 (Lemma 5 of Buranay and Nouman [22]): a) The matrix B in (2.47) is symmetric positive definite matrix.

b) The matrix K in (2.46) is nonsingular M -matrix and is also symmetric positive definite matrix.

Proof. (Proof of Lemma 5 of Buranay and Nouman [22])

a) Using (2.43) if $Q_i \in \text{Patt}(Q_j)$ for $i \neq j$, $1 \leq i, j \leq N$ this implies that $Q_j \in \text{Patt}(Q_i)$ giving $\text{Inc}^T = \text{Inc}$. Thus, B is symmetric and since hexagonal grid is connected grid in a simply connected polygon Ω , using (2.47) one can easily show that the matrix B is irreducibly diagonally dominant matrix with $b_{ii} > 0$, $i = 1, \dots, N$. Hence by Theorem 2.2, B is positive definite matrix.

b) The main diagonal entries $k_{ii} > 0$, $i = 1, \dots, N$ and $k_{ij} \leq 0$ for $i \neq j$, and $1 \leq i, j \leq N$. Since $k_{ii} > \sum_{j=1, j \neq i}^N |k_{ij}|$ for all $i = 1, 2, \dots, N$, the matrix $K = I + \frac{\omega\tau}{h^2}D_1 - \frac{\omega\tau}{3h^2}\text{Inc}$ is strictly diagonally dominant matrix and Lemma 2.1 implies that K is an M -matrix and it's inverse $K^{-1} \geq 0$. Also $K^T = \left(I + \frac{\omega\tau}{h^2}B\right)^T = K$ and K is symmetric real matrix. Therefore, all eigenvalues λ_s of K are real. Using Theorem 2.2 we obtain that $\text{Re}(\lambda_s(K)) = \lambda_s(K) > 0$ for all eigenvalues λ_s of K thus, K is symmetric positive definite matrix. \square

Theorem 2.3 (Theorem 6 of Buranay and Nouman [22]): The implicit scheme of the Difference Problem 1 is unconditionally stable and the solution $u_{h,\tau}$ converges to the exact solution u of (2.9) - (2.11) with order of accuracy $(h^2 + \tau^2)$.

Proof. (Proof of Theorem 6 of Buranay and Nouman [22]) On the basis of Lemma 2.2, the matrices B and K are symmetric and positive definite matrices. Since K is symmetric K^{-1} is also symmetric and the eigenvalues of K^{-1} satisfy $0 < \lambda_s(K^{-1}) \leq$

$\frac{1}{1 + \frac{\omega\tau}{h^2} \min_{1 \leq s \leq N}(\lambda_s(B))} < 1$ for $\frac{\omega\tau}{h^2} > 0$ and we get $\|K^{-1}\|_2 < 1$. Also

$$\begin{aligned}
(K^{-1}S)^T &= SK^{-1} = \left(I - \frac{\omega\tau}{h^2}B\right) \left(I + \frac{\omega\tau}{h^2}B\right)^{-1} \\
&= \frac{1}{\det\left(I + \frac{\omega\tau}{h^2}B\right)} \left(I - \frac{\omega\tau}{h^2}B\right) \text{Adj}\left(I + \frac{\omega\tau}{h^2}B\right) \\
&= \left(I + \frac{\omega\tau}{h^2}B\right)^{-1} \left[I - \frac{1}{\det\left(I + \frac{\omega\tau}{h^2}B\right)} \left(I + \frac{\omega\tau}{h^2}B\right) \right. \\
&\quad \left. \left(\frac{\omega\tau}{h^2}B\right) \text{Adj}\left(I + \frac{\omega\tau}{h^2}B\right) \right] \\
&= \left(I + \frac{\omega\tau}{h^2}B\right)^{-1} \left(I - \frac{\omega\tau}{h^2}B\right) = K^{-1}S. \tag{2.49}
\end{aligned}$$

where, $\det\left(I + \frac{\omega\tau}{h^2}B\right)$ and $\text{Adj}\left(I + \frac{\omega\tau}{h^2}B\right)$ are the determinant and the adjoint matrix of $K = I + \frac{\omega\tau}{h^2}B$, respectively. Thus $K^{-1}S$ is real symmetric matrix therefore, the eigenvalues $\lambda_s(K^{-1}S)$ are real. Using Gershgorin Theorem for the estimation of the spectrum of the matrix B gives

$$0 < \lambda_s(B) \leq 4. \tag{2.50}$$

Since B is symmetric positive definite matrix, it follows that $B = P^T D P$ with P orthogonal and D diagonal matrix of eigenvalues $\lambda_s(B)$. Then $K = I + \frac{\omega\tau}{h^2}B = P^T \left(I + \frac{\omega\tau}{h^2}D\right) P$ and $K^{-1} = P^T \left(I + \frac{\omega\tau}{h^2}D\right)^{-1} P$ and

$$K^{-1}S = P^T \left(I + \frac{\omega\tau}{h^2}D\right)^{-1} P P^T \left(I - \frac{\omega\tau}{h^2}D\right) P \tag{2.51}$$

that is the matrix $K^{-1}S$ is similar to $\left(I + \frac{\omega\tau}{h^2}D\right)^{-1} \left(I - \frac{\omega\tau}{h^2}D\right)$ so from (2.49) we get

$$\begin{aligned}
\|K^{-1}S\|_2 &= \rho(K^{-1}S) = \max_{1 \leq s \leq N} \left| \lambda_s \left(\left(I + \frac{\omega\tau}{h^2}D\right)^{-1} \left(I - \frac{\omega\tau}{h^2}D\right) \right) \right| \\
&\leq \left| \frac{1 - \frac{\omega\tau}{h^2} \min_{1 \leq s \leq N}(\lambda_s(B))}{1 + \frac{\omega\tau}{h^2} \min_{1 \leq s \leq N}(\lambda_s(B))} \right| < 1 \text{ for } \frac{\omega\tau}{h^2} > 0. \tag{2.52}
\end{aligned}$$

Using (2.52) and by induction follows that

$$\begin{aligned}
\|U^{k+1}\|_2 &\leq \|K^{-1}S\|_2 \|U^k\|_2 + \tau \|K^{-1}\|_2 \left(\|F^{k+\frac{1}{2}}\|_2 + \|G^{k*}\|_2 \right) \\
&\leq \|U^0\|_2 + \tau \sum_{k'=0}^k \left(\|F^{k'+\frac{1}{2}}\|_2 + \|G^{k'*}\|_2 \right). \tag{2.53}
\end{aligned}$$

Since $K^{-1}S$ is real symmetric matrix it is also normal matrix hence, Von Neumann condition for stability is sufficient as well as necessary for stability (see Lax and Richtmyer [32]). Therefore, equation (2.53) yields that the implicit scheme in Difference Problem 1 is unconditionally stable. The error function $\epsilon_{h,\tau}$ satisfying (2.40)-(2.42) can be given in the matrix form (2.45) at time level $t = (k+1)\tau$ as

$$KE^{k+1} = SE^k + \tau \widehat{\Psi}^k. \tag{2.54}$$

where, E is vector of order N . Thus, from Theorem 2.1 and (2.53), (2.54) we have

$$\|E^{k+1}\|_2 \leq \tau \sum_{k'=0}^k \|\widehat{\Psi}^{k'}\|_2 \leq c_1 (h^2 + \tau^2), \tag{2.55}$$

where, c_1 is positive constant independent from h and τ and depends on the bounded derivatives of the solution u of the form (2.1) of at most sixth order in the truncation error $\widehat{\Psi}^k$ as given in (2.38) and (2.39). Let

$\|\epsilon_{h,\tau}^{k+1}\|_C = \max_{\Omega^h \gamma_\tau \cap \{t=(k+1)\tau\}} |\epsilon_{h,\tau}^{k+1}| = \|E^{k+1}\|_\infty$, then on the basis of norm concordance and using (2.55) we get

$$\|\epsilon_{h,\tau}^{k+1}\|_C \leq \|E^{k+1}\|_2 \leq c_1 (h^2 + \tau^2). \tag{2.56}$$

Therefore, the solution $u_{h,\tau}$ converges to the exact solution u with order of accuracy $(h^2 + \tau^2)$. □

2.4 Fourth Order Accurate Implicit Difference Problem

Let $f_{P_0}^{k+1} = f(x_1, x_2, t + \tau)$, $f_{P_A}^{k+1} = f(\hat{p}, x_2, t + \tau)$ and $f_{P_A}^k = f(\hat{p}, x_2, t)$ where, \hat{p} is as defined in (2.29). Analogously $\partial_{x_1}^2 f_{P_0}^{k+1} = \frac{\partial^2 f}{\partial x_1^2} \Big|_{(x_1, x_2, t + \tau)}$ and $\partial_{x_2}^2 f_{P_0}^{k+1} = \frac{\partial^2 f}{\partial x_2^2} \Big|_{(x_1, x_2, t + \tau)}$.

We give the following difference problem for the solution of the given BVP1.

Difference Problem 2

$$\tilde{\Theta}_{h,\tau} u_{h,\tau}^{k+1} = \tilde{\Lambda}_{h,\tau} u_{h,\tau}^k + \tilde{\Psi} \text{ on } \Omega^{0h}\gamma_\tau, \quad (2.57)$$

$$\tilde{\Theta}_{h,\tau}^* u_{h,\tau}^{k+1} = \tilde{\Lambda}_{h,\tau}^* u_{h,\tau}^k + \tilde{E}_{h,\tau}^* \phi + \tilde{\Psi}^* \text{ on } \Omega^{*h}\gamma_\tau, \quad (2.58)$$

$$u_{h,\tau} = \varphi(x), \quad t = 0 \text{ on } \bar{\Omega}^h, \quad (2.59)$$

$$u_{h,\tau} = \phi(x, t) \text{ on } S_T^h, \quad (2.60)$$

$k = 0, \dots, M' - 1$, where

$$\tilde{\Psi} = f_{P_0}^{k+1} + \frac{1}{16} h^2 \left(\partial_{x_1}^2 f_{P_0}^{k+1} + \partial_{x_2}^2 f_{P_0}^{k+1} \right), \quad (2.61)$$

$$\begin{aligned} \tilde{\Psi}^* &= \frac{h^2}{96\tau\omega} f_{P_A}^{k+1} - \frac{h^2}{96\tau\omega} f_{P_A}^k - \frac{1}{6} f_{P_A}^{k+1} + f_{P_0}^{k+1} \\ &\quad + \frac{1}{16} h^2 \left(\partial_{x_1}^2 f_{P_0}^{k+1} + \partial_{x_2}^2 f_{P_0}^{k+1} \right) \end{aligned} \quad (2.62)$$

$$\tilde{\Theta}_{h,\tau} u^{k+1} = \left(\frac{3}{4\tau} + \frac{4\omega}{h^2} \right) u_{P_0}^{k+1} + \left(\frac{1}{24\tau} - \frac{2\omega}{3h^2} \right) \sum_{i=1}^6 u_{P_i}^{k+1}, \quad (2.63)$$

$$\tilde{\Lambda}_{h,\tau} u^k = \frac{3}{4\tau} u_{P_0}^k + \frac{1}{24\tau} \sum_{i=1}^6 u_{P_i}^k \quad (2.64)$$

$$\begin{aligned} \tilde{\Theta}_{h,\tau}^* u^{k+1} &= \left(\frac{17}{24\tau} + \frac{14\omega}{3h^2} \right) u_{P_0}^{k+1} + \left(\frac{1}{24\tau} - \frac{2\omega}{3h^2} \right) \left(u(p, x_2 + \frac{\sqrt{3}}{2}h, t + \tau) \right. \\ &\quad \left. + u(p, x_2 - \frac{\sqrt{3}}{2}h, t + \tau) + u(p + \eta, x_2, t + \tau) \right), \end{aligned} \quad (2.65)$$

$$\begin{aligned}
\tilde{E}_{h,\tau}^* \phi &= \left(-\frac{1}{36\tau} + \frac{4\omega}{9h^2} \right) \left(\phi(\hat{p}, x_2 + \frac{\sqrt{3}}{2}h, t + \tau) + \phi(\hat{p}, x_2 - \frac{\sqrt{3}}{2}h, t + \tau) \right) \\
&+ \left(\frac{1}{18\tau} + \frac{16\omega}{9h^2} \right) \phi(\hat{p}, x_2, t + \tau) + \frac{1}{36\tau} \left(\phi(\hat{p}, x_2 + \frac{\sqrt{3}}{2}h, t) \right. \\
&\left. + \phi(\hat{p}, x_2 - \frac{\sqrt{3}}{2}h, t) \right) - \frac{1}{18\tau} \phi(\hat{p}, x_2, t), \tag{2.66}
\end{aligned}$$

$$\begin{aligned}
\tilde{\Lambda}_{h,\tau}^* u^k &= \frac{17}{24\tau} u_{P_0}^k + \frac{1}{24\tau} \left(u(p, x_2 + \frac{\sqrt{3}}{2}h, t) \right. \\
&\left. + u(p, x_2 - \frac{\sqrt{3}}{2}h, t) + u(p + \eta, x_2, t) \right), \tag{2.67}
\end{aligned}$$

and p, \hat{p}, η are as defined in (2.29).

We remark that $\tilde{\Psi}$ in (2.61) can be taken as (see also Lee et al. [19])

$$\tilde{\Psi} = \frac{3}{4} f_{P_0}^{k+1} + \frac{1}{24} \sum_{i=1}^6 f_{P_i}^{k+1}. \tag{2.68}$$

2.4.1 The Stability and Convergence Analysis of Difference Problem 2

Theorem 2.4 (Theorem 7 of Buranay and Nouman [22]): The order of approximation of the implicit scheme in Difference Problem 2 is $O(h^4 + \tau)$.

Proof. (Proof of Theorem 7 of Buranay and Nouman [22]) Let $(x_1, x_2, t + \tau) \in \Omega^{*lh}\gamma_\tau$ be the center of the hexagon (P_0) at time level $t + \tau$. The heat equation (2.9) is also satisfied at the boundary points $(\hat{p}, x_2, t + \tau)$ and (\hat{p}, x_2, t) where, $\hat{p} = x_1 - \frac{h}{2}$. We give the difference approximation of the heat equation (2.9) at these boundary points (P_A)

$$\begin{aligned}
\frac{u_{h,\tau,P_A}^{k+1} - u_{h,\tau,P_A}^k}{\tau} &= \omega \left(\frac{4}{h^2} \left(u_{h,\tau,P_0}^{k+1} - 2u_{h,\tau,P_A}^{k+1} + u_{h,\tau,P_2}^{k+1} \right) \right. \\
&\left. + \frac{4}{3h^2} \left(u_{h,\tau,P_1}^{k+1} - 2u_{h,\tau,P_A}^{k+1} + u_{h,\tau,P_3}^{k+1} \right) \right) + f_{P_A}^{k+1}. \tag{2.69}
\end{aligned}$$

$$\begin{aligned}
\frac{u_{h,\tau,P_A}^{k+1} - u_{h,\tau,P_A}^k}{\tau} &= \omega \left(\frac{4}{h^2} \left(u_{h,\tau,P_0}^k - 2u_{h,\tau,P_A}^k + u_{h,\tau,P_2}^k \right) \right. \\
&\left. + \frac{4}{3h^2} \left(u_{h,\tau,P_1}^k - 2u_{h,\tau,P_A}^k + u_{h,\tau,P_3}^k \right) \right) + f_{P_A}^k. \tag{2.70}
\end{aligned}$$

respectively, both with order of approximation $O(h^2 + \tau)$. For the left ghost points from the equation (2.69) we get.

$$\begin{aligned} u_{h,\tau,P_2}^{k+1} &= \left(\frac{h^2}{4\tau\omega} + \frac{8}{3} \right) u_{h,\tau,P_A}^{k+1} - \frac{h^2}{4\tau\omega} u_{h,\tau,P_A}^k - u_{h,\tau,P_0}^{k+1} - \frac{1}{3} u_{h,\tau,P_1}^{k+1} \\ &\quad - \frac{1}{3} u_{h,\tau,P_3}^{k+1} - \frac{h^2}{4\omega} f_{P_A}^{k+1}, \end{aligned} \quad (2.71)$$

and from (2.70) results

$$u_{h,\tau,P_2}^k = \frac{h^2}{4\tau\omega} u_{h,\tau,P_A}^{k+1} + \left(\frac{8}{3} - \frac{h^2}{4\tau\omega} \right) u_{h,\tau,P_A}^k - u_{h,\tau,P_0}^k - \frac{1}{3} u_{h,\tau,P_1}^k - \frac{1}{3} u_{h,\tau,P_3}^k - \frac{h^2}{4\omega} f_{P_A}^k. \quad (2.72)$$

Analogously, when $(x_1, x_2, t + \tau) \in \Omega^{*rh}\gamma_\tau$ for the right ghost points approximation we obtain

$$\begin{aligned} u_{h,\tau,P_5}^{k+1} &= \left(\frac{h^2}{4\tau\omega} + \frac{8}{3} \right) u_{h,\tau,P_A}^{k+1} - \frac{h^2}{4\tau\omega} u_{h,\tau,P_A}^k - u_{h,\tau,P_0}^{k+1} - \frac{1}{3} u_{h,\tau,P_4}^{k+1} \\ &\quad - \frac{1}{3} u_{h,\tau,P_6}^{k+1} - \frac{h^2}{4\omega} f_{P_A}^{k+1}. \end{aligned} \quad (2.73)$$

$$\begin{aligned} u_{h,\tau,P_5}^k &= \frac{h^2}{4\tau\omega} u_{h,\tau,P_A}^{k+1} + \left(\frac{8}{3} - \frac{h^2}{4\tau\omega} \right) u_{h,\tau,P_A}^k - u_{h,\tau,P_0}^k - \frac{1}{3} u_{h,\tau,P_4}^k \\ &\quad - \frac{1}{3} u_{h,\tau,P_6}^k - \frac{h^2}{4\omega} f_{P_A}^k. \end{aligned} \quad (2.74)$$

Using (2.71)-(2.74) and (2.57) we obtain the scheme (2.58). Let the error function be

$\varepsilon_{h,\tau} = u_{h,\tau} - u$. Then $\varepsilon_{h,\tau}$ satisfies the following difference problem

$$\tilde{\Theta}_{h,\tau} \varepsilon_{h,\tau}^{k+1} = \tilde{\Lambda}_{h,\tau} \varepsilon_{h,\tau}^k + \tilde{\Psi}_1^k \text{ on } \Omega^{0h}\gamma_\tau, \quad (2.75)$$

$$\tilde{\Theta}_{h,\tau}^* \varepsilon_{h,\tau}^{k+1} = \tilde{\Lambda}_{h,\tau}^* \varepsilon_{h,\tau}^k + \tilde{\Psi}_2^k \text{ on } \Omega^{*h}\gamma_\tau, \quad (2.76)$$

$$\varepsilon_{h,\tau} = 0, \quad t = 0 \text{ on } \bar{\Omega}^h, \quad (2.77)$$

$$\varepsilon_{h,\tau} = 0 \text{ on } S_T^h, \quad (2.78)$$

where,

$$\tilde{\Psi}_1^k = \tilde{\Lambda}_{h,\tau} u^k - \tilde{\Theta}_{h,\tau} u^{k+1} + \tilde{\Psi}, \quad (2.79)$$

$$\tilde{\Psi}_2^k = \tilde{\Lambda}_{h,\tau}^* u^k - \tilde{\Theta}_{h,\tau}^* u^{k+1} + \tilde{\Psi}^*. \quad (2.80)$$

Let $\widehat{\Theta}_{h,\tau}$ be the operator that coincides with $\tilde{\Theta}_{h,\tau}$ for the points in $\Omega^{0h}\gamma_\tau$, and coincides with $\tilde{\Theta}_{h,\tau}^*$ for the points in $\Omega^{*h}\gamma_\tau$. Analogously, let $\widehat{\Lambda}_{h,\tau}$ be the operator that coincides with $\tilde{\Lambda}_{h,\tau}$ for the points in $\Omega^{0h}\gamma_\tau$ and coincides with $\tilde{\Lambda}_{h,\tau}^*$ for the points in $\Omega^{*h}\gamma_\tau$. Also $\widehat{\Psi}^k$ denotes the truncation error $\tilde{\Psi}_1^k$ and $\tilde{\Psi}_2^k$ for the points belonging to $\Omega^{0h}\gamma_\tau$ and $\Omega^{*h}\gamma_\tau$ respectively. Then the system (2.75)-(2.78) can be given as

$$\widehat{\Theta}_{h,\tau} \varepsilon_{h,\tau}^{k+1} = \widehat{\Lambda}_{h,\tau} \varepsilon_{h,\tau}^k + \widehat{\Psi}^k \text{ on } \Omega^h \gamma_\tau, \quad (2.81)$$

$$\varepsilon_{h,\tau} = 0, \quad t = 0 \text{ on } \overline{\Omega}^h, \quad (2.82)$$

$$\varepsilon_{h,\tau} = 0 \text{ on } S_T^h. \quad (2.83)$$

Using Taylor's expansion at the point $(x_1, x_2, t + \tau)$ and from the assumption that $u \in C_{x,t}^{6+\alpha, 3+\frac{\alpha}{2}}(\overline{Q}_T)$ we obtain $\widehat{\Psi} = O(h^4 + \tau)$ order of the approximation. Therefore, the order of approximation of the implicit scheme in Difference Problem 2 (2.57)-(2.60) is $O(h^4 + \tau)$. \square

The algebraic linear system of equations obtained by the Difference Problem 2 can be presented in matrix form

$$\tilde{K}U^{k+1} = \tilde{S}U^k + \tau(\tilde{F}^{k*} + \tilde{G}^{k*}), \quad (2.84)$$

where, $\tilde{K}, \tilde{S} \in R^{N \times N}$ are given as

$$\tilde{K} = \left(\tilde{D}_1 + \frac{1}{24} Inc + \frac{\omega\tau}{h^2} \tilde{B} \right), \quad \tilde{S} = \left(\tilde{D}_1 + \frac{1}{24} Inc \right), \quad (2.85)$$

$$\tilde{B} = \tilde{D}_2 - \frac{2}{3} Inc \in R^{N \times N}. \quad (2.86)$$

\tilde{F}^{k*} and \tilde{G}^{k*} are vectors of order N obtained by evaluating the heat source function f

in (2.61), (2.62) and the boundary and initial function values in Difference Problem 2 (2.57)-(2.60) respectively. Also k^* denotes that values from $(k+1)\tau$ and $k\tau$ are used and \tilde{D}_1, \tilde{D}_2 are diagonal matrices with entries

$$\tilde{d}_{1,jj} = \begin{cases} \frac{3}{4} & \text{if } Q_j \in \Omega^{0h}\gamma\tau \\ \frac{17}{24} & \text{if } Q_j \in \Omega^{*h}\gamma\tau \end{cases}, \quad j = 1, 2, \dots, N, \quad (2.87)$$

$$\tilde{d}_{2,jj} = \begin{cases} 4 & \text{if } Q_j \in \Omega^{0h}\gamma\tau \\ \frac{14}{3} & \text{if } Q_j \in \Omega^{*h}\gamma\tau \end{cases}, \quad j = 1, 2, \dots, N, \quad (2.88)$$

respectively.

Lemma 2.3 (Lemma 8 of Buranay and Nouman [22]): The matrices \tilde{K}, \tilde{S} in (2.85) and \tilde{B} in (2.86) are symmetric positive definite matrices.

Proof. (Proof of Lemma 8 of Buranay and Nouman [22]) The matrix \tilde{S} is nonnegative and strictly diagonally dominant matrix and \tilde{B} is irreducibly diagonally dominant matrices with positive main diagonal entries. Since Inc is symmetric we get \tilde{B}, \tilde{S} are also symmetric. Thus, Theorem 2.2 implies that \tilde{B}, \tilde{S} have positive eigenvalues. Therefore \tilde{B}, \tilde{S} are symmetric positive definite matrices. Using $\tilde{K} = \tilde{S} + \frac{\omega\tau}{h^2}\tilde{B}$ and that the sum of two symmetric positive definite matrices is symmetric positive definite gives \tilde{K} is symmetric positive definite. \square

On the basis of Lemma 2.3, \tilde{S} is invertible and algebraic linear system (2.84) can be rewritten as

$$\tilde{A}U^{k+1} = U^k + \tau\tilde{S}^{-1}(\tilde{F}^{k*} + \tilde{G}^{k*}), \quad (2.89)$$

$$\tilde{A} = I + \frac{\omega\tau}{h^2}\tilde{S}^{-1}\tilde{B}. \quad (2.90)$$

Lemma 2.4 (Lemma 9 of Buranay and Nouman [22]): The matrix \tilde{A} in (2.90) is symmetric positive definite.

Proof. (Proof of Lemma 9 of Buranay and Nouman [22]) $\tilde{S} = I - \frac{1}{16}\tilde{B}$ and \tilde{B} have the same basis vectors spanning their eigenspaces therefore on the basis of Lemma 2.3 and using that every real symmetric matrix is orthogonal equivalent to a real diagonal matrix we have $\tilde{S} = P^T \Delta_1 P$ and $\tilde{B} = P^T \Delta_2 P$ where Δ_1 and Δ_2 are diagonal matrices and P is orthogonal matrix of which the columns are the normalized basis vectors spanning the eigenspaces of \tilde{S} and \tilde{B} . From $\Delta_1^{-1} \Delta_2 = \Delta_2 \Delta_1^{-1}$ it follows that

$$\tilde{S}^{-1} \tilde{B} = \left(P^T \Delta_1^{-1} P \right) P^T \Delta_2 P = P^T \Delta_2 \Delta_1^{-1} P = \left(\tilde{S}^{-1} \tilde{B} \right)^T. \quad (2.91)$$

So $\tilde{S}^{-1} \tilde{B}$ is symmetric, thus $\tilde{S}^{-1} \tilde{B}$ commutes. Since the product of two symmetric positive definite matrices that commute is also symmetric positive definite (see Axelsson [31] and Taussky [33]) gives $\lambda_s \left(\tilde{S}^{-1} \tilde{B} \right) > 0$ as:

$$\tilde{S}^{-1} \tilde{B} = \tilde{S}^{-1} \tilde{B}^{\frac{1}{2}} \tilde{B}^{\frac{1}{2}} = \tilde{B}^{-\frac{1}{2}} \tilde{B}^{\frac{1}{2}} \tilde{S}^{-1} \tilde{B}^{\frac{1}{2}} \tilde{B}^{\frac{1}{2}}, \quad (2.92)$$

that is $\tilde{S}^{-1} \tilde{B}$ is similar to the symmetric matrix $\tilde{B}^{\frac{1}{2}} \tilde{S}^{-1} \tilde{B}^{\frac{1}{2}}$. Using that

$$x^T \tilde{B}^{\frac{1}{2}} \tilde{S}^{-1} \tilde{B}^{\frac{1}{2}} x = z^T \tilde{S}^{-1} z > 0, \quad (2.93)$$

for every $z = \tilde{B}^{\frac{1}{2}} x \neq 0$. Thus, the eigenvalues $\lambda_s \left(\tilde{B}^{\frac{1}{2}} \tilde{S}^{-1} \tilde{B}^{\frac{1}{2}} \right) > 0$ implying that $\lambda_s \left(\tilde{S}^{-1} \tilde{B} \right) > 0$ and $\lambda_s \left(\tilde{A} \right) > 0$. \square

Theorem 2.5: Theorem 10 of Buranay and Nouman [22] The implicit scheme of the Difference Problem 2 is unconditionally stable and the solution $u_{h,\tau}$ converges to the exact solution u of (2.9) - (2.11) with order of accuracy $O(h^4 + \tau)$.

Proof. (Proof of Theorem 10 of Buranay and Nouman [22]) using (2.90) and Lemma 2.4 implies that

$$0 < \lambda_s(\tilde{A}^{-1}) \leq \frac{1}{1 + \frac{\omega\tau}{h^2} \min_{1 \leq s \leq N} (\lambda_s(\tilde{S}^{-1}\tilde{B}))} < 1, \quad (2.94)$$

for $\frac{\omega\tau}{h^2} > 0$ and since \tilde{A} is symmetric matrix \tilde{A}^{-1} is also symmetric matrix, therefore $\|\tilde{A}^{-1}\|_2 < 1$. Also using (2.85)-(2.90) and the Gershgorin Theorem to estimate the spectrum of \tilde{B} we get $0 < \lambda_s(\tilde{B}) \leq 8$, and $\|(\tilde{K})^{-1}\|_2 = \|(\tilde{S}\tilde{A})^{-1}\|_2 \leq 2$. Multiplying both sides of (2.89) by \tilde{A}^{-1} and taking second norm and by using norm properties and induction gives

$$\begin{aligned} \|U^{k+1}\|_2 &\leq \|U^k\|_2 + 2\tau \left(\|\tilde{F}^{k*}\|_2 + \|\tilde{G}^{k*}\|_2 \right) \\ &\leq \|U^0\|_2 + 2\tau \sum_{k'=1}^k \left(\|\tilde{F}^{k'*}\|_2 + \|\tilde{G}^{k'*}\|_2 \right). \end{aligned} \quad (2.95)$$

Hence, the inequality (2.94) gives the Von Neumann necessary condition for stability. Since \tilde{A} is real symmetric matrix it is also normal matrix and the condition (2.94) is as well as the sufficient condition for stability (see Lax and Richtmyer [32]). Therefore, equation (2.95) yields that the implicit scheme (2.57), (2.58) is unconditionally stable. The error function $\epsilon_{h,\tau}$ satisfying (2.81)-(2.83) can be given in the matrix form (2.89) at time level $t = (k+1)\tau$ as

$$\tilde{A}E^{k+1} = E^k + \tau\tilde{S}^{-1}\widehat{\Psi}^k. \quad (2.96)$$

where, E is vector of order N . Thus, from Theorem 2.4 and (2.95), (2.96) we have

$$\|E^{k+1}\|_2 \leq 2\tau \sum_{k'=0}^k \|\widehat{\Psi}^{k'}\|_2 \leq c_2 (h^4 + \tau), \quad (2.97)$$

where, c_2 is positive constant independent from h and τ and depends on the bounded

derivatives of the solution u of the form (2.1) of at most sixth order in the truncation error $\widehat{\Psi}^k$ as given in (2.79) and (2.80). Using norm concordance and the inequality (2.97) we get

$$\left\| \boldsymbol{\varepsilon}_{h,\tau}^{k+1} \right\|_C \leq \left\| E^{k+1} \right\|_2 \leq c_2 (h^4 + \tau). \quad (2.98)$$

Hence, the solution $u_{h,\tau}$ converges to the exact solution u on the hexagonal grids with accuracy order of $(h^4 + \tau)$. □

Chapter 3

IMPLICIT METHOD OF HIGH ACCURACY ON HEXAGONAL GRIDS FOR APPROXIMATING THE SOLUTION TO HEAT EQUATION ON RECTANGLE

3.1 Introduction

In this chapter, we give a highly accurate two layer Implicit method on hexagonal grids for approximating the solution to first type boundary value problem of heat equation

$$\frac{\partial u}{\partial t} = \omega \left(\frac{\partial^2 u}{\partial x_1^2} + \frac{\partial^2 u}{\partial x_2^2} \right) - bu + f(x_1, x_2, t) \quad (3.1)$$

on rectangle where, $\omega > 0$, $b \geq 0$ are constants. For the hexagonal grids that have centers $\frac{h}{2}$ units away from the sides of the rectangle at time moment t , which has a neighboring point in the pattern emerging through these sides a special scheme is given. In Section 3.2, we give the boundary value problem of 1st type for the heat equation in (3.1) on a rectangle D under the assumption that the heat source and the initial and boundary functions are given such that on $\bar{Q}_T = \bar{D} \times [0, T]$ the solution belongs to the Hölder space $C_{x,t}^{6+\alpha, 3+\frac{\alpha}{2}}(\bar{Q}_T)$, $0 < \alpha < 1$. Hexagonal grid structure and basic notations are also given. In Section 3.3, a two layer symmetric implicit difference scheme with 14-point on hexagonal grid is proposed and it is proved that this scheme is unconditionally stable and the solution of the given difference problem converges to the exact solution with $O(h^4 + \tau^2)$ order of accuracy on the grids. Here h and $\frac{\sqrt{3}}{2}h$ are the step sizes in space variables x_1 and x_2 respectively and τ being the time step

size. Chapter 4 presents the numerical experiments justifying the obtained theoretical results. Three test problems are constructed of which for the Example 4.4 and Example 4.5 the constant b in (3.1) is zero and also the exact solution of Example 4.5 is not given, and in Example 4.6 the constant b is nonzero. Moreover, for Example 4.4 and Example 4.5 ($b = 0$), the obtained results are compared with the numerical results obtained by the two layer implicit scheme with 14-point on rectangular grids derived by using the 9-point scheme approximation to the Laplacian operator Samarskii [34]. This scheme is also unconditionally stable and has the order of convergence $O(|h|^4 + \tau^2)$ where, $h = \sqrt{h_1^2 + h_2^2}$ and h_1 and h_2 are the step sizes along the spatial variables x_1 and x_2 respectively. We applied incomplete block preconditioning (see Concus et al. [35], Axelsson [36], and Buranay and Iyikal [37]) for the conjugate gradient method to solve the obtained algebraic system of equations in all the examples. Accordingly, it is numerically shown that the proposed scheme is computationally more economical than the 14-point implicit scheme on rectangular grids when the block preconditioning of the conjugate gradient method is used, and approximates more general heat equation in the form (3.1) when b is positive constant as well.

3.2 First Type Problem on Rectangle and Basic Notations

Let $D = \{(x_1, x_2) : 0 < x_1 < a_1, 0 < x_2 < a_2\}$ be an open rectangle where, a_2 is multiple of $\sqrt{3}$ and let v_j , $j = 1, 2, 3, 4$, be its sides. Further, let $S = \bigcup_{j=1}^4 v_j$ be the boundary of D and denote by $\bar{D} = D \cup S$ the closure of D . Let $Q_T = D \times (0, T)$, with lateral surface S_T more accurately the set of points (x, t) , $x = (x_1, x_2) \in S$ and $t \in [0, T]$ also \bar{Q}_T shows the closure of Q_T . We give the boundary value problem of first type for the two space dimensional heat equation BVP2:

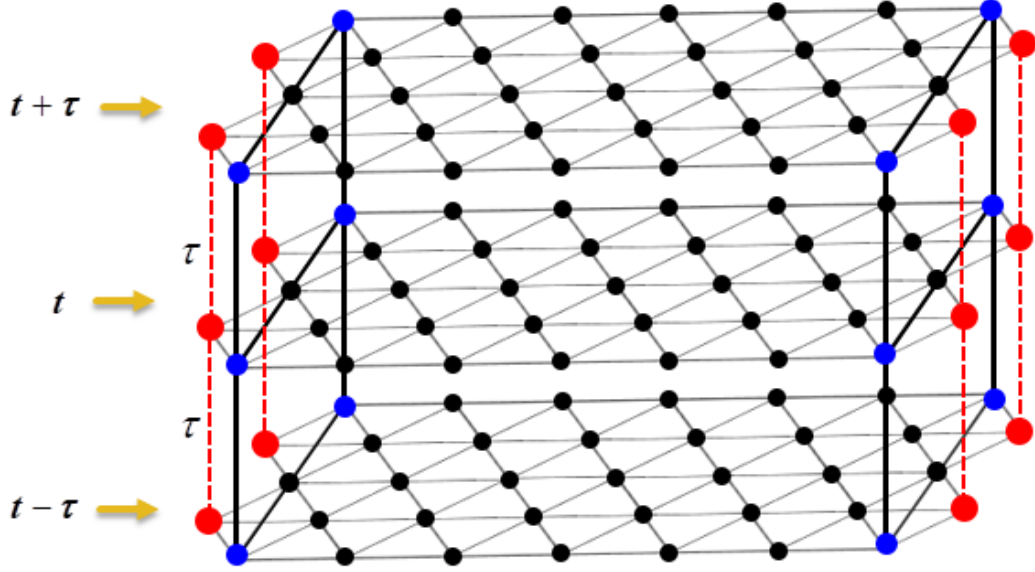


Figure 3.1: Hexagonal grid structure and ghost points on rectangle

$$\frac{\partial u}{\partial t} = \omega \left(\frac{\partial^2 u}{\partial x_1^2} + \frac{\partial^2 u}{\partial x_2^2} \right) - bu + f(x_1, x_2, t) \text{ on } Q_T, \quad (3.2)$$

$$u(x_1, x_2, 0) = \varphi(x_1, x_2) \text{ on } \bar{\Omega}, \quad (3.3)$$

$$u(x_1, x_2, t) = \phi(x_1, x_2, t) \text{ on } S_T, \quad (3.4)$$

where, $\omega > 0$ and $b \geq 0$ are constant. We assume that the heat source function $f(x_1, x_2, t)$ and the initial and boundary functions $\varphi(x_1, x_2)$ and $\phi(x_1, x_2, t)$ respectively, are given such that the problem (3.2)-(3.4) has unique solution u belonging to the Hölder class $C_{x,t}^{6+\alpha, 3+\frac{\alpha}{2}}(\bar{Q}_T)$. Let $h > 0$, with $h = a_1/N_1$, where N_1 is positive integer and assign D^h a hexagonal grid on D , with step size h , defined as the set of nodes

$$D^h = \left\{ x = (x_1, x_2) \in D : x_1 = \frac{i' - j'}{2}h, x_2 = \frac{\sqrt{3}(i' + j')}{2}h, \right. \\ \left. i' = 1, 2, \dots; j' = 0 \pm 1 \pm 2, \dots \right\} \quad (3.5)$$

Let $v_j^h, j = 1, \dots, 4$ be the set of nodes on the interior of v_j and let $\widehat{v}_j^h = v_{j-1} \cap v_j$ be the j -th vertex of D , $S^h = \bigcup_{j=1}^4 (v_j \cup \widehat{v}_j^h)$, $\overline{D}^h = D^h \cup S^h$. Further, let D^{*lh}, D^{*rh} denote the set of interior nodes whose distance from the boundary is $\frac{h}{2}$ and the hexagon has a left ghost point or a right ghost point respectively, emerging through the side of the rectangle. We also denote by $D^{*h} = D^{*lh} \cup D^{*rh}$ and $D^{0h} = D^h \setminus D^{*h}$.

Next, let the set of internal nodes and lateral surface nodes be defined by

$$D^h \gamma_\tau = D^h \times \gamma_\tau = \left\{ (x, t) : x \in D^h, t \in \gamma_\tau \right\}, \quad (3.6)$$

$$S_T^h = S^h \times \overline{\gamma}_\tau = \left\{ (x, t) : x \in S^h, t \in \overline{\gamma}_\tau \right\}. \quad (3.7)$$

respectively, where γ_τ and $\overline{\gamma}_\tau$ are same as given in (2.13) and (2.14) respectively. Let $D^{*lh} \gamma_\tau = D^{*lh} \times \gamma_\tau \subset D^h \gamma_\tau$ and $D^{*rh} \gamma_\tau = D^{*rh} \times \gamma_\tau \subset D^h \gamma_\tau$ and $D^{*h} \gamma_\tau = D^{*lh} \gamma_\tau \cup D^{*rh} \gamma_\tau$, also $D^{0h} \gamma_\tau = D^h \gamma_\tau \setminus D^{*h} \gamma_\tau$. Figure 3.1 shows the hexagonal grid covering of the rectangle D for three time levels $t - \tau, t$ and $t + \tau$.

3.3 Implicit Method of High Accuracy for the Solution of Problem (3.2)-(3.4)

Let P_0 denote the center of the hexagon and $Patt(P_0)$ denote the pattern of the hexagon consisting the neighboring points $P_i, i = 1, \dots, 6$. Also $u_{P_i}^{k+1}$ denotes the exact solution at the point P_i and $u_{P_A}^{k+1}$ denotes the value at the boundary point for the time moment $t + \tau$ same as given in (2.17). Analogously, the values $u_{P_i}^k, i = 0, \dots, 6$ and $u_{P_A}^k$ present the exact solution at the same space coordinates of $P_i, i = 0, \dots, 6$ and P_A respectively, but at time level $t = k\tau$. Further, $u_{h,\tau,P_i}^{k+1}, i = 0, \dots, 6, u_{h,\tau,P_A}^{k+1}$, and $u_{h,\tau,P_i}^k, i = 0, \dots, 6, u_{h,\tau,P_A}^k$

present the numerical solution at the same space coordinates of P_i , $i = 0, \dots, 6$ and P_A for time moments $t + \tau$ and $t = k\tau$, respectively and $f_{P_0}^{k+\frac{1}{2}} = f(x_1, x_2, t + \frac{\tau}{2})$, and $f_{P_A}^{k+1} = f(\widehat{p}, x_2, t + \tau)$. For the numerical solution of BVP2 (3.2)-(3.4) we propose the following difference problem

Highly Accurate Difference Problem (HADP)

$$\Theta_{h,\tau}^1 u_{h,\tau}^{k+1} = \Lambda_{h,\tau}^1 u_{h,\tau}^k + \Psi^1 \text{ on } D^{0h}\gamma_\tau, \quad (3.8)$$

$$\Theta_{h,\tau}^2 u_{h,\tau}^{k+1} = \Lambda_{h,\tau}^2 u_{h,\tau}^k + E_{h,\tau}\phi + \Psi^2 \text{ on } D^{*h}\gamma_\tau, \quad (3.9)$$

$$u_{h,\tau} = \varphi(x_1, x_2), t = 0, \text{ on } \overline{D}^h, \quad (3.10)$$

$$u_{h,\tau} = \phi(x_1, x_2, t) \text{ on } S_T^h, \quad (3.11)$$

$k = 1, 2, \dots, M' - 1$, where

$$\Psi^1 = f_{P_0}^{k+\frac{1}{2}} + \frac{1}{16}h^2 \left(\partial_{x_1}^2 f_{P_0}^{k+\frac{1}{2}} + \partial_{x_2}^2 f_{P_0}^{k+\frac{1}{2}} \right), \quad (3.12)$$

$$\begin{aligned} \Psi^2 = & \frac{h^2}{96\tau\omega} \left(f_{P_A}^{k+1} - f_{P_A}^k \right) - \left(\frac{1}{6} - \frac{h^2 b}{96\omega} \right) f_{P_A}^{k+\frac{1}{2}} + f_{P_0}^{k+\frac{1}{2}} \\ & + \frac{1}{16}h^2 \left(\partial_{x_1}^2 f_{P_0}^{k+\frac{1}{2}} + \partial_{x_2}^2 f_{P_0}^{k+\frac{1}{2}} \right), \end{aligned} \quad (3.13)$$

$$\Theta_{h,\tau}^1 u^{k+1} = \left(\frac{3}{4\tau} + \frac{2\omega}{h^2} + \frac{3}{8}b \right) u_{P_0}^{k+1} + \left(\frac{1}{24\tau} - \frac{\omega}{3h^2} + \frac{b}{48} \right) \sum_{i=1}^6 u_{P_i}^{k+1} \quad (3.14)$$

$$\Lambda_{h,\tau}^1 u^k = \left(\frac{3}{4\tau} - \frac{2\omega}{h^2} - \frac{3}{8}b \right) u_{P_0}^k + \left(\frac{1}{24\tau} + \frac{\omega}{3h^2} - \frac{b}{48} \right) \sum_{i=1}^6 u_{P_i}^k \quad (3.15)$$

$$\begin{aligned} \Theta_{h,\tau}^2 u^{k+1} = & \left(\frac{17}{24\tau} + \frac{7\omega}{3h^2} + \frac{17}{48}b \right) u_{P_0}^{k+1} + \left(\frac{1}{24\tau} - \frac{\omega}{3h^2} + \frac{b}{48} \right) \\ & \left(u(p + \eta, x_2, t + \tau) + u\left(p, x_2 + \frac{\sqrt{3}}{2}h, t + \tau\right) + u\left(p, x_2 - \frac{\sqrt{3}}{2}h, t + \tau\right) \right) \end{aligned}$$

$$\begin{aligned}
E_{h,\tau}\phi &= \left(-\frac{1}{36\tau} + \frac{2\omega}{9h^2} - \frac{b}{72}\right) \left(\phi(\widehat{p}, x_2 + \frac{\sqrt{3}}{2}h, t + \tau) + \phi(\widehat{p}, x_2 - \frac{\sqrt{3}}{2}h, t + \tau)\right) \\
&+ \left(\left(\frac{1}{36\tau} + \frac{2\omega}{9h^2} - \frac{b}{72}\right)\phi(\widehat{p}, x_2 + \frac{\sqrt{3}}{2}h, t) + \phi(\widehat{p}, x_2 - \frac{\sqrt{3}}{2}h, t)\right) \\
&+ \left(\frac{1}{18\tau} + \frac{8\omega}{9h^2} - \frac{h^2b}{48\omega\tau} + \frac{b}{36} - \frac{h^2b^2}{192\omega}\right)\phi(\widehat{p}, x_2, t + \tau) \\
&- \left(\frac{1}{18\tau} - \frac{8\omega}{9h^2} + \frac{h^2b}{48\omega\tau} - \frac{b}{36} + \frac{h^2b^2}{192\omega}\right)\phi(\widehat{p}, x_2, t) \tag{3.16}
\end{aligned}$$

$$\begin{aligned}
\Lambda_{h,\tau}^2 u^k &= \left(\frac{17}{24\tau} - \frac{7\omega}{3h^2} - \frac{17}{48}b\right)u_{P_0}^k + \left(\frac{1}{24\tau} + \frac{\omega}{3h^2} - \frac{b}{48}\right) \left(u(p, x_2 + \frac{\sqrt{3}}{2}h, t) \right. \\
&\quad \left. + u(p, x_2 - \frac{\sqrt{3}}{2}h, t) + u(p + \eta, x_2, t)\right) \tag{3.17}
\end{aligned}$$

and p and \widehat{p} are same as given in (2.29).

3.3.1 The Stability and Convergence Analysis for HADP (3.8)-(3.11)

Theorem 3.1: The order of approximation of the implicit scheme (3.8), (3.9) in HADP is $O(h^4 + \tau^2)$.

Proof. Let $(x_1, x_2, t + \tau) \in D^*\gamma_\tau$ be the center of the hexagon (P_0) at $t = (k + 1)\tau$, $k = 0, \dots, M' - 1$ time levels. The heat equation (3.2) is also satisfied at the boundary points $(\widehat{p}, x_2, t + \frac{\tau}{2})$ denoted by P_A . Therefore, we give $O(h^2 + \tau^2)$ difference approximation of the heat equation (3.2) at $(\widehat{p}, x_2, t + \frac{\tau}{2})$ when $\widehat{p} = x_1 - \frac{h}{2}$ as

$$\begin{aligned}
\frac{u_{h,\tau,P_A}^{k+1} - u_{h,\tau,P_A}^k}{\tau} &= \omega \left(\frac{2}{h^2} \left(u_{h,\tau,P_0}^{k+1} - 2u_{h,\tau,P_A}^{k+1} + u_{h,\tau,P_2}^{k+1} \right) \right. \\
&+ \frac{2}{3h^2} \left(u_{h,\tau,P_1}^{k+1} - 2u_{h,\tau,P_A}^{k+1} + u_{h,\tau,P_3}^{k+1} \right) \\
&+ \frac{2}{h^2} \left(u_{h,\tau,P_0}^k - 2u_{h,\tau,P_A}^k + u_{h,\tau,P_2}^k \right) \\
&+ \left. \frac{2}{3h^2} \left(u_{h,\tau,P_1}^k - 2u_{h,\tau,P_A}^k + u_{h,\tau,P_3}^k \right) \right) \\
&- \frac{1}{2}b \left(u_{h,\tau,P_A}^{k+1} + u_{h,\tau,P_A}^k \right) + f_{P_A}^{k+\frac{1}{2}}. \tag{3.18}
\end{aligned}$$

Using the equation (3.18) the following equation can be derived for the sum of left ghost points P_2 at time moments $t = (k + 1)\tau$, and $t = k\tau$

$$\begin{aligned}
u_{h,\tau,P_2}^{k+1} + u_{h,\tau,P_2}^k &= \frac{h^2}{2\tau\omega} u_{h,\tau,P_A}^{k+1} + \frac{8}{3} u_{h,\tau,P_A}^{k+1} - u_{h,\tau,P_0}^{k+1} - \frac{1}{3} u_{h,\tau,P_1}^{k+1} \\
&\quad - \frac{1}{3} u_{h,\tau,P_3}^{k+1} - \frac{h^2}{2\tau\omega} u_{h,\tau,P_A}^k + \frac{8}{3} u_{h,\tau,P_A}^k - u_{h,\tau,P_0}^k - \frac{1}{3} u_{h,\tau,P_1}^k \\
&\quad - \frac{1}{3} u_{h,\tau,P_3}^k + \frac{h^2 b}{4\omega} \left(u_{h,\tau,P_A}^{k+1} + u_{h,\tau,P_A}^k \right) - \frac{h^2}{2\omega} f_{P_A}^{k+\frac{1}{2}}. \tag{3.19}
\end{aligned}$$

Analogously, we use the following difference approximation of the heat equation (3.2)

at the boundary points $(\widehat{p}, x_2, t + \frac{\tau}{2})$ when $\widehat{p} = x_1 + \frac{h}{2}$

$$\begin{aligned}
\frac{u_{h,\tau,P_A}^{k+1} - u_{h,\tau,P_A}^k}{\tau} &= \omega \left(\frac{2}{h^2} \left(u_{h,\tau,P_0}^{k+1} - 2u_{h,\tau,P_A}^{k+1} + u_{h,\tau,P_5}^{k+1} \right) \right. \\
&\quad + \frac{2}{3h^2} \left(u_{h,\tau,P_4}^{k+1} - 2u_{h,\tau,P_A}^{k+1} + u_{h,\tau,P_6}^{k+1} \right) \\
&\quad + \frac{2}{h^2} \left(u_{h,\tau,P_0}^k - 2u_{h,\tau,P_A}^k + u_{h,\tau,P_5}^k \right) \\
&\quad + \left. \frac{2}{3h^2} \left(u_{h,\tau,P_4}^k - 2u_{h,\tau,P_A}^k + u_{h,\tau,P_6}^k \right) \right) \\
&\quad - \frac{1}{2} b \left(u_{h,\tau,P_A}^{k+1} + u_{h,\tau,P_A}^k \right) + f_{P_A}^{k+\frac{1}{2}}. \tag{3.20}
\end{aligned}$$

with order of approximation $O(h^2 + \tau^2)$. The sum of left ghost points P_5 at time moments $t = (k+1)\tau$, and $t = k\tau$ is obtained from (3.20)

$$\begin{aligned}
u_{h,\tau,P_5}^{k+1} + u_{h,\tau,P_5}^k &= \frac{h^2}{2\tau\omega} u_{h,\tau,P_A}^{k+1} + \frac{8}{3} u_{h,\tau,P_A}^{k+1} - u_{h,\tau,P_0}^{k+1} - \frac{1}{3} u_{h,\tau,P_4}^{k+1} - \frac{1}{3} u_{h,\tau,P_6}^{k+1} \\
&\quad - \frac{h^2}{2\tau\omega} u_{h,\tau,P_A}^k + \frac{8}{3} u_{h,\tau,P_A}^k - u_{h,\tau,P_0}^k - \frac{1}{3} u_{h,\tau,P_4}^k - \frac{1}{3} u_{h,\tau,P_6}^k \\
&\quad + \frac{h^2 b}{4\omega} \left(u_{h,\tau,P_A}^{k+1} + u_{h,\tau,P_A}^k \right) - \frac{h^2}{2\omega} f_{P_A}^{k+\frac{1}{2}}. \tag{3.21}
\end{aligned}$$

Further we give the following difference approximation of the heat equation (3.2) at

the boundary points $(\widehat{p}, x_2, t + \tau)$ and (\widehat{p}, x_2, t) where, $\widehat{p} = x_1 - \frac{h}{2}$.

$$\begin{aligned}
\frac{u_{h,\tau,P_A}^{k+1} - u_{h,\tau,P_A}^k}{\tau} &= \omega \left(\frac{4}{h^2} \left(u_{h,\tau,P_0}^{k+1} - 2u_{h,\tau,P_A}^{k+1} + u_{h,\tau,P_2}^{k+1} \right) \right. \\
&\quad + \left. \frac{4}{3h^2} \left(u_{h,\tau,P_1}^{k+1} - 2u_{h,\tau,P_A}^{k+1} + u_{h,\tau,P_3}^{k+1} \right) \right) \\
&\quad - bu_{h,\tau,P_A}^{k+1} + f_{P_A}^{k+1}, \tag{3.22}
\end{aligned}$$

$$\begin{aligned}
\frac{u_{h,\tau,P_A}^{k+1} - u_{h,\tau,P_A}^k}{\tau} &= \omega \left(\frac{4}{h^2} \left(u_{h,\tau,P_0}^k - 2u_{h,\tau,P_A}^k + u_{h,\tau,P_2}^k \right) \right. \\
&\quad \left. + \frac{4}{3h^2} \left(u_{h,\tau,P_1}^k - 2u_{h,\tau,P_A}^k + u_{h,\tau,P_3}^k \right) \right) \\
&\quad - bu_{h,\tau,P_A}^k + f_{P_A}^k
\end{aligned} \tag{3.23}$$

respectively, both with order of approximation $O(h^2 + \tau)$. From (3.22) and (3.23) we get the difference of the approximate solution on the left ghost points P_2 at time moments $t = (k+1)\tau$, and $t = k\tau$ as;

$$\begin{aligned}
u_{h,\tau,P_2}^{k+1} - u_{h,\tau,P_2}^k &= -u_{h,\tau,P_0}^{k+1} - \frac{1}{3}u_{h,\tau,P_1}^{k+1} - \frac{1}{3}u_{h,\tau,P_3}^{k+1} + \frac{8}{3}u_{h,\tau,P_A}^{k+1} \\
&\quad + u_{h,\tau,P_0}^k + \frac{1}{3}u_{h,\tau,P_1}^k + \frac{1}{3}u_{h,\tau,P_3}^k - \frac{8}{3}u_{h,\tau,P_A}^k \\
&\quad + \frac{h^2b}{4\omega} \left(u_{h,\tau,P_A}^{k+1} - u_{h,\tau,P_A}^k \right) - \frac{h^2}{4\omega} \left(f_{P_A}^{k+1} - f_{P_A}^k \right),
\end{aligned} \tag{3.24}$$

Analogously, when $(x_1, x_2, t + \tau) \in D^{*rh}\gamma_\tau$ for the difference of the right ghost points approximation we obtain

$$\begin{aligned}
u_{h,\tau,P_5}^{k+1} - u_{h,\tau,P_5}^k &= -u_{h,\tau,P_0}^{k+1} - \frac{1}{3}u_{h,\tau,P_6}^{k+1} - \frac{1}{3}u_{h,\tau,P_4}^{k+1} + \frac{8}{3}u_{h,\tau,P_A}^{k+1} \\
&\quad + u_{h,\tau,P_0}^k + \frac{1}{3}u_{h,\tau,P_6}^k + \frac{1}{3}u_{h,\tau,P_4}^k - \frac{8}{3}u_{h,\tau,P_A}^k \\
&\quad + \frac{h^2b}{4\omega} \left(u_{h,\tau,P_A}^{k+1} - u_{h,\tau,P_A}^k \right) - \frac{h^2}{4\omega} \left(f_{P_A}^{k+1} - f_{P_A}^k \right).
\end{aligned} \tag{3.25}$$

Using (3.19), (3.21) and (3.24),(3.25) in (3.8) we obtain the scheme (3.9). Let the error function be $\varepsilon_{h,\tau} = u_{h,\tau} - u$. Then $\varepsilon_{h,\tau}$ satisfies the following difference problem

$$\Theta_{h,\tau}^1 \varepsilon_{h,\tau}^{k+1} = \Lambda_{h,\tau}^1 \varepsilon_{h,\tau}^k + \Psi^1 \text{ on } D^{0h}\gamma_\tau, \tag{3.26}$$

$$\Theta_{h,\tau}^2 \varepsilon_{h,\tau}^{k+1} = \Lambda_{h,\tau}^2 \varepsilon_{h,\tau}^k + \Psi^2 \text{ on } D^{*h}\gamma_\tau, \tag{3.27}$$

$$\varepsilon_{h,\tau} = 0, t = 0, \text{ on } \overline{D}^h, \tag{3.28}$$

$$\varepsilon_{h,\tau} = 0 \text{ on } S_T^h. \tag{3.29}$$

where, $\Psi^1 = \Lambda_{h,\tau}^1 u^k - \Theta_{h,\tau}^1 u^{k+1} + \psi^1$ and $\Psi^2 = \Lambda_{h,\tau}^2 u^k - \Theta_{h,\tau}^2 u^{k+1} + \psi^2$. Using

Taylor's expansion around the point $(x_1, x_2, t + \frac{\tau}{2})$ and from the assumption that $u \in C_{x,t}^{6+\alpha, 3+\frac{\alpha}{2}}(\bar{Q}_T)$, we obtain $\Psi^1 = O(h^4 + \tau^2)$ and $\Psi^2 = O(h^4 + \tau^2)$ accuracy of the approximation. \square

Next we analyze the stability for the HADP using spectral method. The algebraic linear system of equations obtained by HADP can be given in matrix form:

$$K_1 U^{k+1} = K_2 U^k + \tau (F^{k*} + G^{k*}), \quad (3.30)$$

where, $K_1, K_2 \in R^{N \times N}$ given as

$$K_1 = \left(S_1 + \frac{\omega\tau}{h^2} S_2 \right), \quad K_2 = \left(S_1 - \frac{\omega\tau}{h^2} S_2 \right), \quad (3.31)$$

$$S_1 = D_1 + \frac{1}{24} Inc, \quad S_2 = B + \frac{bh^2}{\omega} C \quad (3.32)$$

$$B = D_2 - \frac{1}{3} Inc, \quad C = D_3 + \frac{1}{48} Inc \quad (3.33)$$

where *Inc* is the same as give in (2.44).

Also F^{k*} and G^{k*} are vectors of order N obtained by evaluating the heat source function f in (3.12), (3.13) and the boundary and initial function values in HADP (3.8)-(3.11) respectively and D_1, D_2, D_3 are diagonal matrices with entries

$$d_{1,jj} = \begin{cases} \frac{3}{4} & \text{if } Q_j \in D^{0h}\gamma_\tau \\ \frac{17}{24} & \text{if } Q_j \in D^{*h}\gamma_\tau \end{cases}, \quad j = 1, 2, \dots, N, \quad (3.34)$$

$$d_{2,jj} = \begin{cases} 2 & \text{if } Q_j \in D^{0h}\gamma_\tau \\ \frac{7}{3} & \text{if } Q_j \in D^{*h}\gamma_\tau \end{cases}, \quad j = 1, 2, \dots, N, \quad (3.35)$$

$$d_{3,jj} = \begin{cases} \frac{3}{8} & \text{if } Q_j \in D^{0h}\gamma_\tau \\ \frac{17}{48} & \text{if } Q_j \in D^{*h}\gamma_\tau \end{cases}, \quad j = 1, 2, \dots, N, \quad (3.36)$$

respectively.

Definition 3.1 (Definition 4.2 in Axelsson [31]): A matrix $K = [k_{ij}] \in R^{N \times N}$ is said to be reducible if there exists a nonempty subset $S \in L = \{1, 2, \dots, N\}$ with $S \neq L$, such that $a_{i,j} = 0$ for all index pairs (i, j) where $i \in S$ and $j \in L \setminus S$. A matrix is said to be irreducible if it is not reducible.

Definition 3.2 (Definition 4.3 in Axelsson [31]): A directed path is said to be strongly connected if to each ordered pair of disjoint points P_i, P_j there exists a directed path in the graph, $\overrightarrow{P_{i_0}P_{i_1}}, \overrightarrow{P_{i_1}P_{i_2}}, \dots, \overrightarrow{P_{i_{r-1}}P_{i_r}}$ with $i_0 = i, i_r = j$.

Definition 3.3 (Definition 4.4 in Axelsson [31]): The matrix $K = [k_{ij}] \in R^{N \times N}$ is said to be strictly diagonally dominant if $|k_{ii}| > \sigma_i = \sum_{\substack{j=1 \\ i \neq j}}^N |k_{ij}|, i = 1, 2, \dots, N$ and irreducibly diagonally dominant if A is irreducible and i) $|k_{ii}| \geq \sigma_i, i = 1, 2, \dots, N$, ii) $|k_{kk}| > \sigma_k$ for at least one index k .

Theorem 3.2 (Varga [38]): A matrix K is irreducible if and only if its directed graph is strongly connected.

Lemma 3.1: a) The matrix S_1 , in (3.32) and the matrices B and C in (3.33) are symmetric positive definite matrix.

b) The matrix K_1 in (3.31) and S_2 in (3.32) are symmetric positive definite matrices.

Proof. a) Using (2.43) if $E_i \in \text{Pat}(E_j)$ for $i \neq j, 1 \leq i, j, \leq N$ this implies that

$E_j \in \text{Patt}(E_i)$ giving $\text{Inc}^T = \text{Inc}$. Thus, S_1, B , and C are real symmetric matrices hence the eigenvalues of S_1, B , and C are real. Also because hexagonal grid is connected grid in the rectangle D , using (3.33) and Theorem 3.2 one can easily show that the matrix B is irreducibly diagonally dominant matrices with $b_{ii} > 0, i = 1, \dots, N$. Further, the matrices S_1 , and C are strictly diagonally dominant matrices with positive diagonal entries therefore by Theorem 2.2, S_1, B and C are positive definite matrices

b) From (3.32) since the sum of two symmetric positive definite matrices is also symmetric positive definite, so S_2 and K_1 are symmetric positive definite matrices. □

Theorem 3.3: The implicit scheme of the HADP is unconditionally stable and the solution $u_{h,\tau}$ of (3.8) - (3.11) converges to the exact solution u of BVP2 (3.2) - (3.4) with order of accuracy $O(h^4 + \tau^2)$.

Proof. On the basis of Lemma 3.1, the matrix S_1 is symmetric and positive definite matrix hence invertible. The linear system (3.30) can be written as

$$\left(I + \frac{\omega\tau}{h^2} (S_1)^{-1} S_2\right) U^{k+1} = \left(I - \frac{\omega\tau}{h^2} (S_1)^{-1} S_2\right) U^k + \tau (S_1)^{-1} (F^{k*} + G^{k*}), \quad (3.37)$$

On the other hand from (3.31)-(3.36)

$$S_1 = I - \frac{1}{8}B, \quad C = I - \frac{1}{16}B, \quad S_2 = \left(1 - \frac{1}{16} \frac{bh^2}{\omega}\right) B + \frac{bh^2}{\omega} I \quad (3.38)$$

where, B, C are same as given in (3.33) and $I \in \mathbb{R}^{N \times N}$ is the identity matrix. Because $(S_1)^{-1} S_2$ commutes and S_1 and S_2 are symmetric implies that $(S_1)^{-1} S_2$ is also symmetric matrix. Since the product of two symmetric positive definite matrices that commute is also symmetric positive definite (see Axelsson [31] and Taussky [33]) gives $\lambda_s \left((S_1)^{-1} S_2 \right) > 0$. Let $A = \left(I + \frac{\omega\tau}{h^2} (S_1)^{-1} S_2 \right)$ obviously A is symmetric

positive definite matrix. Let $\widehat{A} = \left(I - \frac{\omega\tau}{h^2}(S_1)^{-1}S_2\right)$.

$$\begin{aligned}
\left(A^{-1}\widehat{A}\right)^T &= \widehat{A}A^{-1} = \left(I - \frac{\omega\tau}{h^2}(S_1)^{-1}S_2\right) \left(I + \frac{\omega\tau}{h^2}(S_1)^{-1}S_2\right)^{-1} \\
&= \frac{1}{\det\left(I + \frac{\omega\tau}{h^2}(S_1)^{-1}S_2\right)} \left(I - \frac{\omega\tau}{h^2}(S_1)^{-1}S_2\right) \text{Adj}\left(I + \frac{\omega\tau}{h^2}(S_1)^{-1}S_2\right) \\
&= \left(I + \frac{\omega\tau}{h^2}(S_1)^{-1}S_2\right)^{-1} \left[I - \frac{1}{\det\left(I + \frac{\omega\tau}{h^2}(S_1)^{-1}S_2\right)} \left(I + \frac{\omega\tau}{h^2}(S_1)^{-1}S_2\right) \right. \\
&\quad \left. \left(\frac{\omega\tau}{h^2}(S_1)^{-1}S_2\right) \text{Adj}\left(I + \frac{\omega\tau}{h^2}(S_1)^{-1}S_2\right) \right] \\
&= \left(I + \frac{\omega\tau}{h^2}(S_1)^{-1}S_2\right)^{-1} \left(I - \frac{\omega\tau}{h^2}(S_1)^{-1}S_2\right) = A^{-1}\widehat{A}. \tag{3.39}
\end{aligned}$$

Thus $A^{-1}\widehat{A}$ is symmetric matrix. Also let P be orthogonal and \widetilde{D} be diagonal matrix of eigenvalues $\lambda_s\left((S_1)^{-1}S_2\right)$. Then $\left(I + \frac{\omega\tau}{h^2}(S_1)^{-1}S_2\right) = P^T \left(I + \frac{\omega\tau}{h^2}\widetilde{D}\right) P$ and $\left(I + \frac{\omega\tau}{h^2}(S_1)^{-1}S_2\right)^{-1} = P^T \left(I + \frac{\omega\tau}{h^2}\widetilde{D}\right)^{-1} P$ and

$$\left(I + \frac{\omega\tau}{h^2}(S_1)^{-1}S_2\right)^{-1} \left(I - \frac{\omega\tau}{h^2}(S_1)^{-1}S_2\right) = P^T \left(I + \frac{\omega\tau}{h^2}\widetilde{D}\right)^{-1} P P^T \left(I - \frac{\omega\tau}{h^2}\widetilde{D}\right) P \tag{3.40}$$

that is the matrix $A^{-1}\widehat{A}$ is similar to $\left(I + \frac{\omega\tau}{h^2}\widetilde{D}\right)^{-1} \left(I - \frac{\omega\tau}{h^2}\widetilde{D}\right)$ so from (3.39)

$$\begin{aligned}
\left\|A^{-1}\widehat{A}\right\|_2 &= \rho\left(A^{-1}\widehat{A}\right) = \max_{1 \leq s \leq N} \left| \lambda_s \left[\left(I + \frac{\omega\tau}{h^2}\widetilde{D}\right)^{-1} \left(I - \frac{\omega\tau}{h^2}\widetilde{D}\right) \right] \right| \\
&\leq \left| \frac{1 - \frac{\omega\tau}{h^2} \min_{1 \leq s \leq N} (\lambda_s((S_1)^{-1}S_2))}{1 + \frac{\omega\tau}{h^2} \min_{1 \leq s \leq N} (\lambda_s((S_1)^{-1}S_2))} \right| < 1 \text{ for } \frac{\omega\tau}{h^2} > 0. \tag{3.41}
\end{aligned}$$

and from Gerchgorin's circle theorem we have

$$0 < \lambda_s(B) \leq 4 \tag{3.42}$$

From (3.38) and (3.42) and on the basis of Lemma 3.1 that $K_1 = S_1 + \frac{\omega\tau}{h^2}S_2$ is symmetric positive definite matrix we have

$$\begin{aligned}
K_1 &= S_1 + \frac{\omega\tau}{h^2}S_2 = (1 + \tau b)I + \left(-\frac{1}{8} + \frac{\omega\tau}{h^2} - \frac{b\tau}{16}\right)B \\
\lambda_s(K_1) &= \lambda_s\left(S_1 + \frac{\omega\tau}{h^2}S_2\right) = (1 + \tau b) + \left(-\frac{1}{8} + \frac{\omega\tau}{h^2} - \frac{b\tau}{16}\right)\lambda_s(B) \\
\rho\left((K_1)^{-1}\right) &= \rho\left(\left(S_1 + \frac{\omega\tau}{h^2}S_2\right)^{-1}\right) = \left\|\left(S_1 + \frac{\omega\tau}{h^2}S_2\right)^{-1}\right\|_2 \\
&\leq \frac{1}{\eta}
\end{aligned}$$

where $\eta = \min\left\{1 + \tau b, \frac{1}{2} + \frac{15}{16}b\tau + \frac{\omega\tau}{h^2}\right\}$ then

$$\left\|(K_1)^{-1}\right\|_2 \leq \frac{1}{\eta} < 2 \quad (3.43)$$

Next using (3.41) and (3.43) by induction results

$$\begin{aligned}
\left\|U^{k+1}\right\|_2 &\leq \left\|A^{-1}\widehat{A}\right\|_2 \left\|U^k\right\|_2 + \tau \left\|(K_1)^{-1}\right\|_2 \left(\left\|F^{k+\frac{1}{2}}\right\|_2 + \left\|G^{k*}\right\|_2\right) \\
&\leq \left\|U^0\right\|_2 + 2 \sum_{k'=0}^k \tau \left(\left\|F^{k'+\frac{1}{2}}\right\|_2 + \left\|G^{k'}\right\|_2\right). \quad (3.44)
\end{aligned}$$

The error function $\varepsilon_{h,\tau}$ satisfying (3.26)-(3.29) can also be given in the matrix form (3.37) as

$$\left(I + \frac{\omega\tau}{h^2}(S_1)^{-1}S_2\right)\varepsilon^{k+1} = \left(I - \frac{\omega\tau}{h^2}(S_1)^{-1}S_2\right)\varepsilon^k + \tau(S_1)^{-1}\widehat{\Psi}^{k+\frac{1}{2}}, \quad (3.45)$$

where ε^{k+1} , ε^k and $\widehat{\Psi}^{k+\frac{1}{2}}$ are vectors of order N . Thus, from Theorem 3.1 and (3.44), (3.45) we have

$$\left\|\varepsilon^{k+1}\right\|_2 \leq 2 \sum_{k'=0}^k \tau \left\|\widehat{\Psi}^{k'+\frac{1}{2}}\right\|_2 \leq c_3(h^4 + \tau^2), \quad (3.46)$$

where, c_3 is positive constant independent from h and τ and depends on the bounded derivatives of the solution u of the form (2.1), where $2r + s_1 + s_2 < 6 + \alpha$, in the truncation errors Ψ and Ψ^* . Since $A^{-1}\widehat{A}$ is symmetric real matrix it is also normal matrix and Von Neuman Condition for stability is sufficient as well as necessary for

stability (see Lax and Richtmyer [32]). Therefore, equation (3.44) yields that the implicit scheme (3.8), (3.9) is unconditionally stable. Let $\left\| \boldsymbol{\epsilon}_{h,\tau}^{k+1} \right\|_C = \max_{D^h \gamma_\tau \cap \{t=(k+1)\tau\}} \left| \boldsymbol{\epsilon}_{h,\tau}^{k+1} \right| = \left\| \boldsymbol{\epsilon}^{k+1} \right\|_\infty$, then on the basis of norm concordance and using (3.46) we get

$$\left\| \boldsymbol{\epsilon}_{h,\tau}^{k+1} \right\|_C \leq \left\| \boldsymbol{\epsilon}^{k+1} \right\|_2 \leq c_3 (h^4 + \tau^2). \quad (3.47)$$

Therefore, the solution $u_{h,\tau}$ of (3.8) - (3.11) converges to the exact solution u of (3.2) - (3.4) with order of accuracy $(h^4 + \tau^2)$. \square

Chapter 4

NUMERICAL RESULTS

4.1 Introduction

To justify the theoretical results given in Chapter 2 and Chapter 3, we construct several test examples. Numerical results are presented via tables and figures.

In section 4.2 we apply Difference Problem 1 and Difference Problem 2 to show that the order of convergence of the approximate solution to the exact solution of the problem (2.9) - (2.11) is $O(h^2 + \tau^2)$ and $O(h^4 + \tau)$ respectively.

In section 4.3 we apply Highly Accurate Difference Problem to illustrate that the order of convergence of the approximate solution to the exact solution of the problem (3.2) - (3.4) is of order $O(h^4 + \tau^2)$.

4.2 Numerical Results for the Problem (2.9) - (2.11)

We consider three examples for the problem (2.9) - (2.11), when the value of $\omega = 1$ for the operator $L \equiv \frac{\partial}{\partial t} - \omega \left(\frac{\partial^2}{\partial x_1^2} + \frac{\partial^2}{\partial x_2^2} \right)$

We take the open polygon Ω , as the rectangle,

$$\Omega_{Rec} = \left\{ (x_1, x_2) : 0 < x_1 < 1, 0 < x_2 < \frac{\sqrt{3}}{2} \right\} \quad (4.1)$$

the trapezoid,

$$\Omega_{Tra} = \left\{ (x_1, x_2) : 0 < x_2 < \frac{\sqrt{3}}{2}, 0 < x_1 < \frac{x_2}{\sqrt{3}} + 1 \right\} \quad (4.2)$$

and the parallelogram,

$$\Omega_{Par} = \left\{ (x_1, x_2) : 0 < x_2 < \frac{\sqrt{3}}{2}, \frac{x_2}{\sqrt{3}} < x_1 < \frac{x_2}{\sqrt{3}} + 1 \right\} \quad (4.3)$$

All the computations are performed using Mathematica in double precision on a personal computer with properties AMD Ryzen 7 1800X Eight Core Processor 3.60GHz. Also we used conjugate gradient method to solve the obtained algebraic linear system of equations at each time level. All tables given in this section adopt the following notations:

$CT^{Exi}, i = 1, 2, 3$ present the total Central Processing Unit time in seconds per time level for the Example 4.1, Example 4.2 and Example 4.3 respectively. *neg* means that $CT^{Exi}, i = 1, 2, 3$ is less than one milliseconds.

Example 4.1 (Example 1 of Buranay and Nouman [22]): Test problem with smooth boundary and initial functions in the pure diffusion case $f = \mathbf{0}$

$$\begin{aligned} Lu &= 0 \text{ on } Q_T, \\ u(x_1, x_2, 0) &= \sin\left(\frac{\pi}{6}x_1 + \frac{\pi}{3}x_2\right) \text{ on } \bar{\Omega} \\ u(x_1, x_2, t) &= e^{\frac{-5\pi^2}{36}t} \sin\left(\frac{\pi}{6}x_1 + \frac{\pi}{3}x_2\right) \text{ on } S_T, \end{aligned}$$

and, the exact solution is $u(x_1, x_2, t) = e^{\frac{-5\pi^2}{36}t} \sin\left(\frac{\pi}{6}x_1 + \frac{\pi}{3}x_2\right)$.

Example 4.2 (Example 2 of Buranay and Nouman [22]): Test problem with decreased smoothness on the boundary, initial functions and heat source.

$$\begin{aligned} Lu &= - \left(\frac{37}{12} t^{\frac{25}{12}} \sin \left(t^{\frac{37}{12}} \right) + \frac{1147}{72} x_1^{\frac{25}{6}} + \frac{1147}{36} x_2^{\frac{25}{6}} \right) \text{ on } Q_T, \\ u(x_1, x_2, 0) &= \frac{1}{2} x_1^{\frac{37}{6}} + x_2^{\frac{37}{6}} + 1 \text{ on } \overline{\Omega} \\ u(x_1, x_2, t) &= \frac{1}{2} x_1^{\frac{37}{6}} + x_2^{\frac{37}{6}} + \cos \left(t^{\frac{37}{12}} \right) \text{ on } S_T, \end{aligned}$$

and the exact solution is $u(x_1, x_2, t) = \frac{1}{2} x_1^{\frac{37}{6}} + x_2^{\frac{37}{6}} + \cos \left(t^{\frac{37}{12}} \right)$.

On the grid points $\overline{\Omega^h \gamma_\tau}$, which is the closure of $\Omega^h \gamma_\tau$ we denote the error function $\epsilon_{h,\tau}$ by $\epsilon_{Rec}^{Exi(h,\tau)}$, $\epsilon_{Tra}^{Exi(h,\tau)}$ and $\epsilon_{Par}^{Exi(h,\tau)}$ $i = 1, 2$ when Ω is the rectangle (Ω_{Rec}), trapezoid (Ω_{Tra}) and parallelogram (Ω_{Par}) respectively, for the Example 4.1 and Example 4.2. Also maximum norm of the errors $\max_{\overline{\Omega^h \gamma_\tau}} |\epsilon_{h,\tau}|$ for the Example 4.1 and Example 4.2 ($i = 1, 2$) are denoted by $\left\| \epsilon_{Rec}^{Exi(h,\tau)} \right\|_\infty$, $\left\| \epsilon_{Tra}^{Exi(h,\tau)} \right\|_\infty$ and $\left\| \epsilon_{Par}^{Exi(h,\tau)} \right\|_\infty$ on Ω_{Rec} , Ω_{Tra} and Ω_{Par} respectively. Further, we denote the order of convergence of the approximate solution $u_{h,\tau}$ to the exact solution u for the Example 4.1 and Example 4.2 obtained by using the Difference Problem 1 with

$${}_2\mathfrak{R}_{Rec}^{Exi} = \log_2 \left(\frac{\left\| \epsilon_{Rec}^{Exi(2^{-\mu}, 2^{-\lambda})} \right\|_\infty}{\left\| \epsilon_{Rec}^{Exi(2^{-(\mu+1)}, 2^{-(\lambda+1)})} \right\|_\infty} \right), \quad i = 1, 2, \quad (4.4)$$

$${}_2\mathfrak{R}_{Tra}^{Exi} = \log_2 \left(\frac{\left\| \epsilon_{Tra}^{Exi(2^{-\mu}, 2^{-\lambda})} \right\|_\infty}{\left\| \epsilon_{Tra}^{Exi(2^{-(\mu+1)}, 2^{-(\lambda+1)})} \right\|_\infty} \right), \quad i = 1, 2, \quad (4.5)$$

$${}_2\mathfrak{R}_{Par}^{Ex1} = \log_2 \left(\frac{\left\| \epsilon_{Par}^{Exi(2^{-\mu}, 2^{-\lambda})} \right\|_\infty}{\left\| \epsilon_{Par}^{Exi(2^{-(\mu+1)}, 2^{-(\lambda+1)})} \right\|_\infty} \right), \quad i = 1, 2, \quad (4.6)$$

for the considered domains respectively. Table 4.1, Table 4.2, Table 4.3 demonstrate the CT^{Ex1} , CT^{Ex2} and the maximum norm of the errors for $h = 2^{-\mu}$, $\mu = 3, 4, 5, 6, 7, 8$

when $\tau = 2^{-\lambda}$, $\lambda = 8, 9, 10, 11, 12, 13$ and the convergence order of $u_{h,\tau}$ to the exact solution u with respect to h and τ obtained by using the constructed Difference Problem 1 for the Example 4.1 and Example 4.2 on rectangle, trapezoid and parallelogram respectively. These tables show that the proposed Difference Problem 1 has quadratic convergence order in both the spatial and time variables.

Next we solve both examples by using the Difference Problem 2 and denote the obtained order of convergence of the approximate solution $u_{h,\tau}$ to the exact solution u for the Example 4.1 and Example 4.2 ($i = 1, 2$) by

$${}_4\mathfrak{R}_{Rec}^{Exi} = \log_2 \left(\frac{\left\| \left\| \mathfrak{E}_{Rec}^{Exi(2^{-\mu}, 2^{-\lambda})} \right\| \right\|_{\infty}}{\left\| \left\| \mathfrak{E}_{Rec}^{Exi(2^{-(\mu+1)}, 2^{-(\lambda+4)})} \right\| \right\|_{\infty}} \right), \quad i = 1, 2, \quad (4.7)$$

$${}_4\mathfrak{R}_{Tra}^{Exi} = \log_2 \left(\frac{\left\| \left\| \mathfrak{E}_{Tra}^{Exi(2^{-\mu}, 2^{-\lambda})} \right\| \right\|_{\infty}}{\left\| \left\| \mathfrak{E}_{Tra}^{Exi(2^{-(\mu+1)}, 2^{-(\lambda+4)})} \right\| \right\|_{\infty}} \right), \quad i = 1, 2, \quad (4.8)$$

$${}_4\mathfrak{R}_{Par}^{Exi} = \log_2 \left(\frac{\left\| \left\| \mathfrak{E}_{Par}^{Exi(2^{-\mu}, 2^{-\lambda})} \right\| \right\|_{\infty}}{\left\| \left\| \mathfrak{E}_{Par}^{Exi(2^{-(\mu+1)}, 2^{-(\lambda+4)})} \right\| \right\|_{\infty}} \right), \quad i = 1, 2, \quad (4.9)$$

for the considered domains respectively. Table 4.4, Table 4.5, Table 4.6 show the CT^{Ex1} , CT^{Ex2} , maximum norm of the errors for $h = 2^{-\mu}$, $\mu = 4, 5, 6, 7, 8$ when $\tau = 2^{-\lambda}$, $\lambda = 6, 10, 14, 18, 22$ and the order of convergence of $u_{h,\tau}$ to the exact solution u with respect to h and τ obtained by using the constructed Difference Problem 2 for the Example 4.1 and Example 4.1 on rectangle, trapezoid and parallelogram respectively. These tables demonstrate that the approximate solution $u_{h,\tau}$ of the proposed Difference Problem 2 converges to the exact solution u with fourth order in the spatial variables and linearly with respect to time variable t . Figure 4.1, Figure 4.2 and Figure 4.3 demonstrate the absolute error functions $\left| \mathfrak{E}_{Rec}^{Ex2(2^{-6}, 2^{-14})} \right|$,

Table 4.1: Computational time, maximum norm of the errors and the order of convergence by using Difference Problem 1 for the Example 4.1 and Example 4.2 on rectangle.

(h, τ)	CT^{Ex1}	$\ \epsilon_{Rec}^{Ex1(h,\tau)}\ _{\infty}$	${}_2\mathfrak{R}_{Rec}^{Ex1}$	CT^{Ex2}	$\ \epsilon_{Rec}^{Ex2(h,\tau)}\ _{\infty}$	${}_2\mathfrak{R}_{Rec}^{Ex2}$
$(2^{-3}, 2^{-8})$	<i>neg</i>	$6.24429E-5$	1.978	<i>neg</i>	$9.35402E-3$	1.983
$(2^{-4}, 2^{-9})$	0.02	$1.58525E-5$	1.999	0.02	$2.36716E-3$	2.001
$(2^{-5}, 2^{-10})$	0.03	$3.96648E-6$	1.999	0.03	$5.91299E-4$	2.002
$(2^{-6}, 2^{-11})$	0.16	$9.92099E-7$	2.000	0.19	$1.47588E-4$	2.003
$(2^{-7}, 2^{-12})$	1.52	$2.48027E-7$	2.000	1.66	$3.68223E-5$	2.004
$(2^{-8}, 2^{-13})$	3.50	$6.19891E-8$		3.76	$9.17993E-6$	

Table 4.2: Computational time, maximum norm of the errors and the order of convergence by using Difference Problem 1 for the Example 4.1 and Example 4.2 on trapezoid.

(h, τ)	CT^{Ex1}	$\ \epsilon_{Tra}^{Ex1(h,\tau)}\ _{\infty}$	${}_2\mathfrak{R}_{Tra}^{Ex1}$	CT^{Ex2}	$\ \epsilon_{Tra}^{Ex2(h,\tau)}\ _{\infty}$	${}_2\mathfrak{R}_{Tra}^{Ex2}$
$(2^{-3}, 2^{-8})$	<i>neg</i>	$7.47982E-5$	1.971	<i>neg</i>	$1.40022E-2$	1.989
$(2^{-4}, 2^{-9})$	0.02	$1.90801E-5$	1.999	0.02	$3.52824E-3$	2.001
$(2^{-5}, 2^{-10})$	0.05	$4.77247E-6$	1.999	0.05	$8.81499E-4$	2.002
$(2^{-6}, 2^{-11})$	0.20	$1.19371E-6$	2.000	0.25	$2.20072E-4$	2.002
$(2^{-7}, 2^{-12})$	2.20	$2.98412E-7$	2.000	2,33	$5.49334E-5$	2.002
$(2^{-8}, 2^{-13})$	4.41	$7.45783E-8$		4.88	$1.37127E-5$	

$|\epsilon_{Par}^{Ex2(2^{-6}, 2^{-14})}|$ and $|\epsilon_{Tra}^{Ex2(2^{-6}, 2^{-14})}|$ respectively, at time moments $t = 0.25$ and $t = 0.75$ obtained by using the Difference Problem 2 for the numerical solution of Example 4.2 when $h = 2^{-6}$ and $\tau = 2^{-14}$.

Example 4.3 (Example 3 of Buranay and Nouman [22]): A benchmark problem

$$\begin{aligned}
 Lu &= f(x_1, x_2, t) \text{ on } Q_T, \\
 u(x_1, x_2, 0) &= 0 \text{ on } \bar{\Omega}_{Rec} \\
 u(0, x_2, t) &= u(1, x_2, t) = u(x_1, 0, t) = u\left(x_1, \frac{\sqrt{3}}{2}, t\right) = 0 \text{ on } S_T,
 \end{aligned}$$

where,

Table 4.3: Computational time, maximum norm of the errors and the order of convergence by using Difference Problem 1 for the Example 4.1 and Example 4.2 on parallelogram.

(h, τ)	CT^{Ex1}	$\ \epsilon_{Par}^{Ex1(h,\tau)}\ _{\infty}$	${}_2\mathfrak{R}_{Par}^{Ex1}$	CT^{Ex2}	$\ \epsilon_{Par}^{Ex2(h,\tau)}\ _{\infty}$	${}_2\mathfrak{R}_{Par}^{Ex2}$
$(2^{-3}, 2^{-8})$	<i>neg</i>	$6.63405E-5$	1.980	<i>neg</i>	$1.31396E-2$	1.992
$(2^{-4}, 2^{-9})$	0.02	$1.68183E-5$	1.997	0.02	$3.30422E-3$	2.002
$(2^{-5}, 2^{-10})$	0.03	$4.21369E-6$	2.000	0.05	$8.24839E-4$	2.001
$(2^{-6}, 2^{-11})$	0.16	$1.05350E-6$	2.001	0.19	$2.06009E-4$	2.002
$(2^{-7}, 2^{-12})$	1.58	$2.63097E-7$	2.002	1.63	$5.14365E-5$	2.002
$(2^{-8}, 2^{-13})$	3.69	$6.56738E-8$		4.62	$1.28391E-5$	

Table 4.4: Computational time, maximum norm of the errors and the order of convergence by using Difference Problem 2 for the Example 4.1 and Example 4.2 on rectangle.

(h, τ)	CT^{Ex1}	$\ \epsilon_{Rec}^{Ex1(h,\tau)}\ _{\infty}$	${}_4\mathfrak{R}_{Rec}^{Ex1}$	CT^{Ex2}	$\ \epsilon_{Rec}^{Ex2(h,\tau)}\ _{\infty}$	${}_4\mathfrak{R}_{Rec}^{Ex2}$
$(2^{-4}, 2^{-6})$	<i>neg</i>	$4.95534E-4$	3.965	0.02	$4.66691E-3$	3.981
$(2^{-5}, 2^{-10})$	0.03	$3.17373E-5$	3.997	0.08	$2.95518E-4$	3.999
$(2^{-6}, 2^{-14})$	0.14	$1.98759E-6$	3.999	0.34	$1.84851E-5$	4.000
$(2^{-7}, 2^{-18})$	1.13	$1.24291E-7$	4.000	1.88	$1.15518E-6$	4.000
$(2^{-8}, 2^{-22})$	3.24	$7.76738E-9$		3.98	$7.21861E-8$	

Table 4.5: Computational time, maximum norm of the errors and the order of convergence by using Difference Problem 2 for the Example 4.1 and Example 4.2 on trapezoid.

(h, τ)	CT^{Ex1}	$\ \epsilon_{Tra}^{Ex1(h,\tau)}\ _{\infty}$	${}_4\mathfrak{R}_{Tra}^{Ex1}$	CT^{Ex2}	$\ \epsilon_{Tra}^{Ex2(h,\tau)}\ _{\infty}$	${}_4\mathfrak{R}_{Tra}^{Ex2}$
$(2^{-4}, 2^{-6})$	<i>neg</i>	$5.97349E-4$	3.967	0.02	$5.24608E-3$	3.980
$(2^{-5}, 2^{-10})$	0.03	$3.81931E-5$	3.997	0.09	$3.32497E-4$	3.999
$(2^{-6}, 2^{-14})$	0.20	$2.39154E-6$	4.000	0.45	$2.08008E-5$	4.000
$(2^{-7}, 2^{-18})$	1.63	$1.49520E-7$	4.000	2.61	$1.29993E-6$	4.000
$(2^{-8}, 2^{-22})$	4.18	$9.34338E-9$		4.53	$8.12356E-8$	

Table 4.6: Computational time, maximum norm of the errors and the order of convergence by using Difference Problem 2 for the Example 4.1 and Example 4.2 on parallelogram.

(h, τ)	CT^{Ex1}	$\ \epsilon_{Par}^{Ex1(h,\tau)}\ _{\infty}$	${}_4\mathfrak{R}_{Par}^{Ex1}$	CT^{Ex2}	$\ \epsilon_{Par}^{Ex2(h,\tau)}\ _{\infty}$	${}_4\mathfrak{R}_{Par}^{Ex2}$
$(2^{-4}, 2^{-6})$	<i>neg</i>	$5.25821E-4$	3.963	0.02	$4.35263E-3$	3.981
$(2^{-5}, 2^{-10})$	0.03	$3.37165E-5$	3.998	0.06	$2.75544E-4$	3.999
$(2^{-6}, 2^{-14})$	0.17	$2.11066E-6$	4.000	0.30	$1.72353E-5$	4.000
$(2^{-7}, 2^{-18})$	1.19	$1.31906E-7$	4.000	1.81	$1.07708E-6$	4.000
$(2^{-8}, 2^{-22})$	3.98	$8.24304E-9$		4.78	$6.73085E-8$	

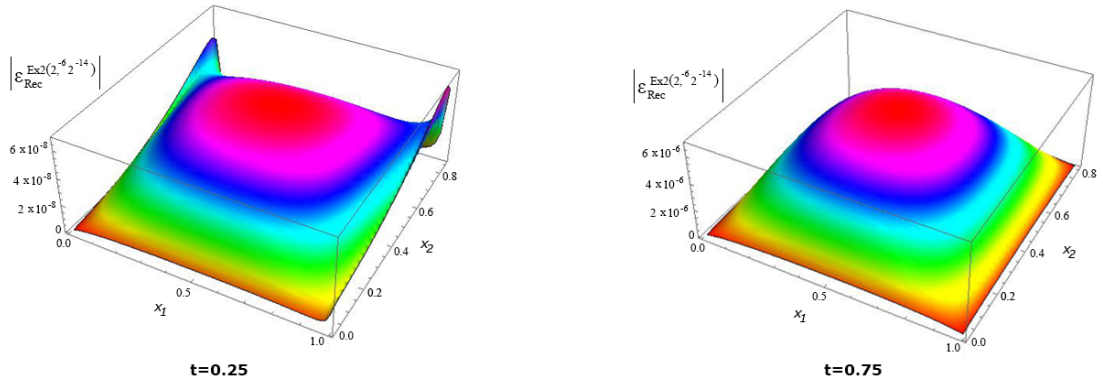


Figure 4.1: Absolute error function $\left| \epsilon_{Rec}^{Ex2(2^{-6}, 2^{-14})} \right|$ at $t = 0.25$ and $t = 0.75$ obtained by using Difference Problem 2 for the Example 4.2.

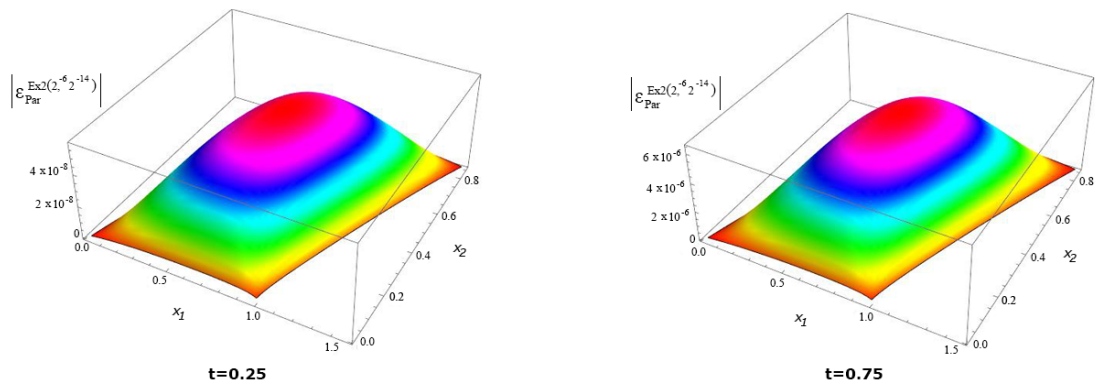


Figure 4.2: Absolute error function $\left| \epsilon_{Par}^{Ex2(2^{-6}, 2^{-14})} \right|$ at $t = 0.25$ and $t = 0.75$ obtained by using Difference Problem 2 for the Example 4.2.

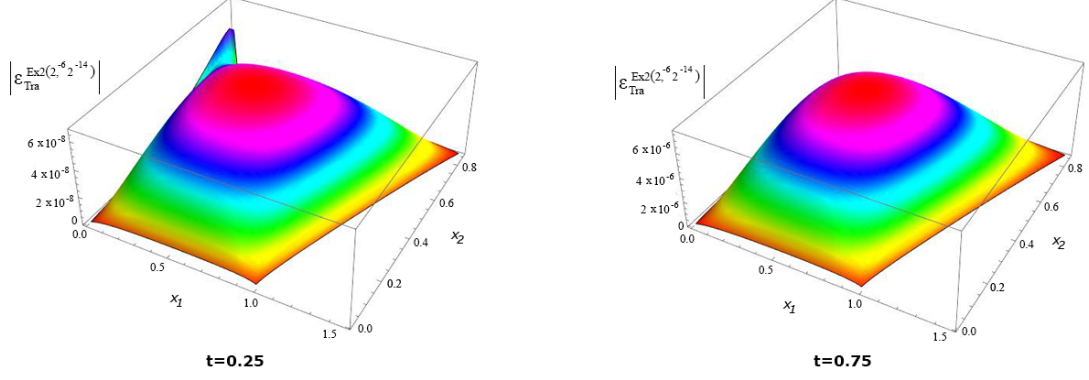


Figure 4.3: Absolute error function $\left| \epsilon_{Tra}^{Ex2(2^{-6}, 2^{-14})} \right|$ at $t = 0.25$ and $t = 0.75$ obtained by using Difference Problem 2 for the Example 4.2.

$$\begin{aligned}
 f(x_1, x_2, t) &= x_1^{\frac{49}{8}} \left(x_2^2 - \frac{\sqrt{3}}{2} x_2 \right) \sin(x_1 - 1) \cos t \\
 &\quad - \left(x_2^2 - \frac{\sqrt{3}}{2} x_2 \right) \sin t \left[\frac{2009}{64} x_1^{\frac{33}{8}} \sin(x_1 - 1) + \frac{49}{4} x_1^{\frac{41}{8}} \cos(x_1 - 1) \right. \\
 &\quad \left. + x_1^{\frac{49}{8}} \sin(x_1 - 1) \right] - 2x_1^{\frac{49}{8}} \sin(x_1 - 1) \sin t.
 \end{aligned}$$

The exact solution of Example 4.3 is not given. Using the proposed Difference Problem 1 we obtain the approximate solution $u_{2-\mu, 2-\lambda}(x_1, x_2, t)$ at each time level for $\mu = 4, 5, 6$, and $\lambda = 9, 10, 11$ respectively. Table 4.7 presents $u_{2-\mu, 2-\lambda}(x_1, x_2, t)$ at the grid points $\left(0.125, \frac{\sqrt{3}}{16}, 1\right)$, $\left(0.25, \frac{\sqrt{3}}{16}, 1\right)$, $\left(0.375, \frac{\sqrt{3}}{16}, 1\right)$, $\left(0.5, \frac{\sqrt{3}}{16}, 1\right)$, $\left(0.625, \frac{\sqrt{3}}{16}, 1\right)$, $\left(0.75, \frac{\sqrt{3}}{16}, 1\right)$ and $\left(0.875, \frac{\sqrt{3}}{16}, 1\right)$ and the order of convergence at the point $P(x_1, x_2, t)$ denoted by

$${}_2\mathfrak{R}_{Rec}^{Ex3}(P) = \log_2 \left| \frac{u_{2-4, 2-9}(P) - u_{2-5, 2-10}(P)}{u_{2-5, 2-10}(P) - u_{2-6, 2-11}(P)} \right|. \quad (4.10)$$

Next by applying the given Difference Problem 2 we obtain the approximate solution $u_{2-\mu, 2-\lambda}(x_1, x_2, t)$ at each time level for $\mu = 4, 5, 6$, and $\lambda = 6, 10, 14$ respectively. The approximate solution at the same chosen grid points and the order of convergence at

Table 4.7: Solution at some points on $t = 1$, and the order of convergence by using Difference Problem 1 for the Example 4.3.

P	$u_{2^{-4}, 2^{-9}}(P)$	$u_{2^{-5}, 2^{-10}}(P)$	$u_{2^{-6}, 2^{-11}}(P)$	${}_2\mathfrak{R}_{Rec}^{Ex3}(P)$
$(0.125, \frac{\sqrt{3}}{16}, 1)$	$-4.58409E - 6$	$-1.03024E - 6$	$-1.4070E - 7$	1.998
$(0.25, \frac{\sqrt{3}}{16}, 1)$	$-1.80759E - 6$	$6.79206E - 6$	$8.94335E - 6$	1.999
$(0.375, \frac{\sqrt{3}}{16}, 1)$	$7.67420E - 5$	$9.37204E - 5$	$9.79542E - 5$	2.004
$(0.5, \frac{\sqrt{3}}{16}, 1)$	$4.35627E - 4$	$4.64628E - 4$	$4.71821E - 4$	2.011
$(0.625, \frac{\sqrt{3}}{16}, 1)$	$1.36634E - 3$	$1.40760E - 3$	$1.41775E - 3$	2.023
$(0.75, \frac{\sqrt{3}}{16}, 1)$	$2.87207E - 3$	$2.91762E - 3$	$2.92870E - 3$	2.039
$(0.875, \frac{\sqrt{3}}{16}, 1)$	$3.75741E - 3$	$3.78878E - 3$	$3.79627E - 3$	2.066

these points

$${}_4\mathfrak{R}_{Rec}^{Ex3}(P) = \log_2 \left| \frac{u_{2^{-4}, 2^{-6}}(P) - u_{2^{-5}, 2^{-10}}(P)}{u_{2^{-5}, 2^{-10}}(P) - u_{2^{-6}, 2^{-14}}(P)} \right|. \quad (4.11)$$

are shown in Table 4.8. By analyzing the values of (4.10) and (4.11) in the fifth columns of Table 4.7 and Table 4.8 respectively, we conclude that the convergence follow the $2n$ order in both in spatial and time variables on $t = 1$ when Difference Problem 1 is used, and it is fourth order in the spatial variables and linear in time variable while Difference Problem 2 is applied. Figure 4.4 illustrates the approximate solution $u_{2^{-6}, 2^{-14}}(x_1, x_2, t)$ of the Example 4.3 obtained by using Difference Problem 2 at time moments $t = 0.25$ and $t = 1$.

4.3 Numerical Results for the Problem (3.2) - (3.4)

We consider the open rectangle $D = \left\{ (x_1, x_2) : 0 < x_1 < 1, 0 < x_2 < \frac{\sqrt{3}}{2} \right\}$ which is same as Ω_{Rec} in (4.1), and we take $t \in [0, 1]$. Three examples are considered for which the exact solution of Example 4.4 and Example 4.6 are known and the exact solution of Example 4.5 is not given explicitly. To solve the obtained algebraic system of equations in all the examples, we applied incomplete block-matrix factorization of the block tridiagonal stiffness matrices and use as preconditioners for the conjugate

Table 4.8: Solution at some points on $t = 1$, and the order of convergence by using Difference Problem 2 for the Example 4.3.

P	$u_{2^{-4}, 2^{-6}}(P)$	$u_{2^{-5}, 2^{-10}}(P)$	$u_{2^{-6}, 2^{-14}}(P)$	$4\mathfrak{R}_{Rec}^{Ex3}(P)$
$(0.125, \frac{\sqrt{3}}{16}, 1)$	$1.21289E-7$	$1.53563E-7$	$1.55701E-7$	3.916
$(0.25, \frac{\sqrt{3}}{16}, 1)$	$9.57959E-6$	$9.6543E-6$	$9.65919E-6$	3.933
$(0.375, \frac{\sqrt{3}}{16}, 1)$	$9.91752E-5$	$9.93431E-5$	$9.93539E-5$	3.958
$(0.5, \frac{\sqrt{3}}{16}, 1)$	$4.73794E-4$	$4.74143E-4$	$4.74165E-4$	3.988
$(0.625, \frac{\sqrt{3}}{16}, 1)$	$1.42033E-3$	$1.42094E-3$	$1.42098E-3$	3.931
$(0.75, \frac{\sqrt{3}}{16}, 1)$	$2.93121E-3$	$2.93202E-3$	$2.93207E-3$	4.018
$(0.875, \frac{\sqrt{3}}{16}, 1)$	$3.79768E-3$	$3.79832E-3$	$3.79836E-3$	4.000

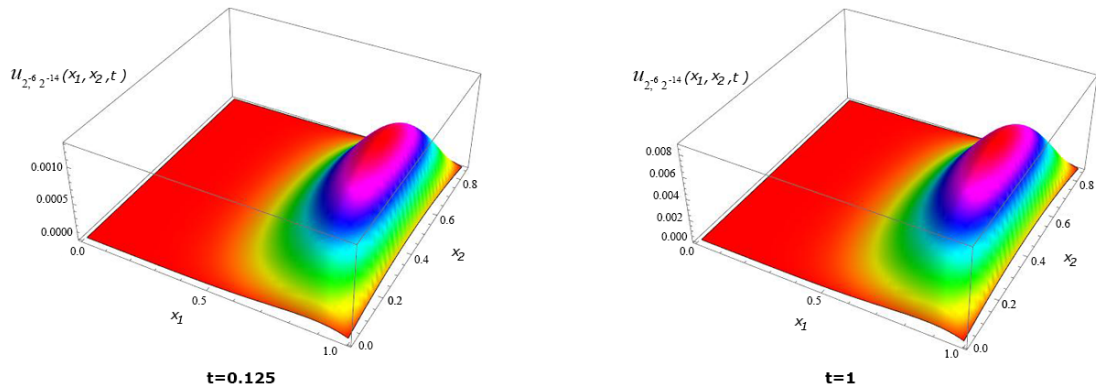


Figure 4.4: The approximate solution $u_{2^{-6}, 2^{-14}}(x_1, x_2, t)$ at time moments $t = 0.25$ and $t = 1$ for the Example 4.3 obtained by using Difference Problem 2.

gradient method (see Concus et al. [35], Axelsson [36] and Buranay and Iyikal [37]).

For experimental investigation of the computational efficiency we also consider the rectangular grids on D with step sizes $h_1 = \frac{a_1}{M_1}$ along the spatial variable x_1 and $h_2 = \frac{a_2}{M_2}$ along x_2 where, M_1 and M_2 are positive integers

$$D^{h_1, h_2} = \{x = (x_1, x_2) \in D : x_1 = ih_1, x_2 = jh_2, i = 1, 2, \dots, M_1 - 1, \\ j = 1, 2, \dots, M_2 - 1\}. \quad (4.12)$$

Let \bar{D}^{h_1, h_2} be the closure of D^{h_1, h_2} and denotes the set of interior and boundary grid points and

$$D^{h_1, h_2} \gamma_\tau = D^{h_1, h_2} \times \gamma_\tau = \{(x, t) : x \in D^{h_1, h_2}, t \in \gamma_\tau\},$$

where, γ_τ is as given in (2.13). The following unconditionally stable 14-point implicit method on rectangular grids is taken which is derived from using the 9-point scheme for the approximation of the Laplacian operator and approximates the first type boundary value problem (3.2)-(3.4) when the value of the constant $b = 0$ in (3.2) (see Samarskii [34]).

$$\Gamma u_{h, \tau} = \omega \sigma_1 \Lambda_1 u_{h, \tau}^{k+1} + \omega (1 - \sigma_1) \Lambda_1 u_{h, \tau}^k + \omega \sigma_2 \Lambda_2 u_{h, \tau}^{k+1} + \omega (1 - \sigma_2) \Lambda_2 u_{h, \tau}^k \\ + \omega \frac{h_1^2 + h_2^2}{24} \Lambda_1 \Lambda_2 u_{h, \tau}^{k+1} + \beta \text{ on } D^{h_1, h_2} \gamma_\tau \quad (4.13)$$

$$u_{h, \tau} = \varphi(x_1, x_2), t = 0, \text{ on } \bar{D}^{h_1, h_2}, \quad (4.14)$$

$$u_{h, \tau} = \phi(x_1, x_2, t) \text{ on } S_T^h \quad (4.15)$$

where,

$$\sigma_1 = \frac{1}{2} - \frac{h_1^2}{12\tau}, \quad \sigma_2 = \frac{1}{2} - \frac{h_2^2}{12\tau} \quad (4.16)$$

$$\Gamma u = \frac{u(x_1, x_2, t + \tau) - u(x_1, x_2, t)}{\tau} \quad (4.17)$$

$$\Lambda_1 u^k = (u(x_1 + h_1, x_2, t) - 2u(x_1, x_2, t) + u(x_1 - h_1, x_2, t)) / h_1^2 \quad (4.18)$$

$$\Lambda_2 u^k = (u(x_1, x_2 + h_2, t) - 2u(x_1, x_2, t) + u(x_1, x_2 - h_2, t)) / h_2^2 \quad (4.19)$$

$$\beta = \tilde{f} + \frac{h_1^2}{12} \Lambda_1 \tilde{f} + \frac{h_2^2}{12} \Lambda_2 \tilde{f} \text{ and } \tilde{f} = f\left(x_1, x_2, t + \frac{\tau}{2}\right) \quad (4.20)$$

In Example 4.4 and Example 4.5 the value of the constant b in (3.2) is zero, hence both problems are solved by the given implicit method HADP and by the implicit method (4.13)-(4.15). In Example 4.6 the constant b is 0.5 and the problem is solved by HADP. Tables and figures given in this section adopt the following notations:

M_{14P}^H denotes the proposed implicit method HADP on hexagonal grids.

M_{14P}^R denotes the 14-point implicit method on rectangular grids given in (4.13)-(4.15).

$N^{h,\tau}(M_{14P}^H)$ shows the number of grid points in the stiffness matrix obtained by the method M_{14P}^H for the the corresponding values of h and τ .

$N^{h,\tau}(M_{14P}^R)$ shows the number of grid points in the stiffness matrix obtained by the method M_{14P}^R for the the corresponding values of h and τ

$Pre^{h,\tau}(M_{14P}^H)$ is the preconditioning time of the stiffness matrix obtained by the method M_{14P}^H .

$Pre^{h,\tau}(M_{14P}^R)$ is the preconditioning time of the stiffness matrix obtained by the method M_{14P}^R .

$Con^{h,\tau}(M_{14P}^H)$ is the condition number of the preconditioned stiffness matrix obtained by the method M_{14P}^H .

$Con^{h,\tau}(M_{14P}^R)$ is the condition number of the preconditioned stiffness matrix obtained by the method M_{14P}^R .

$CT^{M_{14P}^H}$ presents the Central Processing Unit time in seconds per time level for the method M_{14P}^H .

$CT^{M_{14P}^R}$ presents the Central Processing Unit time in seconds per time level for the method M_{14P}^R .

$TCT^{M_{14P}^H}$ shows the total Central Processing Unit time in seconds required for the solution at $t = 1$, by the method M_{14P}^H .

$TCT^{M_{14P}^R}$ shows the total Central Processing Unit time in seconds required for the solution at $t = 1$, by the method M_{14P}^R .

$TCT^{M_{An(S')}} is the total Central Processing Unit time in seconds required for the solution at $t = 1$, by the analytical method when the infinite series in the formula are approximated by taking S' number of terms.$

neg means that *CPUs* is less than one milliseconds.

The numerical solution obtained by the proposed method M_{14P}^H is denoted by $u_{2^{-\mu}, 2^{-\lambda}}^H$ for $h = 2^{-\mu}$ and $\tau = 2^{-\lambda}$ where μ, λ are positive integers. Analogously the numerical solution obtained by the method M_{14P}^R is denoted by $u_{2^{-\mu}, 2^{-\lambda}}^R$. On the grid points $\overline{D^h \gamma_\tau}$, which is the closure of $D^h \gamma_\tau$ we present the error function $\epsilon_{h, \tau}$ obtained by the given method M_{14P}^H by $\epsilon^{M_{14P}^H(h, \tau)}$ and on the grid points $\overline{D^{h_1, h_2} \gamma_\tau}$, (closure of $D^{h_1, h_2} \gamma_\tau$) we use $\epsilon^{M_{14P}^R(h, \tau)}$ to show the error function $\epsilon_{h, \tau}$ obtained by the method M_{14P}^R . Also maximum norm of the errors $\max_{\overline{D^h \gamma_\tau}} \left| \epsilon^{M_{14P}^H(h, \tau)} \right|$ and $\max_{\overline{D^{h_1, h_2} \gamma_\tau}} \left| \epsilon^{M_{14P}^R(h, \tau)} \right|$ are denoted by $\left\| \epsilon^{M_{14P}^H(h, \tau)} \right\|_\infty$, and $\left\| \epsilon^{M_{14P}^R(h, \tau)} \right\|_\infty$, respectively. Further, we give the order of convergence of the approximate solution $u_{2^{-\mu}, 2^{-\lambda}}^H$ and $u_{2^{-\mu}, 2^{-\lambda}}^R$ to the exact solution u obtained by using the methods M_{14P}^H and M_{14P}^R respectively with

$$\mathfrak{R}^{M_{14P}^H} = \log_2 \left(\frac{\left\| \mathfrak{E}^{M_{14P}^H(2^{-\mu}, 2^{-\lambda})} \right\|_{\infty}}{\left\| \mathfrak{E}^{M_{14P}^H(2^{-(\mu+1)}, 2^{-(\lambda+2)})} \right\|_{\infty}} \right), \quad (4.21)$$

$$\mathfrak{R}^{M_{14P}^R} = \log_2 \left(\frac{\left\| \mathfrak{E}^{M_{14P}^R(2^{-\mu}, 2^{-\lambda})} \right\|_{\infty}}{\left\| \mathfrak{E}^{M_{14P}^R(2^{-(\mu+1)}, 2^{-(\lambda+2)})} \right\|_{\infty}} \right) \quad (4.22)$$

accordingly. In Example 4.1 and Example 4.2 the realization of the method M_{14P}^R is given by taking $h_1 = h$ and $h_2 = \frac{\sqrt{3}}{2}h$.

Example 4.4:

$$\begin{aligned} \frac{\partial u}{\partial t} &= \frac{\partial^2 u}{\partial x_1^2} + \frac{\partial^2 u}{\partial x_2^2} + f(x_1, x_2, t) \text{ on } Q_T, \\ u(x_1, x_2, 0) &= 0.07x_1^{6+\alpha} + 0.3x_2^{6+\alpha} + 1 \text{ on } \bar{D} \\ u(x_1, x_2, t) &= v(x_1, x_2, t) \text{ on } S_T, \end{aligned} \quad (4.23)$$

where the heat source and the exact solution are,

$$\begin{aligned} f(x_1, x_2, t) &= \left(3 + \frac{\alpha}{2}\right) t^{2+\frac{\alpha}{2}} \cos\left(t^{3+\frac{\alpha}{2}}\right) - e^{-t} - (6+\alpha)(5+\alpha) [0.07x_1^{4+\alpha} + 0.3x_2^{4+\alpha}] \\ v(x_1, x_2, t) &= 0.07x_1^{6+\alpha} + 0.3x_2^{6+\alpha} + \sin\left(t^{3+\frac{\alpha}{2}}\right) + e^{-t} \end{aligned} \quad (4.24)$$

respectively.

Table 4.9, demonstrates the $CT^{M_{14P}^H}$, $CT^{M_{14P}^R}$ and the maximum norm of the errors for $h = 2^{-\mu}$, $\mu = 4, 5, 6, 7, 8$ when $\tau = 2^{-\lambda}$, $\lambda = 6, 8, 10, 12, 14$ and the order of convergences $\mathfrak{R}^{M_{14P}^H}$, $\mathfrak{R}^{M_{14P}^R}$ when $\alpha = 0.8$. Table 4.10, shows the same quantities by using the methods M_{14P}^H and M_{14P}^R when $\alpha = 0.01$. These tables show that both methods have fourth order convergence in spatial variables and second order convergence in time variable. On the other hand the second column and fifth columns of these tables show the computational time required in seconds per time level $CT^{M_{14P}^H}$ and $CT^{M_{14P}^R}$ for the method M_{14P}^H and M_{14P}^R respectively. By analyzing the

Table 4.9: Computational time, maximum norm of the errors and the order of convergence obtained by using the proposed method M_{14P}^H and the method M_{14P}^R for the Example 4.4 when $\alpha = 0.8$.

(h, τ)	$CT^{M_{14P}^H}$	$\ \epsilon^{M_{14P}^H(h, \tau)}\ _{\infty}$	$\mathfrak{R}^{M_{14P}^H}$	$CT^{M_{14P}^R}$	$\ \epsilon^{M_{14P}^R(h, \tau)}\ _{\infty}$	$\mathfrak{R}^{M_{14P}^R}$
$(2^{-4}, 2^{-6})$	<i>neg</i>	$4.19389E - 5$		<i>neg</i>	$4.26584E - 5$	
$(2^{-5}, 2^{-8})$	0.047	$2.62266E - 6$	3.9992	0.047	$2.66787E - 6$	3.9991
$(2^{-6}, 2^{-10})$	0.156	$1.63922E - 7$	3.9999	0.234	$1.66749E - 7$	3.9999
$(2^{-7}, 2^{-12})$	0.641	$1.02449E - 8$	4.0000	1.016	$1.04224E - 8$	3.9999
$(2^{-8}, 2^{-14})$	2.578	$6.40304E - 10$	4.0000	4.312	$6.51384E - 10$	4.0000

values of $CT^{M_{14P}^H}$ and $CT^{M_{14P}^R}$ we conclude that the proposed method is more economical in computational time per time when the block preconditioning of the conjugate gradient method is used. This conclusion is also supported by the results given in Table 4.11 which demonstrates the number of grid points $N^{h, \tau}(M_{14P}^H)$ and $N^{h, \tau}(M_{14P}^R)$ in the stiffness matrices, the preconditioning times $Pre^{h, \tau}(M_{14P}^H)$ and $Pre^{h, \tau}(M_{14P}^R)$, the condition numbers of the preconditioned matrices $Con^{h, \tau}(M_{14P}^H)$ and $Con^{h, \tau}(M_{14P}^R)$ and the total computational time required in seconds $TCT^{M_{14P}^H}$ and $TCT^{M_{14P}^R}$ by the methods M_{14P}^H and M_{14P}^R , respectively for the Example 4.1. The Figure 4.5, demonstrates the absolute error function $\left| \epsilon^{M_{14P}^H(2^{-6}, 2^{-10})} \right|$, at time moments $t = 0.25, 0.5, 0.75, 1$ obtained by using the proposed method M_{14P}^H for the numerical solution of Example 4.4 when $h = 2^{-6}$ and $\tau = 2^{-10}$ for $\alpha = 0.8$. Analogously, Figure 4.6 shows the absolute error function $\left| \epsilon^{M_{14P}^R(2^{-6}, 2^{-10})} \right|$ at the same time moments obtained by the method M_{14P}^R when $h = 2^{-6}$ and $\tau = 2^{-10}$ for $\alpha = 0.8$.

Next we consider the test problem in Example 4.5 taken from Henner et al. [39]:

Table 4.10: Computational time, maximum norm of the errors and the order of convergence obtained by using the proposed method M_{14P}^H and the method M_{14P}^R for the Example 4.4 when $\alpha = 0.01$.

(h, τ)	$CT^{M_{14P}^H}$	$\ \mathcal{E}^{M_{14P}^H(h, \tau)}\ _{\infty}$	$\mathfrak{R}^{M_{14P}^H}$	$CT^{M_{14P}^R}$	$\ \mathcal{E}^{M_{14P}^R(h, \tau)}\ _{\infty}$	$\mathfrak{R}^{M_{14P}^R}$
$(2^{-4}, 2^{-6})$	neg	$4.19389E-5$		neg	$2.98695E-5$	
$(2^{-5}, 2^{-8})$	0.047	$2.62266E-6$	3.9994	0.047	$1.86757E-6$	3.9994
$(2^{-6}, 2^{-10})$	0.188	$1.63922E-7$	3.9999	0.219	$1.16726E-7$	3.9999
$(2^{-7}, 2^{-12})$	0.64	$1.02449E-8$	4.0000	1.016	$7.29597E-9$	3.9999
$(2^{-8}, 2^{-14})$	2.5	$6.40298E-10$	4.0000	4.25	$4.56001E-10$	3.9999

Table 4.11: sizes of the stiffness matrices, preconditioning times and the condition numbers of the preconditioned stiffness matrices and the total computational time required by the methods M_{14P}^H and M_{14P}^R for the Example 4.4 when $\alpha = 0.8$.

(h, τ)	$(2^{-4}, 2^{-6})$	$(2^{-5}, 2^{-8})$	$(2^{-6}, 2^{-10})$	$(2^{-7}, 2^{-12})$	$(2^{-8}, 2^{-14})$
$N^{h, \tau}(M_{14P}^H)$	233	977	4001	16193	65153
$N^{h, \tau}(M_{14P}^R)$	225	961	3969	16129	65025
$Pre^{h, \tau}(M_{14P}^H)$	neg	neg	0.063	0.36	2.797
$Pre^{h, \tau}(M_{14P}^R)$	neg	neg	0.062	0.359	2.625
$Con^{h, \tau}(M_{14P}^H)$	0.99997	0.99993	0.99989	0.99986	0.99983
$Con^{h, \tau}(M_{14P}^R)$	0.99991	0.99988	0.99987	0.99985	0.99981
$TCT^{M_{14P}^H}$	0.61	9.09	194.84	2659.03	42582.52
$TCT^{M_{14P}^R}$	0.70	11.83	272.91	4258.53	71073.79

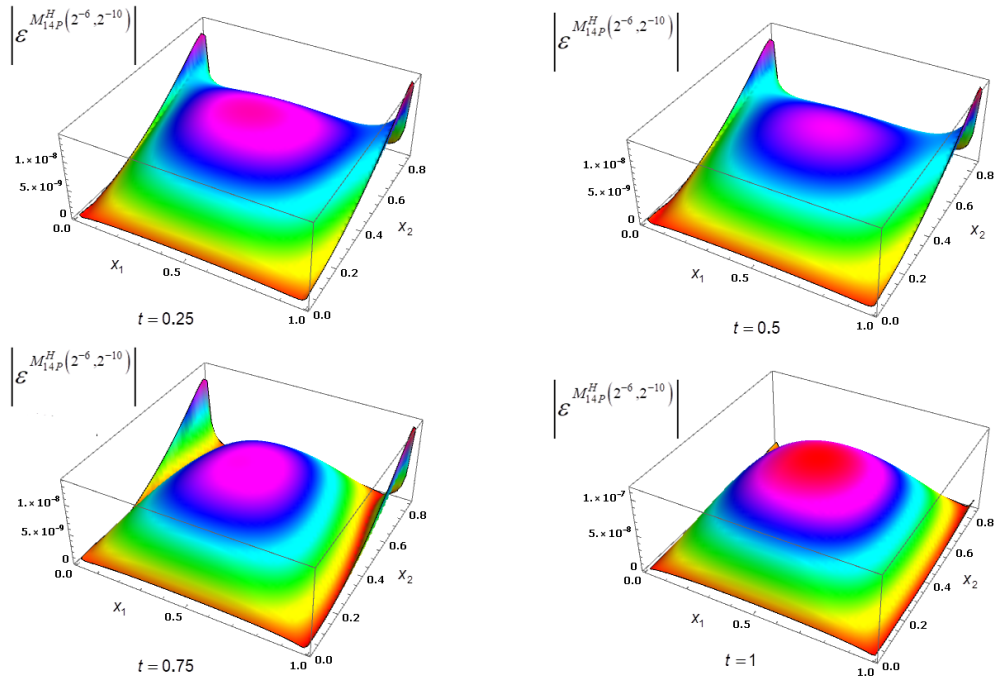


Figure 4.5: The absolute error function $|\mathcal{E}^{M_{14P}^H(2^{-6}, 2^{-10})}|$, at time moments $t = 0.25, 0.5, 0.75, 1$ obtained by using the proposed method M_{14P}^H for the Example 4.4.

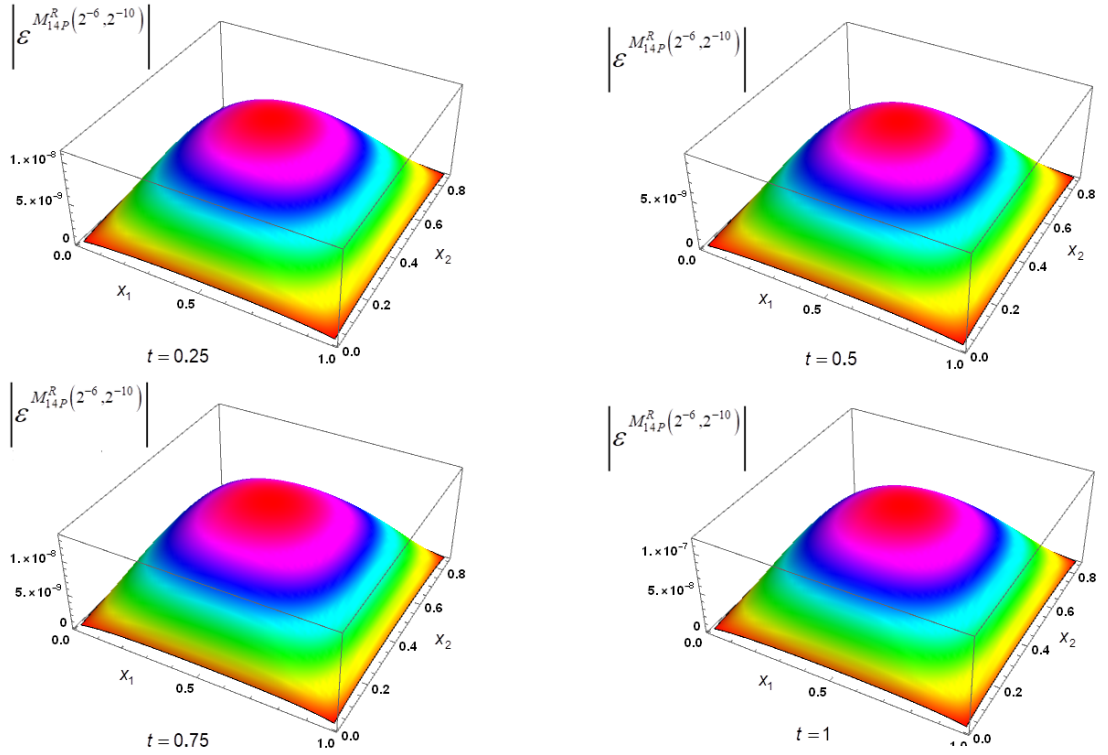


Figure 4.6: The absolute error function $\left| \mathcal{E}^{M_{14P}^R(2^{-6}, 2^{-10})} \right|$, at time moments $t = 0.25, 0.5, 0.75, 1$ obtained by using the proposed method M_{14P}^R for the Example 4.4.

Example 4.5:

$$\begin{aligned} \frac{\partial u}{\partial t} &= 0.25 \left(\frac{\partial^2 u}{\partial x_1^2} + \frac{\partial^2 u}{\partial x_2^2} \right) \text{ on } Q_T, \\ u(x_1, x_2, 0) &= 0.01x_1x_2(1-x_1) \left(\frac{\sqrt{3}}{2} - x_2 \right) \text{ on } \bar{D}, \\ u(x_1, x_2, t) &= 0 \text{ on } S_T, \end{aligned}$$

The exact solution of the problem in Example 4.5 is not given. However, using Fourier method the analytical solution was obtained in Henner et al. [39] as follows

$$\begin{aligned} u(x_1, x_2, t) &= \frac{64Al_{x_1}^2 l_{x_2}^2}{\pi^6} \sum_{n,m=1}^{\infty} \frac{e^{-\lambda_{nm} a^2 t}}{(2n+1)^2 (2m+1)^2} \sin \frac{(2n+1)\pi x_1}{l_{x_1}} \\ &\quad \sin \frac{(2m+1)\pi x_2}{l_{x_2}} \end{aligned} \quad (4.25)$$

For the given example we take, $a^2 = \omega = 0.25, A = 0.01, l_{x_1} = 1, l_{x_2} = \frac{\sqrt{3}}{2}$, and

$$\lambda_{nm} = \pi^2 \left(\frac{n^2}{l_{x_1}^2} + \frac{m^2}{l_{x_2}^2} \right). \quad (4.26)$$

By applying the proposed implicit method M_{14P}^H we obtain the approximate solution $u_{2^{-\mu}, 2^{-\lambda}}^H(x_1, x_2, t)$ at each time level for $\mu = 4, 5, 6$, and $\lambda = 10, 12, 14$ respectively. Table 4.12 presents $u_{2^{-\mu}, 2^{-\lambda}}^H(x_1, x_2, t)$ at the grid points $\left(0.125, \frac{\sqrt{3}}{16}, 1\right)$, $\left(0.25, \frac{\sqrt{3}}{16}, 1\right)$, $\left(0.375, \frac{\sqrt{3}}{16}, 1\right)$, $\left(0.5, \frac{\sqrt{3}}{16}, 1\right)$, $\left(0.625, \frac{\sqrt{3}}{16}, 1\right)$, $\left(0.75, \frac{\sqrt{3}}{16}, 1\right)$ and $\left(0.875, \frac{\sqrt{3}}{16}, 1\right)$ and the order of convergence $\mathfrak{R}_{h,\tau}^{M_{14P}^H}(P)$ at the point $P(x_1, x_2, t)$ given as

$$\mathfrak{R}_{h,\tau}^{M_{14P}^H}(P) = \log_2 \left| \frac{u_{2^{-4}, 2^{-10}}^H(P) - u_{2^{-5}, 2^{-12}}^H(P)}{u_{2^{-5}, 2^{-12}}^H(P) - u_{2^{-6}, 2^{-14}}^H(P)} \right|. \quad (4.27)$$

Table 4.13 shows the numerical solution $u_{2^{-\mu}, 2^{-\lambda}}^R(x_1, x_2, t)$ obtained by the method M_{14P}^R at the same grid points and the corresponding order of convergence $\mathfrak{R}_{h,\tau}^{M_{14P}^R}(P)$ at the point $P(x_1, x_2, t)$ given by

$$\mathfrak{R}_{h,\tau}^{M_{14P}^R}(P) = \log_2 \left| \frac{u_{2^{-4}, 2^{-10}}^R(P) - u_{2^{-5}, 2^{-12}}^R(P)}{u_{2^{-5}, 2^{-12}}^R(P) - u_{2^{-6}, 2^{-14}}^R(P)} \right|. \quad (4.28)$$

Analyzing the values of (4.27) and (4.28) in the fifth columns of Table 4.12, and Table 4.13 we conclude that for both methods the convergence follow the 4th order in the spatial variables and 2nd order in time variable. Further, Table 4.14 illustrates the computational cost comparisons of the methods M_{14P}^H, M_{14P}^R and by the analytical method $TCT^{M_{An(200)}}$ when the infinite series in the explicit solution are computed by taking 200. This table shows the number of grid points in the stiffness matrices $N^{h,\tau}(M_{14P}^H)$ and $N^{h,\tau}(M_{14P}^R)$, the preconditioning times $Pre^{h,\tau}(M_{14P}^H)$ and $Pre^{h,\tau}(M_{14P}^R)$, the condition numbers of the preconditioned stiffness matrices $Con^{h,\tau}(M_{14P}^H), Con^{h,\tau}(M_{14P}^R)$ and the total computational time required in seconds

Table 4.12: Solution at some points on $t = 1$, and the order of convergence obtained by M_{14P}^H for the Example 4.5.

P	$u_{2^{-4}, 2^{-10}}^H(P)$	$u_{2^{-5}, 2^{-12}}^H(P)$	$u_{2^{-6}, 2^{-14}}^H(P)$	$\mathfrak{R}_{h, \tau}^{M_{14P}^H}(P)$
$\left(0.125, \frac{\sqrt{3}}{16}, 1\right)$	$4.84787E - 5$	$4.84769E - 5$	$4.84768E - 5$	4.00078
$\left(0.25, \frac{\sqrt{3}}{16}, 1\right)$	$8.31064E - 5$	$8.31033E - 5$	$8.31031E - 5$	4.00027
$\left(0.375, \frac{\sqrt{3}}{16}, 1\right)$	$1.03883E - 4$	$1.03879E - 4$	$1.03879E - 4$	4.00016
$\left(0.5, \frac{\sqrt{3}}{16}, 1\right)$	$1.10808E - 4$	$1.10804E - 4$	$1.10804E - 4$	4.00001
$\left(0.625, \frac{\sqrt{3}}{16}, 1\right)$	$1.03883E - 4$	$1.03879E - 4$	$1.03879E - 4$	4.00016
$\left(0.75, \frac{\sqrt{3}}{16}, 1\right)$	$8.31064E - 5$	$8.31033E - 5$	$8.31032E - 5$	4.00027
$\left(0.875, \frac{\sqrt{3}}{16}, 1\right)$	$4.84787E - 5$	$4.84769E - 5$	$4.84768E - 5$	4.00078

$TCT^{M_{14P}^H}$, $TCT^{M_{14P}^R}$ of the methods M_{14P}^H and M_{14P}^R respectively for the Example 4.4.

Analyzing the data in Table 4.14 we conclude that the given implicit method M_{14P}^H is computationally more time efficient when block preconditioning for the conjugate gradient method is used. Although the stiffness matrix in the obtained algebraic linear systems at each time level has 7 nonzero diagonals the method M_{14P}^H requires the value of 7 net points of each hexagon from the previous time level. When M_{14P}^R is used the stiffness matrix has 5 nonzero diagonals and the method uses the values of 9 points of the pattern of the rectangular net from the previous time level. Since the constructed preconditioner for specific h and τ values is reused over the time levels the cost of the preconditioner is amortized but the use of 9 points rather than 7 points from the previous time level increases the computational time required by the method M_{14P}^R to solve the algebraic system of equations over the time moments. Figure 4.7 illustrates the approximate solution $u_{2^{-6}, 2^{-10}}^H(x_1, x_2, t)$ for the Example 4.5 obtained by using the given method M_{14P}^H at time moments $t = 0.25, 0.5, 0.75, 1$, whereas the approximate solution $u_{2^{-6}, 2^{-10}}^R(x_1, x_2, t)$ at the same time moments is presented in Figure 4.8 obtained by the method M_{14P}^R .

Table 4.13: Solution at some points on $t = 1$, and the order of convergence obtained by M_{14P}^R for the Example 4.5.

P	$u_{2^{-4}, 2^{-10}}^R(P)$	$u_{2^{-5}, 2^{-12}}^R(P)$	$u_{2^{-6}, 2^{-14}}^R(P)$	$\mathfrak{R}_{h, \tau}^{M_{14P}^R}(P)$
$(0.125, \frac{\sqrt{3}}{16}, 1)$	$4.847746E - 5$	$4.847687E - 5$	$4.847683E - 5$	4.00011
$(0.25, \frac{\sqrt{3}}{16}, 1)$	$8.310411E - 5$	$8.310320E - 5$	$8.310314E - 5$	4.00003
$(0.375, \frac{\sqrt{3}}{16}, 1)$	$1.038801E - 4$	$1.038790E - 4$	$1.038789E - 4$	4.00001
$(0.5, \frac{\sqrt{3}}{16}, 1)$	$1.108054E - 4$	$1.108042E - 4$	$1.108041E - 4$	4.00001
$(0.625, \frac{\sqrt{3}}{16}, 1)$	$1.038801E - 4$	$1.0387890E - 4$	$1.038790E - 4$	4.00001
$(0.75, \frac{\sqrt{3}}{16}, 1)$	$8.310411E - 5$	$8.310320E - 5$	$8.310314E - 5$	4.00003
$(0.875, \frac{\sqrt{3}}{16}, 1)$	$4.847746E - 5$	$4.847687E - 5$	$4.847683E - 5$	4.00011

Table 4.14: Computational efficiency comparison of the methods M_{14P}^H , M_{14P}^R , and $M_{An(200)}$ for the solution at $t = 1$ for the Example 4.5.

(h, τ)	$(2^{-4}, 2^{-8})$	$(2^{-5}, 2^{-10})$	$(2^{-6}, 2^{-12})$
$N^{h, \tau}(M_{14P}^H)$	233	977	4001
$N^{h, \tau}(M_{14P}^R)$	225	961	3969
$Pre^{h, \tau}(M_{14P}^H)$	neg	0.016	0.078
$Pre^{h, \tau}(M_{14P}^R)$	neg	0.015	0.063
$Con^{h, \tau}(M_{14P}^H)$	0.99997	0.99993	0.99989
$Con^{h, \tau}(M_{14P}^R)$	0.99991	0.99988	0.99987
$TCT^{M_{14P}^H}$	2.45	38.20	864.88
$TCT^{M_{14P}^R}$	2.78	47.25	983.63
$TCT^{M_{An(200)}}$	53,124	891,024	14,595,648

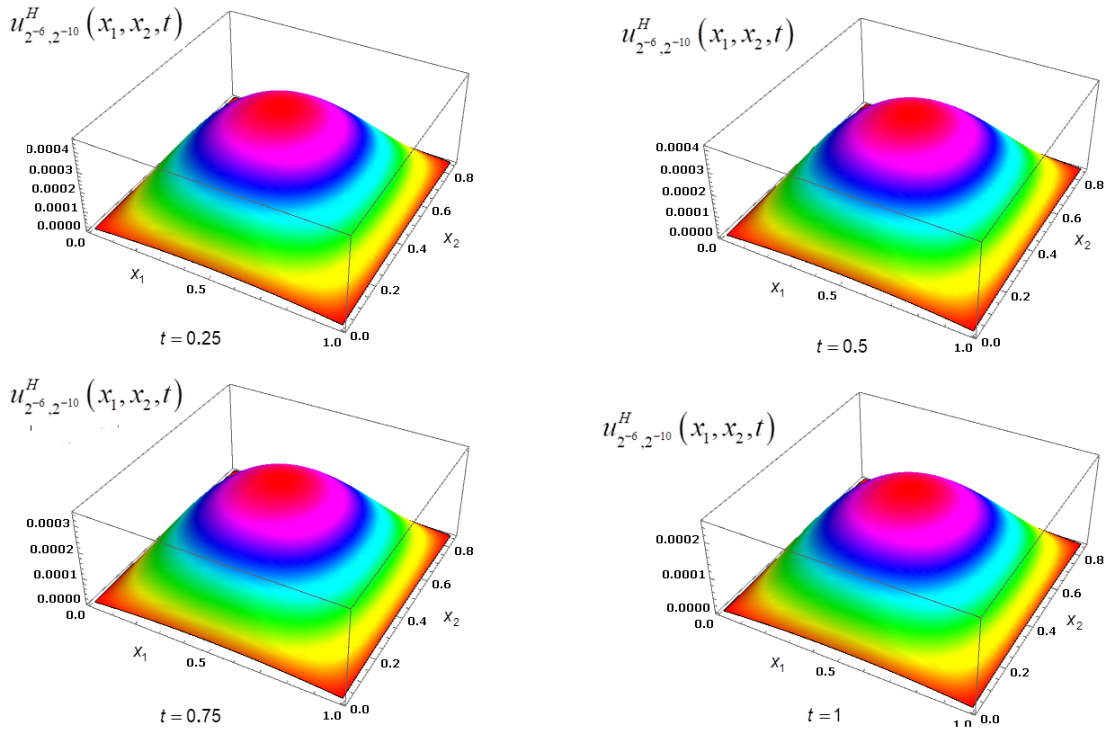


Figure 4.7: The approximate solution $u_{2^{-6}, 2^{-10}}^H(x_1, x_2, t)$ for the Example 4.5 obtained by using the given method M_{14P}^H at time moments $t = 0.25, 0.5, 0.75, 1$.

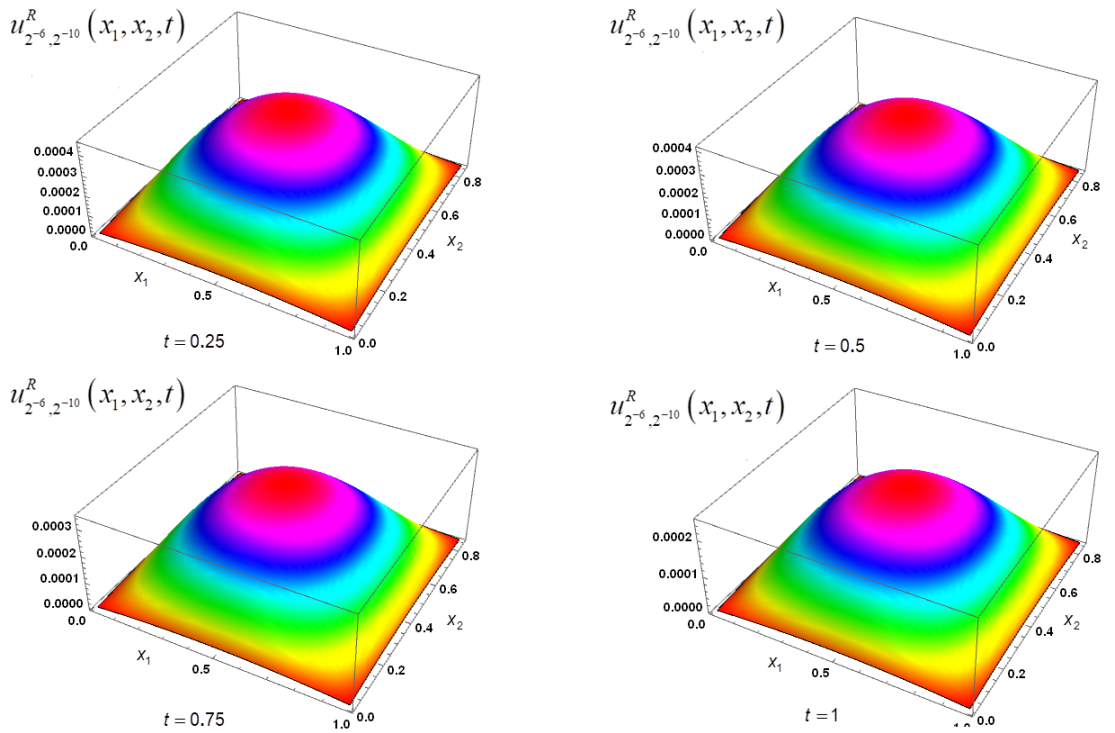


Figure 4.8: The approximate solution $u_{2^{-6}, 2^{-10}}^R(x_1, x_2, t)$ for the Example 4.5 obtained by using the given method M_{14P}^R at time moments $t = 0.25, 0.5, 0.75, 1$.

Table 4.15: Computational times, maximum norm of the errors and the order of convergence obtained by using the proposed method M_{14P}^H for the Example 4.6.

(h, τ)	$CT^{M_{14P}^H}$	$TCT^{M_{14P}^H}$	$\ \epsilon^{M_{14P}^H(h, \tau)}\ _{\infty}$	$\mathfrak{R}^{M_{14P}^H}$
$(2^{-4}, 2^{-6})$	neg	0.61	$2.378442E - 5$	
$(2^{-5}, 2^{-8})$	0.047	9.907	$1.543029E - 6$	3.9462
$(2^{-6}, 2^{-10})$	0.172	207.547	$1.015411E - 7$	3.9256
$(2^{-7}, 2^{-12})$	0.735	2904.99	$6.623985E - 9$	3.9382
$(2^{-8}, 2^{-14})$	2.829	50743	$4.251592E - 10$	3.9616

Example 4.6:

$$\begin{aligned} \frac{\partial u}{\partial t} &= \frac{\partial^2 u}{\partial x_1^2} + \frac{\partial^2 u}{\partial x_2^2} - 0.5u + f(x_1, x_2, t) \text{ on } Q_T, \\ u(x_1, x_2, 0) &= \frac{1}{2}x_1^{\frac{37}{6}} + x_2^{\frac{37}{6}} + 1 \text{ on } \bar{D} \\ u(x_1, x_2, t) &= v(x_1, x_2, t) \text{ on } S_T, \end{aligned}$$

where the heat source and the exact solution are,

$$\begin{aligned} f(x_1, x_2, t) &= -\left(\frac{37}{12}t^{\frac{25}{12}} \sin\left(t^{\frac{37}{12}}\right) + \frac{1147}{72}x_1^{\frac{25}{6}} + \frac{1147}{36}x_2^{\frac{25}{6}}\right) \\ &\quad + 0.5\left(\frac{1}{2}x_1^{\frac{37}{6}} + x_2^{\frac{37}{6}} + \cos\left(t^{\frac{37}{12}}\right)\right) \\ v(x_1, x_2, t) &= \frac{1}{2}x_1^{\frac{37}{6}} + x_2^{\frac{37}{6}} + \cos\left(t^{\frac{37}{12}}\right) \end{aligned}$$

respectively.

Table 4.15, demonstrates the $CT^{M_{14P}^H}$, $TCT^{M_{14P}^H}$ and the maximum norm of the errors for $h = 2^{-\mu}$, $\mu = 4, 5, 6, 7, 8$ when $\tau = 2^{-\lambda}$, $\lambda = 6, 8, 10, 12, 14$ and the order of convergences $\mathfrak{R}^{M_{14P}^H}$ of $u_{h, \tau}^H(x_1, x_2, t)$ to the exact solution u with respect to h and τ obtained by using the proposed method M_{14P}^H . Figure 4.9 shows the absolute error function $\left|\epsilon^{M_{14P}^H(2^{-6}, 2^{-10})}\right|$ at time moments $t = 0.25, 0.5, 0.75, 1$ obtained by the given method M_{14P}^H for the Example 4.6.

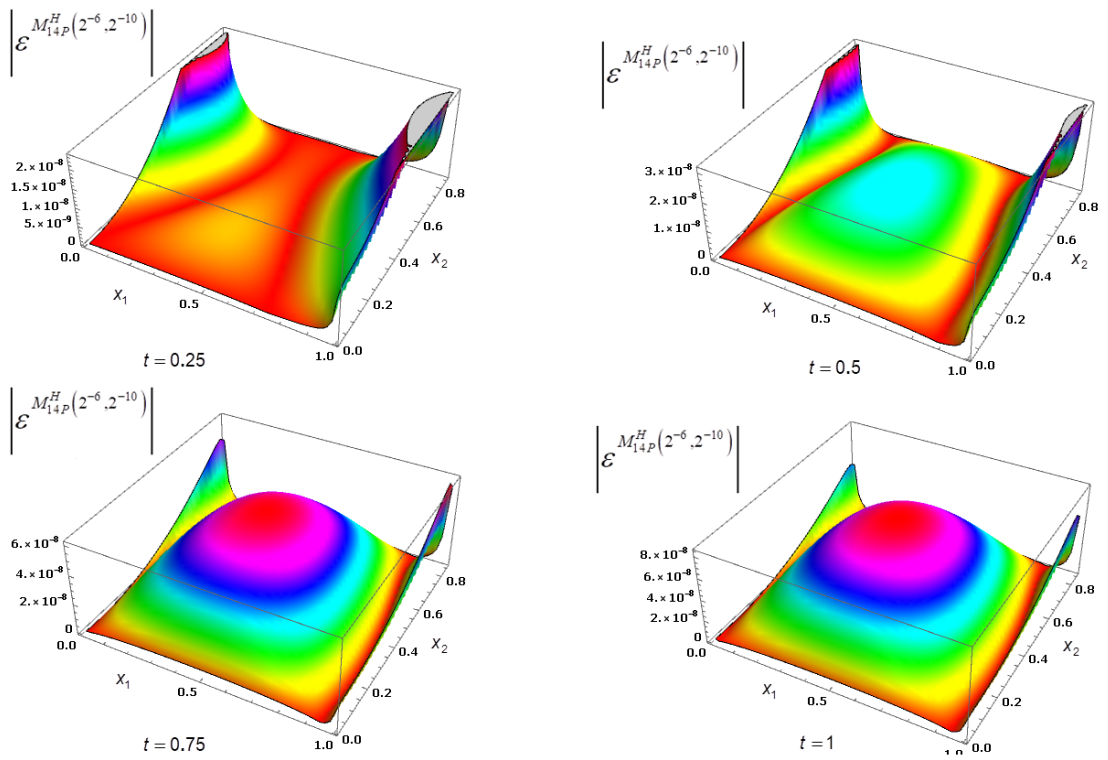


Figure 4.9: The absolute error function $\left| \mathcal{E}^{M_{14P}^H(2^{-6}, 2^{-10})} \right|$, at time moments $t = 0.25, 0.5, 0.75, 1$ obtained by using the proposed method M_{14P}^H for the Example 4.6.

Chapter 5

CONCLUSION AND FURTHER RESEARCH

Using hexagonal grids we proposed two unconditionally stable two layer implicit difference problems with 14-point for the solution of first type boundary value problem of heat equation (2.9) - (2.11) in two space dimensions on special polygons. Furthermore, an implicit method of high accuracy on hexagonal grids for the approximation of the solution of first type boundary value problem (3.2) - (3.4) is given. The methodology given in this research may be extended to the following research topics.

1. Construction of the highly accurate splitting schemes (fractional step methods) and using alternating direction methods (ADI) (see Peaceman and Rachford [40], Douglas [41], Bagrinovskii and Godunov [42] and Marchuk [43]) for the solution of first type boundary value problem of heat equation in three space dimension.
2. Construction of the special difference problems for the first order derivatives of the solution of first type boundary value problem of two dimensional heat equation on rectangle with respect to the space variables. For the derivative of the solution of first type boundary value problem of one dimensional heat equation, with respect to the space variable see Buranay and Farinola [44].
3. Construction of implicit method for the approximation of the solution to heat equation on domains with smooth boundary.

REFERENCES

- [1] Dryja M.: Difference and finite-element methods for the dynamical problem of thermodiffusion in an elastic solid. *Archives of Mechanics, Archivum Mechaniki Stosowanej*, **29**(1), 81-96, (1977).
- [2] Ehrlich R., Hurwitz H.JR.: Multigroup methods for neutron problems. *Nucleonics*, **12**, p.23(1954).
- [3] Ahmed N., Ali M., Baleanu D., Rafiq M., ur Rehman, M. A.: Numerical analysis of diffusive susceptible-infected-recovered epidemic model in three space dimension. *Chaos, Solitons and Fractals*, **132**, UNSP 109535, 1-10(2020)
- [4] Iqbal Z., Ahmed N., Baleanu D., Rafiq M., Iqbal M.S., ur-Rehman M. A.: Structure preserving computational technique for fractional order Schnakenberg model. *Computational and Applied Mathematics* 39 (2), 61,1-18(2020).
- [5] Sadourney R., Arakawa A., Mintz Y.: Integration of the nondivergent barotropic vorticity equation with an icosahedral-hexagonal grid for the sphere. *Mon. Wea. Rev.*, **96**, 351-356(1968).
- [6] Williamson D.: Integration of the barotropic vorticity equation on a spherical

geodesic grid. *Tellus*, **20**, 642-653(1968).

[7] Sadourney R.: Numerical integration of the primitive equation on a spherical grid with hexagonal cells. Proceedings of the WMOTUGG Symposium on Numerical Weather Prediction, Vol. VII. WMO., 45-77(1969).

[8] Sadourney R., Morel P.: A finite-difference approximation of the primitive equations for a hexagonal grid on a plane. *Mon. Wea. Rev.*, **97**, 439-445(1969).

[9] Masuda Y.: A finite difference scheme by making use of hexagonal mesh-points, Proceedings of the WMO/IUGG Symposium on Numerical Weather Prediction in Tokyo, Nov. 26-Dec. 4, 1968. *Teck.Rep. of JMA*, VII35-VII44, (1969).

[10] Masuda Y., Ohnishi H.: An integration scheme of the primitive equation model with an icosahedral-hexagonal grid system and its application to the shallow water equation, Short and Medium range Numerical weather Prediction collection of Papers Presented at the WMO/IUGG Symposium on Numerical Weather Prediction, in Tokyo, 4-8 August, 317-326, (1986).

[11] Thacker W.C.: Irregular grid finite difference techniques: Simulations of oscillations in shallow circular basins. *J. Phys. Oceanogr.*, **7**, 284-292(1977).

- [12] Thacker W.C.: Comparison of finite element and finite difference schemes, Part II: Two dimensional gravity wave motion. *J. Phys. Oceanogr.*, **8**, 680-689(1978).
- [13] Salmon R., Talley M.L.: Generalization of Arakawa Jacobian. *J. Comput. Physics*, **83**, 246-259(1989).
- [14] Ničkovič S.: On the use of hexagonal grids for simulation of atmospheric processes. *Contrib. Atmos. Phys.*, **67**, 103-107(1994).
- [15] Ničkovič S., Gavrilov M.B., Tosič, I.A.: Geostrophic Adjustment on Hexagonal Grids. *Mon. Wea. Rev.*, **130**. 668-683(2002).
- [16] Pruess K., Bodvarsson G.S.: A seven-point finite difference method for improved grid orientation performance in pattern steam floods, Lawrence Berkeley National Laboratory, LBL-16430, 1-32, (1983).
- [17] Richtmyer R.D., Morton K.W.: Difference methods for initial-value problems. Interscience Publishers a division of Jhon Wiley and Sons, Second Edition, 1967.
- [18] Kara S.: High-order approximation of 2D convection-diffusion equation on hexagonal grids, Wiley Interscience, 1239-1246, (2005), DOI

10.1002/num.20149.

- [19] Lee D., Tien H. C., Luo C. P. and Luk H.-N.: Hexagonal grid methods with applications to partial differential equations. *Int. J. of Comput, Math.*, **91**(9), 1986-2009(2014).
- [20] Dosiyevev A.A., Celiker E.: Approximation on the hexagonal grid of the Dirichlet problem for Laplace's equation. *Boundary Value Problems*, 2014:**73**, 1-19(2014).
- [21] Dosiyevev A.A., Celiker E.: A fourth order block-hexagonal grid approximation for the solution of Laplace's equation with singularities. *Advances in Difference Equations*, 2015:59, 1-17 (2015).
- [22] Buranay S.C., Arshad N.: Hexagonal grid approximation of the solution of the heat equation on special polygons. *Advances in Difference Equations*, 2020:309(2020).
- [23] Volkov E.A.: Differentiability properties of solutions of boundary value problems for the Laplace equation on a polygon. *Trudy Mat. Inst. Steklov.*, 77, 113-142(1965).

- [24] Kondrat'ev V.A.: Singularities of a solution of Dirichlet's problem for a second order elliptic equation in the neighborhood of an edge. *Diff. Urevnen.*, **13**, 2026-2033(1977).
- [25] Ladyženskaja O.A., Solonnikov V.A., Ural'ceva, N.N.: *Linear and Quasi-linear Equations of Parabolic Type*, Translation of Mathematical Monographs. **23**, American Mathematical Society, USA(1967).
- [26] Friedman A.: *Partial differential equations of parabolic type*, Robert E. Krieger Publishing Company, Malabar Florida(1983).
- [27] Azzam A., Kreyszig E.: On solutions of parabolic equations in regions with edges. *Bull. Austral. Math. Soc.*, **22**, 219-230(1980).
- [28] Azzam A., Kreyszig E.: Smoothness of solutions of parabolic equations in regions with edges. *Nagoya Math. J.*, **84**, 159-168(1981).
- [29] Dosiyevev A.A.: The high accurate block-grid method for solving Laplace's boundary value problem with singularities. *SIAM J. Numer. Anal.* **42** (1), 153-178(2004).

- [30] Dosiyevev A.A., Buranay S.C., Subasi D.: The highly accurate block-grid method in solving Laplace's equation for nonanalytic boundary condition with corner singularity. *Computers and Mathematics with Applications*, **64**, 616-632(2012).
- [31] Axelsson O.: *Iterative Solution Methods*, Cambridge University Press, New York(1996).
- [32] Lax P.D., Richtmyer R.D.: Survey of the stability of linear finite difference equations, *Communications on Pure and Applied Mathematics* **9**, 267-293(1956).
- [33] Taussky O.: Positive-definite matrices and their role in the study of the characteristic roots of general matrices. *Advances in Mathematics*, **2**(2), 175-186 (1968).
- [34] Samarskii A.A.: *The Theory of Difference Schemes*, Marcel Dekker, Inc. New York, 2001.
- [35] Concus P., Golub G.H., Meurant G.: Block preconditioning for the conjugate gradient method. *SIAM Journal*, 6 (1): 220-252, (1985).
- [36] Axelsson O.: A general incomplete block matrix factorization method, *Linear*

Algebra and Its Applications, 74: 179-190, (1986).

- [37] Buranay S.C., Iyikal O.C.: Incomplete Block-Matrix Factorization of M -Matrices using two step iterative method for matrix inversion and preconditioning, *Mathematical Methods in Applied Sciences*, (2020), (in press).
- [38] Varga R.S.: *Matrix Iterative Analysis*, Prentice-Hall, Englewood Cliffs, NJ. 1962.
- [39] Henner V, Belozerova T., Forinash, K.: *Mathematical methods in physics, partial differential equations, Fourier series, and special functions*. K Peters, Ltd. 888 Worcester Street, Suite 230, Wellesley, MA 02482(2009).
- [40] Peaceman D., Rachford, H.H. JR.: The numerical solution of parabolic and elliptic differential equations. *J. Soc. Industrial Appl. Math.* **3**, p.28(1955)
- [41] Douglas J.: On the numerical integration of $\frac{\partial^2 u}{\partial x^2} + \frac{\partial^2 u}{\partial y^2} = \frac{\partial u}{\partial t}$ by implicit methods. *J. Soc. Industrial Appl. Math.*, **3**, p.42(1955)
- [42] Bagrinovskii K.A., Godunov S.K.: Difference schemes for multidimensional problems, *Dokl. Akad. Nauk USSR*, **115**, p.431(1957)

[43] Marchuk G.I.: Splitting and Alternating Methods, Handbook of Numerical Analysis. Elsevier Science Publisher vol **1**, 1990.

[44] Buranay S.C., Farinola L.A.: Implicit methods for the first derivative of the solution to heat equation. *Advances in Difference Equations*, 2018:430(2018).